UNIVERSITAT DE BARCELONA

Origen de la estructura de la caldera Cañas Dulces y su relación con el recurso geotérmico de alta entalpía

Fernando Molina Zúñiga

Anexos

Anexo

A

Stratigraphy and structure of the Cañas Dulces caldera (Costa Rica).

Publicado en:

Geological Society of America Bulletin

Autores del artículo:

Fernando Molina[1]

Joan Martí[2]

Gerardo Aguirre[3]

Eduardo Vega[1]

Leyner Chavarría[1]

1) Área de Geociencias, Centro de Servicios Recursos Geotérmicos, Instituto Costarricense de Electricidad, 50601 Guanacaste, Costa Rica.

2) Institute of Earth Sciences Jaume Almera, Spanish National Research Council (CSIC), 08028 Barcelona, Spain.

3) Centro de Geociencias, Universidad Nacional Autónoma de México, 76230 Querétaro, Mexico.

Molina, F., Martí, J., Aguirre, G., Vega, E. y Chavarría, L. (2014). Stratigraphy and structure of the Cañas Dulces caldera (Costa Rica). *Geol. Soc. Amer. Bull.*, 126(11-12). pp. 1465-1480. Doi: 10.1130/B31012.1.

Geological Society of America Bulletin, published online on 23 June 2014 as doi:10.1130/B31012.1

Geological Society of America Bulletin

Stratigraphy and structure of the Cañas Dulces caldera (Costa Rica)

F. Molina, J. Martí, G. Aguirre, E. Vega and L. Chavarría

Geological Society of America Bulletin published online 23 June 2014;
doi: 10.1130/B31012.1

Notes

Geological Society of America Bulletin, published online on 23 June 2014 as doi:10.1130/B31012.1

Stratigraphy and structure of the Cañas Dulces caldera (Costa Rica)

F. Molina[1], J. Martí[2,†], G. Aguirre[3], E. Vega[1], and L. Chavarría[1]
[1]*Área de Geociencias, Centro de Servicios Recursos Geotérmicos, Instituto Costarricense de Electricidad, 50601 Guanacaste, Costa Rica*
[2]*Institute of Earth Sciences Jaume Almera, Spanish National Research Council (CSIC), 08028 Barcelona, Spain*
[3]*Centro de Geociencias, Universidad Nacional Autónoma de México, 76230 Querétaro, Mexico*

ABSTRACT

The Cañas Dulces caldera is home to the Rincón de la Vieja–Santa María active volcanic complex and forms part of the northwestern sector of the inner magmatic arc of Costa Rica, together with other calderas and the active volcanoes of Miravalles, Tenorio, and Orosí-Cacao. This caldera is the site of one of the main geothermal reservoirs in Costa Rica, on which it is planned to build two geothermal plants, each with a capacity of 55 MW. Nevertheless, the characteristics of the Cañas Dulces caldera are not well known due to the fact that most of its morphological and structural traits are masked by the products emitted recently by the Rincón de la Vieja–Santa María volcanoes. Based on a revision of extensive deep boreholes and geophysical data obtained by the Instituto Costarricense de Electricidad (ICE) since 1970, combined with new geological work and radiometric dating, we describe in the present study the stratigraphy, structure, and volcanic evolution of this collapse caldera and define a comprehensive model to describe its evolution. The Cañas Dulces caldera resulted from the massive eruption at 1.43 ± 0.09 Ma of ~200 km^3 of rhyolitic magma that was largely responsible for the formation of the Liberia ignimbrite. The caldera was formed under strong structural control dominated by two parallel NE-SW regional faults and was followed by the construction of the Rincón de la Vieja–Santa María volcanic complex on one of the caldera's structural borders. The formation of this caldera and of a new shallow magmatic system facilitated the installation of the highly productive geothermal system inside the caldera.

INTRODUCTION

Like other volcanic phenomena, caldera-forming eruptions represent the culmination of a long geological process involving the generation of magma at depth, its ascent and differentiation, and, finally, its eruption onto Earth's surface (Gottsmann and Marti, 2008, and references therein). More than in any other volcanic environment, collapse calderas are places in which a large amount of Earth's internal energy is accumulated at relatively shallow (2–5 km) depths. This, together with their structural characteristics, makes collapse calderas optimal locations for developing geothermal fields. Examples of high-enthalpy geothermal fields in collapse calderas are found throughout the world and include sites such as Los Azufres in Mexico (Ferrari et al., 1991), the Taupo volcanic zone in New Zealand (Wood, 1995), and Menengai in Kenya (Mibei, 2012).

Costa Rica is home to another good example of this type of energetic resource, and geothermal exploration and exploitation currently take place in two extensive geothermal areas on the southern slopes of the Miravalles and Rincón de la Vieja–Santa María volcanoes, which now supply ~10% of the country's total energy production. These geothermal areas have traditionally been associated with the existence of collapse calderas, hidden by the products of postcaldera volcanism (Chiesa, 1991; Chiesa et al., 1992; Deering et al., 2007), which to date have not been clearly identified or characterized. Both these geothermal areas are located in the northwestern sector of the inner Costa Rica magmatic arc (Fig. 1) and have been thoroughly explored since the Instituto Costarricense de Electricidad (ICE) first discovered their great geothermal potential in the early 1970s.

To successfully exploit geothermal energy, it is necessary to determine—among other aspects—the spatial distribution of the resource. If it is constrained by a caldera structure, it is essential to obtain a volcanological and structural model of the events that led to the formation of both the caldera and the pre- and postcaldera structures (Wood, 1995; Tamanyu and Wood, 2003); this in turn will provide the necessary information for inferring the circulation dynamics of the fluids that are responsible for transporting the heat energy used to produce electricity.

Despite their economic importance, the geothermal areas associated with the volcanoes of Miravalles and Rincón de La Vieja–Santa María and their inferred calderas have never been properly studied. This is probably in part due to the fact that an important part of these calderas is buried below the products of the postcaldera volcanic complexes; field work, however, is also hampered by the lack of erosion—which would reveal significant outcrops—and the dense vegetation cover. Consequently, the name and limits of these calderas and their products have never been consistently described and vary from one study to another (Chiesa, 1991; Kempter, 1997; Vogel et al., 2004; Deering et al., 2007). Nevertheless, after four decades of geothermal exploration by ICE (including the boring of wells up to depths of 2000 m, numerous geophysical studies, and complementary field work), the amount and quality of available information are now sufficient to define a precise model of the formation and evolution of these volcanic complexes, which will help define better guidelines for further geothermal exploration in the area.

In this study, we concentrate on the Rincón de la Vieja–Santa María geothermal area and the related caldera structure(s) that have been postulated in previous works (Chiesa, 1991; Kempter, 1997; Vogel et al., 2004; Deering et al., 2007). Our main goal is to identify the stratigraphic, structural, and volcanological criteria that confirm the existence of collapse caldera(s) and to infer their structural limits and evolution. We present here information obtained from geological field surveys, remote sensing, the stratigraphic logging of cores from exploratory and exploited geothermal wells, radiometric dating,

†E-mail: joan.marti@ictja.csic.es.

GSA Bulletin; doi: 10.1130/B31012.1; 11 figures; 1 table; Data Repository item 2014226.

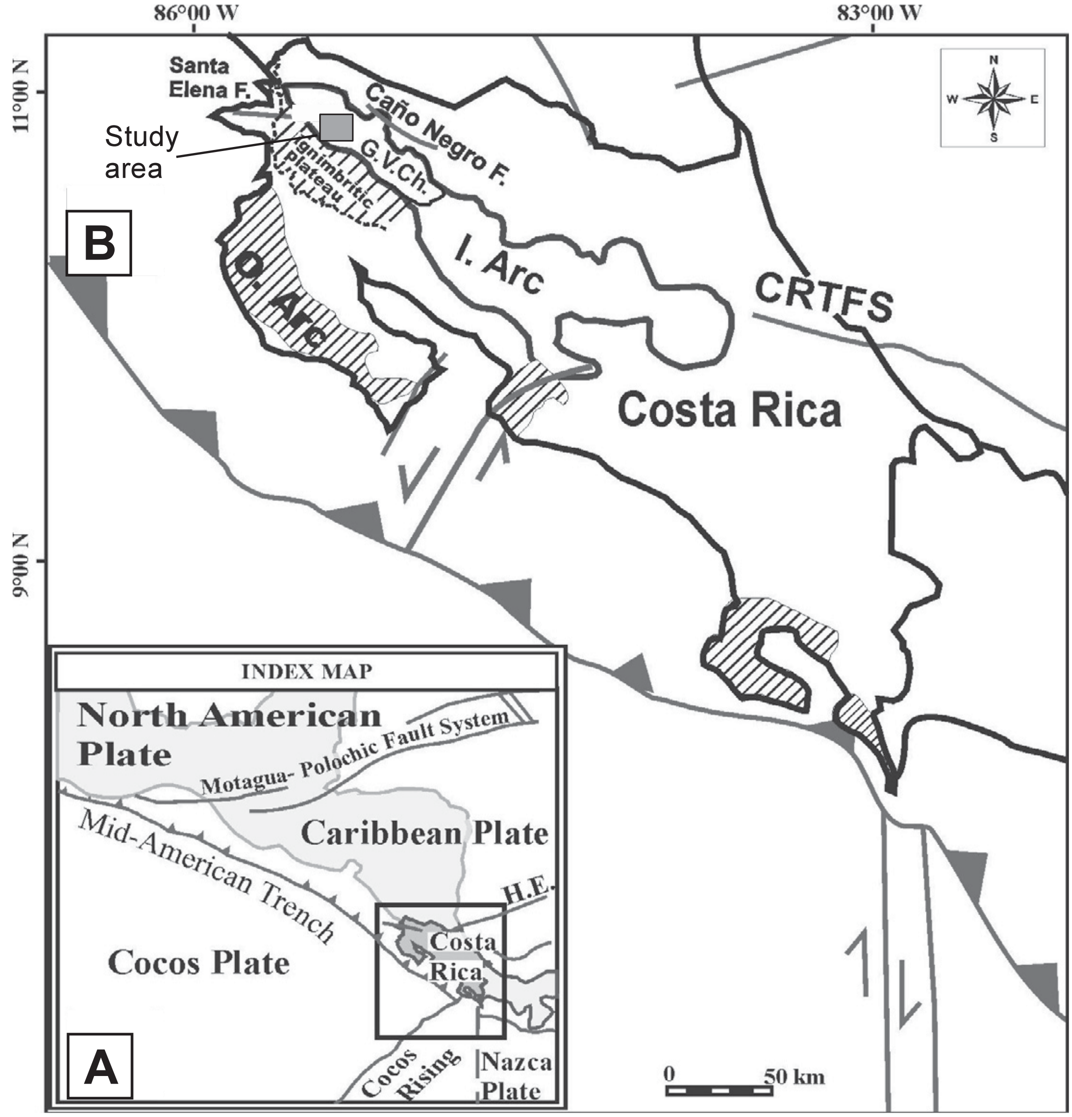

Figure 1. Present-day tectonic map of Costa Rica (simplified from Pindell and Kennan, 2009) and location of the study area. Santa Elena F—Santa Elena fault; Caño Negro F—Caño Negro fault; G.V.Ch—Guanacaste Volcanic Chain; O. Arc—outer arc; I. Arc—inner arc; CRTFS—transcurrent faults system of Costa Rica; H.E.—Hess escarpment.

and structural geophysical data, all of which we use to construct a comprehensive model of the origin and evolution of the caldera system(s) associated with the Rincón de la Vieja–Santa María volcanic complex.

GEOLOGICAL BACKGROUND

Costa Rica is located on the southwestern margin of the Caribbean plate (Fig. 1), below which the Cocos plate subducts slightly obliquely in a northeastern direction at a convergence rate of 8.5 cm/yr (DeMets, 2001; Pindell and Kennan, 2009). Two volcanic arcs are present (Fig. 1): The outer arc is a remnant of the island arc created during the subduction of the Farallon plate below the southwestern margin of the Caribbean plate in the Late Cretaceous (Meschede and Frisch, 1998; Pindell and Barrett, 1990; Pindell and Kennan, 2009), while the inner arc is the result of the subduction of the Cocos plate below the Caribbean plate from the Miocene to present (Syracuse et al., 2008).

The inner arc is oriented NW-SE and includes an alignment of active volcanoes and calderas that run parallel to the Middle America Trench (Fig. 1). The northwestern sector of the inner arc is known as the Guanacaste volcanic chain. It extends for ~75 km and includes four major Quaternary andesitic stratovolcanoes (from north to south): Orosí-Cacao, Rincón de la Vieja–Santa María, Miravalles, and Tenorio-Montezuma. This andesitic volcanism was immediately preceded by several episodes of intense silicic volcanism, the products of which mainly extend toward the Pacific slope and form the Santa Rosa ignimbritic plateau (Chiesa et al., 1992; Vogel et al., 2004; Deering et al., 2007). This andesitic-rhyolitic volcanism generated several hundreds of cubic kilometers of ignimbrites and related deposits, which were emplaced in the period 6–0.65 Ma (Vogel et al., 2004). The most representative unit is the Liberia Formation (1.43 Ma, this work), a pyroclastic succession of white fallout and pyroclastic density current deposits containing distinctive plagioclase, quartz, biotite, and hornblende phenocrysts, which constitutes a marker horizon for the whole region of ~4000 km^2 (Chiesa, 1991). The presence of this silicic volcanism is interpreted as evidence of the evolution of the oceanic crust into continental crust (Vogel et al., 2004).

The possible sites of the vents of the Santa Rosa plateau ignimbrites are not well known because they have been partially destroyed or are covered by products from younger episodes that culminated with the construction of the still-active stratovolcanoes. Based on strati-

Geological Society of America Bulletin, published online on 23 June 2014 as doi:10.1130/B31012.1

graphic relationships and the areal distribution of the deposits, Kempter (1997) identified at least three caldera structures—Cañas Dulces, Guachipelín, and Guayabo—as being responsible for these ignimbritic eruptions, with ages of 1.7 Ma, 1.5 Ma, and 1.4–0.6 Ma, respectively. Kempter located the Cañas Dulces caldera in the foothills of the Rincón de la Vieja stratovolcano and assigned it a diameter at least 8 km, with a border running around the Cañas Dulces domes (Fig. 2). The Guachipelín caldera was assumed to be the result of the Liberia ignimbrite eruption and to have erased much of the Cañas Dulces caldera, generating in the process a new caldera ~20 km in diameter (Fig. 2). Finally, the Guayabo caldera is located ~20 km southeast of Rincón de la Vieja. Based on petrological correlations, Deering et al. (2007) associated the formation of the Guachipelín caldera with the emplacement of seven pyroclastic units (including, among others, the Liberia ignimbrite) during the early Pleistocene with a period of deposition lasting 0.75 m.y. Carr et al. (1985) and Molina (2000) named a 5-km-diameter circular structure in the area corresponding to the Las Pailas geothermal field as the San Vicente caldera (Fig. 2).

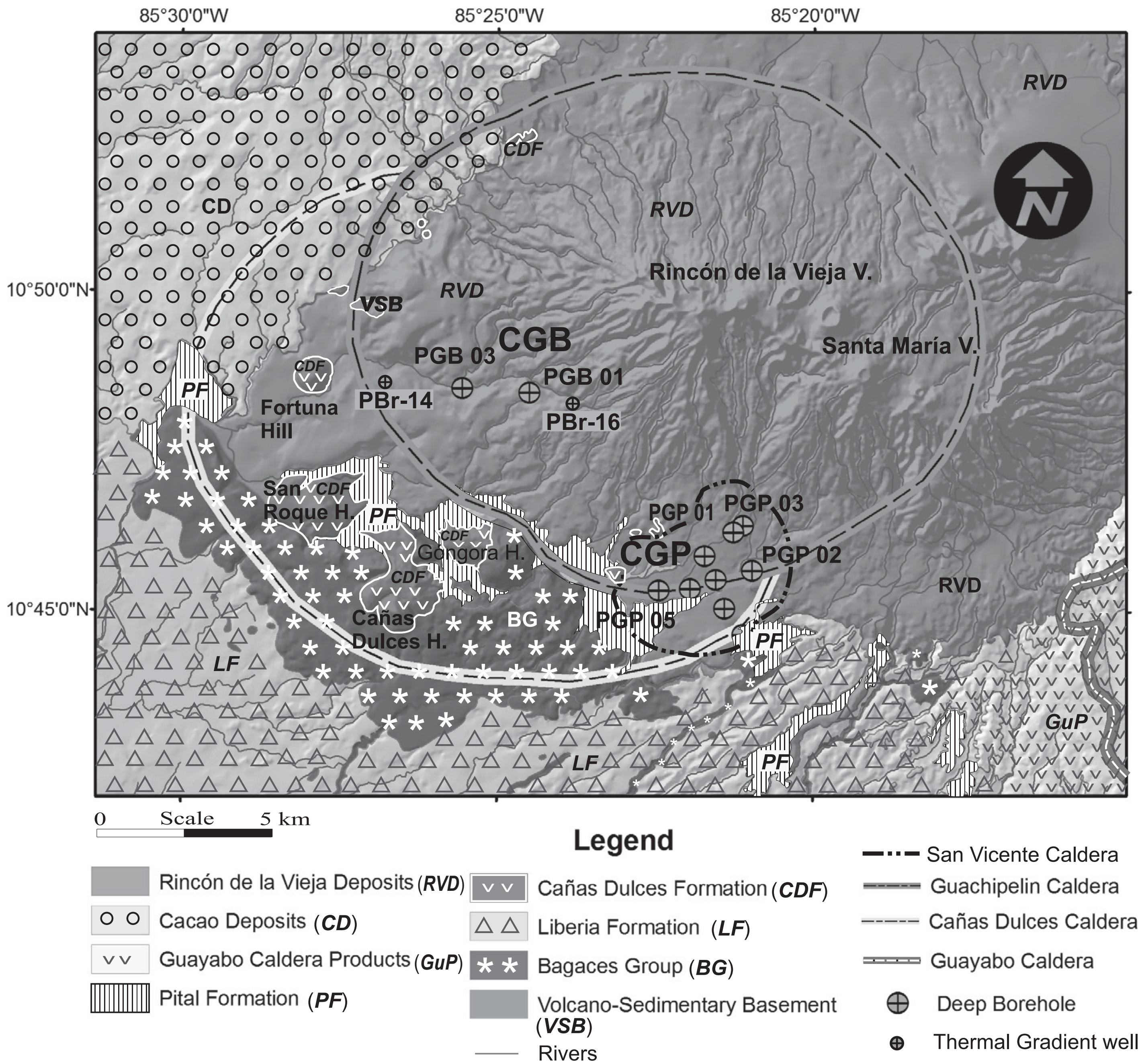

Figure 2. Simplified geological map of the study area based on previous studies (Kempter, 1997; Zamora et al., 2004) and this work. The limits of the caldera structures originally proposed for the study area by Kempter (1997) (Cañas Dulces and Guachipelin) and Molina (2000) (San Vicente) are indicated with different types of lines. CGP—Las Pailas geothermal field; CGB—Borinquen geothermal field.

TABLE 1. RADIOMETRIC AGES OF ROCKS FROM THE STUDY AREA

Code	Lithology	Location	Latitude (°N)	Longitude (°W)	Minerals analyzed	Age (Ma)	Reference
PSL-16-16-9-10	Dacitic pyroclastic flow	I Griega Creek	10°42′60″	85°21′40″	K-feldspar	8.75 ± 0.87	This work
CGO-1-12-10-10	Hornblende-rich dacite	Góngora Viejo Hill	10°45′47″	85°24′47″	Plagioclase	7.96 ± 0.53	This work
πG49s	Dacite	Cabuyal	10°67′93″	85°63′94″	Glass Plagioclase	7.810 ± 0.160 7.990 ± 0.160 7.850 ± 0.160	Gillot et al. (1994)
πG49O	Ignimbrite	Pijije	10°52′31″	85°33′17″	Glass Plagioclase biotite	1.393 ± 0.030 1.420 ± 0.030 1.83 ± 0.030 1.61 ± 0.060	Gillot et al. (1994)
πG49A	Ignimbrite	Salitral, Bagaces	10°59′48″	85°24′52″	Glass Plagioclase	1.600 ± 0.050 1.551 ± 0.060 1.270 ± 0.030 1.310 ± 0.030	Gillot et al. (1994)
Cu-38	Hornblende dacite	San Roque Hill	10°77′40″	85°46′42″	?	1.6 ± 0.5	Bellon and Tournon (1978)
SJL-1-19-8-10	Rhyolitic pyroclastic flow	San Jorge	10°42′16″	85°20′59″	K-feldspar	1.43 ± 0.09	This work
CSR-2-6-10-10	Hornblende-rich dacite	San Roque Hill	10°46′41″	85°27′39″	K-feldspar	1.41 ± 0.18	This work
CSV-1-14-10-10	Hornblende-rich dacite	San Vicente Hill	10°45′30″	85°23′0″	K-feldspar	1.37 ± 0.07	This work
CFO-1-18-9-10	Hornblende-rich dacite	Fortuna Hill	10°48′45″	85°27′49″	K-feldspar	1.31 ± 0.01	This work
CHO-1-12-10-10	Hornblende-rich dacite	Hornillas Hill	10°46′10″	85°22′28″	K-feldspar	1.25 ± 0.07	This work
Cr-RV-02-06	?	Cuesta Diablo	10°78′0″	85°42′1″	Matrix	1.14 ± 0.030	Carr et al. (2007)
CCD-1-6-10-10	Hornblende-rich dacite	Cañas Dulces Hill	10°44′58″	85°26′36″	Plagioclase	0.98 ± 0.05	This work
CGO-2-69-10	Hornblende-rich dacite	Góngora Joven Hill	10°46′1″	85°25′30″	K-feldspar	0.80 ± 0.04	This work
?	Amber	Quebrada Grande	10°84′44″	85°49′28″	C	3490 ± 105	Melson (1988)

METHODOLOGY

We concentrated our study on the area corresponding to the Cañas Dulces caldera (CDC) as defined by Kempter (1997), which contains the Borinquen (CGB) and Las Pailas (CGP) geothermal fields (Fig. 2). The study involved (1) new geological mapping aimed at establishing the relative stratigraphy of the outcropping units and identifying main structural features; (2) stratigraphic logging of the available borehole cores to identify the intracaldera stratigraphy; (3) remote sensing to study regional morphotectonic traits; (4) radiometric dating; and (5) a reinterpretation of the available geophysical data.

During field work, which lasted for several months from 2006 to present and covered all of the study area (Fig. 2), we conducted macroscopic descriptions of the different outcrops, confirmed or updated the stratigraphy established by previous studies, mapped tectonic features that were clearly identifiable in the field, obtained kinematic indicators when possible, and collected samples for petrographic and mineralogical analysis. Samples were also taken from the drilling cores in the Borinquen (CGB) and Las Pailas (CGP) geothermal fields for petrographic and mineralogical study. The total coring recovered from each borehole ranges from 50% to 90%, with the remaining material corresponding to cuttings. The stratigraphic logging of the available borehole samples was carried out by macroscopic and microscopic inspection and by using the primary mineralogy as fingerprints for correlating samples with the products observed on the surface. In addition, nine representative rock samples for geochronological study were selected and sent to Activation Laboratories, Ltd. (http://www.actlabs.com/), in Canada to obtain the Ar/Ar ages of each different unit (Table 1; Data Repository Tables DR1a and DR1b[1]).

For the study of regional and local morphotectonic lineaments, we used satellite images acquired by the Aster platform in 2008 (especially the three bands of visible near-infrared [VNIR], with a resolution of 15 m) and part of the colored shaded digital elevation model (DEM) of Central America, with a spatial resolution of 90 m, obtained by the Shuttle Radar Topography Mission (SRTM) mission in February 2000. In order to draw up a comprehensive analysis of the local morphotectonic lineaments in the Cañas Dulces caldera area, we used analogue aerial panchromatic photographs from November 1987 (scale 1:35,000), true-color digital photographs from January 1996 (resolution of 3 m), a RapydAye image from 2010 with a resolution of 5 m, and a DEM generated from contour lines every 20 m from the 1:50,000 topographic maps of the National Geographic Institute of Costa Rica. The morphotectonic analysis included the determination and comparison of lineaments obtained from the Aster images and different illumination-shaded relief DEM models, as well as a statistical analysis of the length and orientation of lineations. No significant differences were found between the data obtained from the digital terrain model (DTM) and the satellite images (see following), and so the preferred orientations cannot be attributed to any artifact of the construction of the Aster image or to the lighting direction of the DTM, given we used different lighting models. We also analyzed the profile and direction of more than 100 streams and rivers in order to detect abrupt changes in slope direction that could be related to tectonic movements.

In order to check the tectonic character of the lineaments patterns obtained through remote sensing, structural data were complemented with field studies aimed at recognizing these lineaments and identifying, whenever possible, their kinematic characteristics. Structural field data (fractures and faults) were organized into symmetrical-strike rose diagrams showing the relative abundance of the different distribution patterns. In addition, we identified and located with precision the main thermal manifestations in the study area and correlated their spatial distribution with previously identified lineaments to confirm their structural character. In a similar manner, we also located natural and induced seismic events recorded by the ICE monitoring network over the previous 12 yr and correlated their epicentral locations with the identified lineaments. Finally, available gravimetric data previously gathered by the ICE (1993, personal commun.) using a Lacoste-Rombert G-840 gravimeter, which provided gravity data from 348 sites, were also integrated into the study and used to identify major structural discontinuities.

[1]GSA Data Repository item 2014226, Analytical condition and results of samples analyzed for Ar-Ar dating (see Table 1 in main text for samples location), is available at http://www.geosociety.org/pubs/ft2014.htm or by request to editing@geosociety.org.

Geological Society of America Bulletin, published online on 23 June 2014 as doi:10.1130/B31012.1

STRATIGRAPHY

Previous studies addressing the volcano-stratigraphy of this area (Kempter, 1997; Zamora et al., 2004; Deering et al., 2007) indicated the presence of activity cycles that began with the establishment of a number of central volcanic edifices. These were later destroyed by caldera events taking place near the axis of the current volcanic arc, the products of which contributed to the formation of the Santa Rosa ignimbritic plateau. In this study, we make use of the general stratigraphy established by previous authors, but we partially modify it in light of our field work and the borehole data (Fig. 3). In this section, we introduce and describe the temporal and spatial distribution of the pre–Rincón de La Vieja–Santa María products. As we show here, the Liberia Formation is the main unit that can be stratigraphically and volcanologically correlated with a caldera formation and so can be used as the reference horizon for separating pre- and postcaldera rocks wherever the corresponding caldera structure is identified. Therefore, to facilitate the description of rocks in the study area, the stratigraphy has been divided informally and chronologically into pre–, syn–, and post–Liberia Formation products (Figs. 2 and 3).

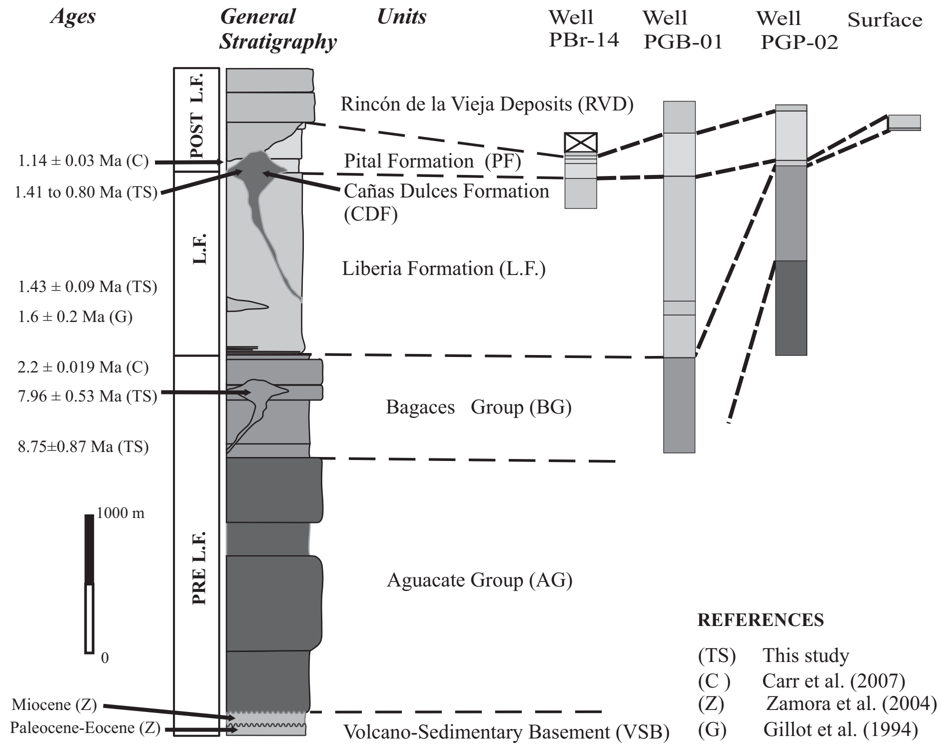

Figure 3. General stratigraphy of the study area based on previous studies (Zamora et al., 2004; Deering et al., 2007) and this work. Location of boreholes is shown in Figure 2. Data regarding new radiometric ages are given in Table 1, and locations of dated samples (stratigraphic units) are in Figure 2.

Pre–Liberia Formation Unit

This stratigraphic unit forms the substrate of the Liberia ignimbrite in most parts of the study area. It includes at its base a volcano-sedimentary basement of Upper Paleocene–Middle Miocene material formed of strongly hydrothermally altered sandstones and gray siltstones, silicified volcaniclastic breccias, and some minor pyroclastic deposits (Zamora et al., 2004). This volcano-sedimentary basement (Fig. 3) is unconformably overlain by the Aguacate Group (Tertiary period), which is mostly composed of pyroclastic deposits and lava flows of andesitic composition, occasionally intruded by andesitic and granodioritic dikes (Figs. 2 and 3; Laguna, 1984; Kussmaul, 2000). The Aguacate Group does not outcrop in the study area but has been identified in the boreholes of the Las Pailas geothermal field (Fig. 3) and has a maximum thickness of 1868 m.

The pre–Liberia Formation stratigraphic unit continues with the Bagaces Group, which forms most of the ignimbrite plateau of Santa Rosa. It extends from the base of the current volcanic edifices to the Pacific coast and is unconformably overlain by the Liberia Formation. It is mainly composed of scoria-rich ignimbrites of dacitic composition, and silicic ignimbrites and lava flows. Based on the borehole stratigraphy, the Bagaces Group has a maximum thickness of 1077 m (PGP 05) in the Las Pailas area (Fig. 2) and, given that the borehole did not reach its basal contact, a minimum thickness of 749 m in the Borinquen area (PGB 01) (Fig. 2). The Bagaces Group is interpreted as covering a depositional period spanning from 8.75 to 1.43 Ma (this work). According to the lithology of the exposed rocks, this group is divided into several stratigraphic units (I Griega, Góngora Viejo, Santa Fe units, Alcantaro Formation, and Curubandé unit) with stratigraphic discontinuities (Kempter, 1997; Zamora et al., 2004) that were not distinguished in this study.

Liberia Formation

According to its extension, volume, facies, and variations in thickness, the Liberia Formation is the only unit that can be stratigraphically correlated with the formation of a collapse caldera in the study area. Although several authors (Chiesa, 1991; Kempter, 1997; Vogel et al., 2004; Deering et al., 2007) have studied this ignimbrite and suggest that it derived from a caldera eruption, none has ever established any clear correlation with the formation of any particular caldera. However, all suggested that it could derive from the Guachipelin caldera (see Fig. 2) located east of the Borinquen geothermal field (Fig. 2).

Our field revision indicates that the Liberia Formation is radially distributed around the southwestern flank of Rincón de la Vieja volcano in the area of the Borinquen and Las Pailas geothermal fields (Fig. 2). In the Borinquen area, boreholes PGB01 and PGB03 reveal that this formation has a total thickness of over 1350 m (Fig. 3), while to the southeast, in the area corresponding to the Las Pailas geothermal field, boreholes PGP01, PGP02, and PGP03 revealed a thickness of only up to 40 m for the same unit (Fig. 3). Field mapping shows that the Liberia Formation extends mainly on the Pacific side of the Rincón de la Vieja–Santa María volcanoes, from La Cruz to Bijagua (Fig. 4), with a thickness ranging from 0.8 to 120 m; also, some isolated outcrops exist on the Caribbean slopes, with total thicknesses of up to 4 m, over a total area of ~4000 km^2.

The Liberia Formation includes at its base a well-stratified succession of alternating, thinly laminated pyroclastic surge and pumice-rich fallout deposits, which have a total thickness of between 0.3 and 2.5 m and an irregular areal

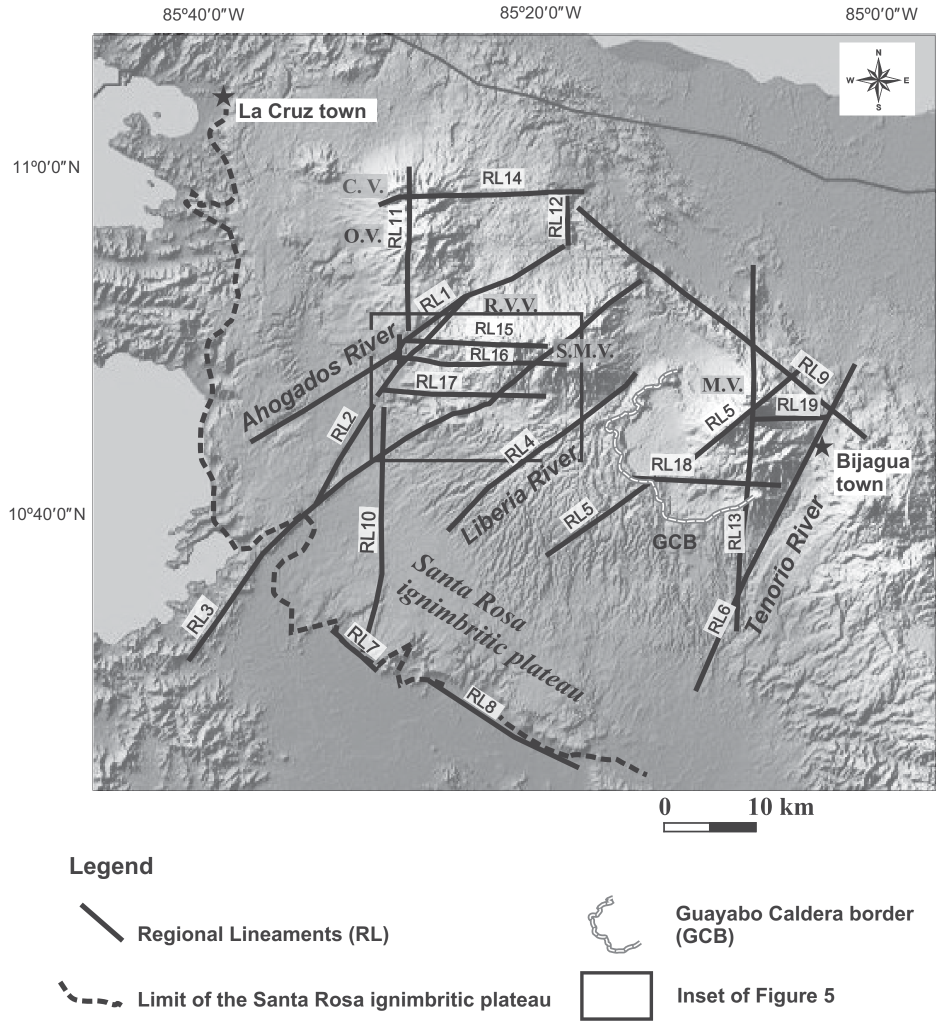

Figure 4. The most relevant regional geological and morphological features of the Rincón de la Vieja–Santa María and Miravalles volcanic complexes and adjacent zones: the volcanic edifices of Orosí (O.V.)-Cacao (C.V.), Rincón de la Vieja (R.V.V.)–Santa María (S.M.V.), and Miravalles (M.V.), the Santa Rosa ignimbritic plateau, the regional lineament systems, the main rivers, and the topographic rim of the Guayabo caldera.

distribution. These basal deposits grade into an apparently massive flow unit that corresponds to the Liberia ignimbrite. They consist of a pumice-rich ignimbrite in which rounded pumice clasts (with 10% of crystals) and lithic fragments, mainly derived from the Aguacate and Bagaces Groups and subvolcanic intrusions, are embedded in an abundant ash-rich matrix composed of glass shards and crystal fragments of plagioclase, quartz, biotite, amphibole, and, sporadically, pyroxene. Occasionally, this ignimbrite is internally stratified, a fact that probably reflects the superposition of several flow units, and it has irregularly distributed lithic-rich horizons with clasts up to 1 m in diameter. Some boreholes have revealed thinly stratified, fine-grained fallout and surge deposits on top of the Liberia ignimbrite that have not been identified on the surface, probably due to subsequent erosion. The Liberia Formation deposits have a characteristic white color but in some places are slightly reddish-to-pink in color. In some of the studied boreholes, the Liberia Formation is intruded by andesitic rocks, which are associated with subvolcanic intrusions related to the Rincón de la Vieja volcano. Using K/Ar dating, Gillot et al. (1994) assigned an age of 1.6 ± 0.2 Ma to the Liberia ignimbrite; nevertheless, new Ar/Ar results obtained in this study assign it an age of 1.43 ± 0.09 Ma (Table 1), which corresponds more closely to the observable stratigraphic relationships and the existing ages for pre- and post-caldera rocks (Fig. 3).

Post–Liberia Formation

Here, we include all the volcanic material outcropping in the study area that postdates the Liberia Formation: the deposits in-filling the caldera depression, which include a series of dacitic domes (Cañas Dulces Formation) emplaced around an inferred caldera border (Chiesa, 1991; Kempter, 1997; Vogel et al., 2004; Deering et al., 2007), a sequence of interbedded pyroclastic materials with lacustrine sediments and epiclastic deposits (Pital Formation), and lava flows of andesitic to basaltic-andesitic composition related to the volcanism that occurred before and during the establishment of the Rincón de la Vieja–Santa María volcanic complex (Figs. 2 and 3). Additionally, two further units lying outside the study area were also mapped in order to complete the region's geological map: the Guayabo caldera products (pyroclasts and lavas flows) to the southeast and the Cacao volcano deposits (andesitic lavas flows and debris avalanche) to the northwest (Fig. 2).

The Cañas Dulces Formation includes a group of seven dacitic domes containing phenocrysts of plagioclase, green hornblende, clinopyroxenes and orthopyroxenes, minor biotite, and opaques in a devitrified groundmass, emplaced on the periphery of the southwestern border of the Cañas Dulces depression (Fig. 2; Kempter, 1997). Similar rocks have been described on the northwestern border of this depression (Fig. 2) in small, dispersed outcrops. Although these domes were initially dated at 1.5 and 1.6 Ma (ICE, 1976, personal commun.; Bellon and Tournon, 1978), the new Ar/Ar ages (from 1.41 to 0.8 Ma) obtained in this study (Table 1) are more consistent with the relative stratigraphy and the new ages given for the Liberia Formation. The Pital Formation (Kempter, 1997) consists of a succession of pumice-rich dacitic fallout and pyroclastic density current deposits containing some minor epiclastic and lacustrine deposits, as well as some andesitic lavas, and it is restricted to the interior of the study area. In thickness, it ranges from 180 m (PGP-05) to 347 m (PGP-03) in the Las Pailas geothermal field and from 5 m (PBr 16) to 384 m (PBr 14) in the Borinquen geothermal field (Figs. 2 and 3). This unit was emplaced over an estimated period of 1.43–0.8 Ma. Finally, the deposits from the Rincón de la Vieja volcano, mostly corresponding to andesitic lava flows with a total thickness of up to 200 m, cover the previous formations discontinuously and range in age from around 1.14 ± 0.030 Ma (Carr et al., 2007) to the present day. Some pyroclastic and debris avalanche deposits are also present in the uppermost part of the sequence. An age of 3490 ± 105 yr was obtained for one of these pyroclastic deposits (Melson, 1988).

Geological Society of America Bulletin, published online on 23 June 2014 as doi:10.1130/B31012.1

STRUCTURAL GEOLOGY

In order to identify the main structural features (fractures and faults) that affect the study area, we collated structural data published in previous studies (Denyer et al., 2003; Denyer and Alvarado, 2007) and conducted a remote-sensing study in which we identified the main morphological lineaments of the area (Figs. 4 and 5). In order to confirm the tectonic nature of the morphological lineaments identified by the remote-sensing analysis, we conducted a structural field study (Figs. 5 and 6; Data Repository Table DR2 [see footnote 1]) and analyzed the location of thermal anomalies (Fig. 5), gravimetric anomalies (Fig. 7), and seismicity (Fig. 8). These three elements are all good indicators of the existence and location of tectonic faults and fractures (Price and Cosgrove, 1990; Gudmundsson, 2011).

Remote-Sensing Analysis

Using the methodology described previously and several morphological criteria such as morphological alignments and/or inflections in riverbeds, hills, watersheds, domes, landslide scars, and slope maps, we identified the main lineaments in the study area.

We distinguished four main lineament systems oriented NE-SW, NW-SE, N-S, and E-W. The NE-SW regional system (from RL1 to RL6 in Fig. 4) affects the Rincón de la Vieja, Santa María, and Miravalles volcanoes. The courses of a number of rivers also run in this direction, mainly in the valleys that separate the volcanic massifs (RL1, Ahogados River; RL4 Liberia River; and RL6, Tenorio River). RL3 defines a main lineament with a total length of more than 65 km and a nearly constant azimuth averaging 45°, extending from near the Pacific coast to the foothills of the Caribbean sector of the Rincón de la Vieja–Santa María complex (Fig. 4). Several domes—Góngora Viejo (7.96 ± 0.53 Ma), Hornillas (1.25 ± 0.07 Ma), and Cañas Dulces (0.80 ± 0.04 Ma)—were emplaced along this lineament at various times, thereby suggesting its tectonic nature. Lineament RL5, known as the Guayabo fault (W. Taylor, 2011, personal commun.), affects the ignimbrites of the Santa Rosa Plateau and the Quaternary rocks of

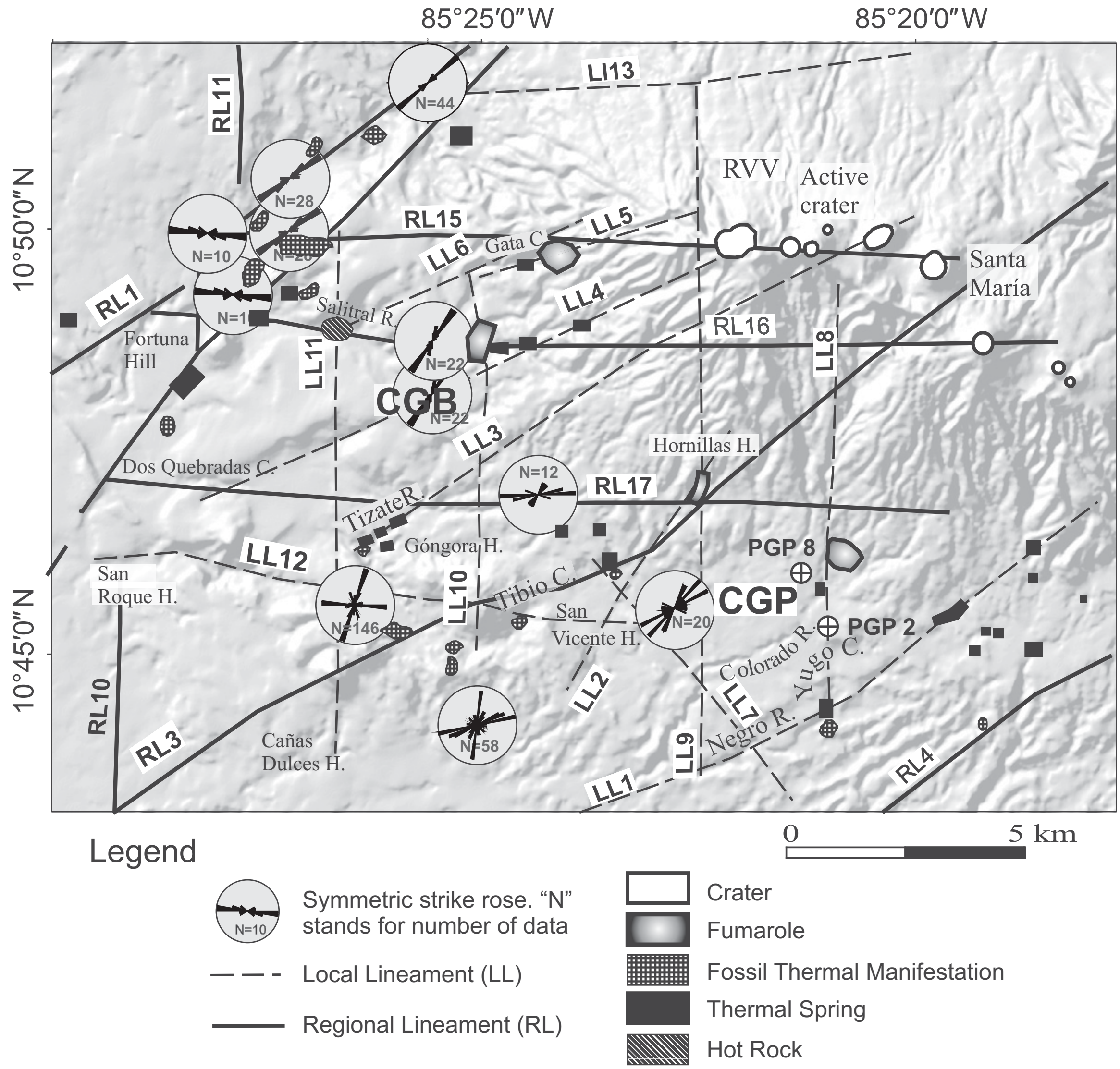

Figure 5. Major morphological lineaments and structural data, and spatial distribution of the main manifestations of the thermal activity (fumaroles, hot rock, thermal springs, fossil hydrothermal alterations, and craters) from the study area. RVV—Rincón de la Vieja; CGP—Las Pailas geothermal field; CGB—Borinquen geothermal field.

Geological Society of America Bulletin, published online on 23 June 2014 as doi:10.1130/B31012.1

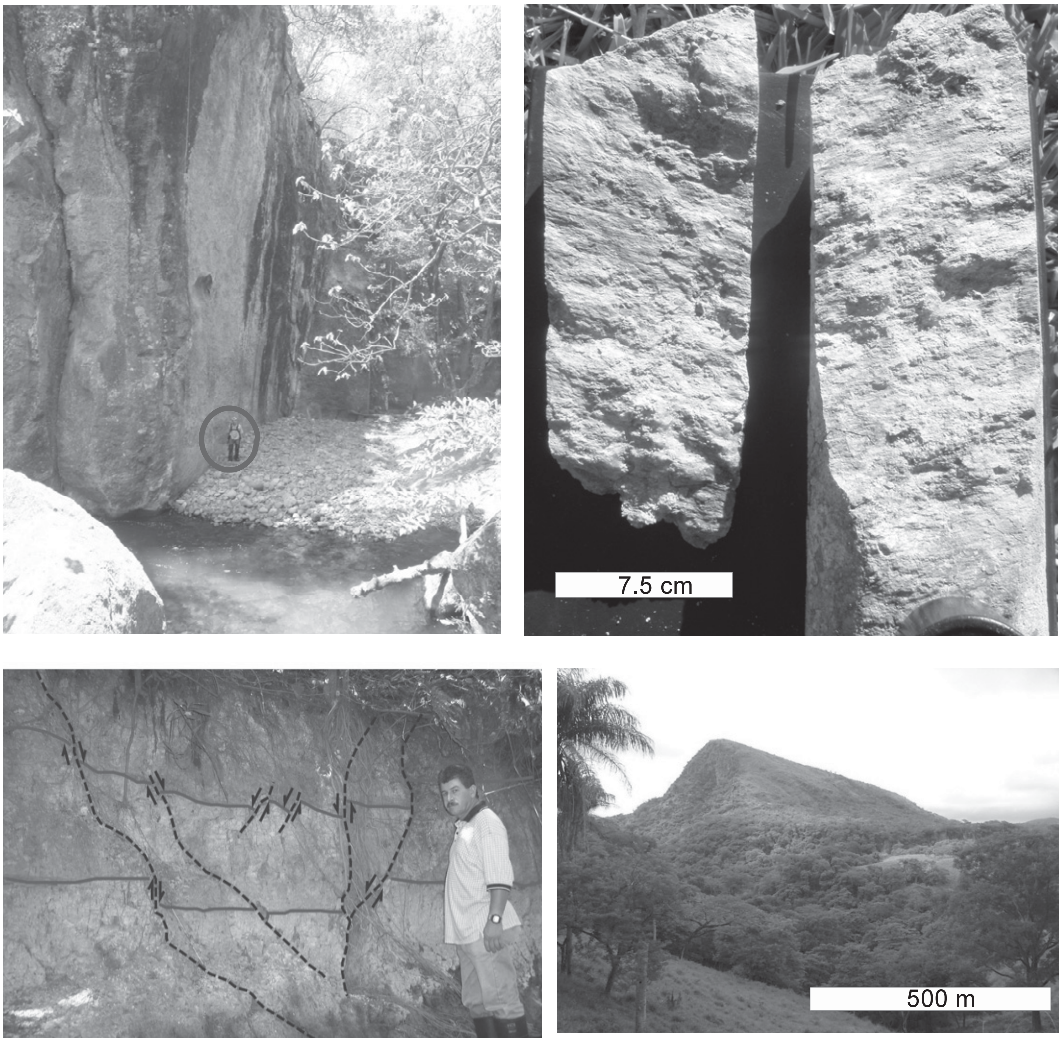

Figure 6. Photographs showing field and borehole evidence of the tectonic nature of some of the morphological lineaments identified from the remote-sensing study. (Upper left) Vertical fault plane affecting the Pital Formation probably related to the movement of LL9 lineament at the point where it changes the course of the Colorado River from E-W to N-S (see Fig. 5 for location). (Upper right) Sample of a rock core showing slickensides from the PB3 23 borehole at the vicinity of RL2 (see Figs. 9 and 10 for location). These slickensides are almost pure strike-slip striae that affect post–Liberia Formation rocks. These structural indicators do not correspond to the kinematics of the RL2 lineament at the moment of the caldera formation but indicate the tectonic nature of this lineament, which has had different movements along its long-lived history. (Lower left) Extensional faulting affecting the Pital Formation at the Quebrada de Gata, probably related to joint movement of LL5 and LL6 (see Fig. 5 for location). (Lower right) View from the ESE of the San Roque dome (Figs. 2 and 5), the morphology of which is truncated by the normal movement of LL12.

the Miravalles volcano. At a more local level (Fig. 5), the NE-SW system with six main lineaments (from LL1 to LL6, in Fig. 5) is also evident in the study area and its surroundings. The influence of this group of lineaments is revealed by the orientation of drainage patterns and the manifestations of thermal activity that occur along them. In addition, the morphology of the active crater of Rincón de La Vieja suggests that it was affected by lineament LL3 (Fig. 5).

The NW-SE system is less prominent at a regional scale but still includes three main lineaments (labeled as RL7, RL8, and RL9 in Fig. 4). RL7 and RL8 are located on the Pacific slope and delimit the southern edge of the Santa Rosa ignimbrite plateau (Fig. 4). The southeastern end of RL8 is identified as a thrust fault on the 2007 geological map of Costa Rica (Denyer and Alvarado, 2007). Lineament RL9 is located on the Caribbean side and separates the volcanic edifices of Rincón de la Vieja and Miravalles from the northern plains of Costa Rica. Astorga et al. (1991) suggested that this lineament is a continuation of the Nicaragua graben. Locally, we traced LL7 south of the Las Pailas geothermal field to where it affects the direction of the Negro and Colorado Rivers (Figs. 5 and 6).

The N-S system is also well defined at a regional scale. We identified four main lineaments, labeled from RL10 to LR13 (Fig. 4). RL10, part of which was previously identified as the Liberia fault (Denyer et al., 2003), has an average azimuth of 5° and a length of 27 km. RL11 can be seen in the north of the study zone cutting through the Orosi-Cacao volcanic complex, the southern end of which is visually truncated by RL1 and shifted westward. RL13, which crosses the Miravalles volcano and has a maximum length of 39 km, is the most important lineament in the N-S system. At a more detailed level (Fig. 5), we identified four N-S lineaments. LL8 is marked by the riverbeds of the Colorado River and Yugo Creek, and its tectonic nature was confirmed by directional drilling from PGP-2 and PGP-8 (Fig. 5), as they intersected a fault plane with the same direction and position as LL8. The existence of other lineaments (LL9, LL10, and LL11) is also suggested by their effect on riverbeds and presence of thermal manifestations (Fig. 5).

The E-W system includes lineaments RL14 to RL19 (Fig. 4), which have an average azimuth of 95° and are clearly visible in the volcanic edifices of Rincón de la Vieja, Santa María, and Miravalles. In the vicinity of the study area, we identified three of these lineaments (RL15–RL17, Fig. 4) within a 7.5-km-wide zone. A segment of RL15 atop Rincón de la Vieja is defined by the alignment of six craters

Geological Society of America Bulletin, published online on 23 June 2014 as doi:10.1130/B31012.1

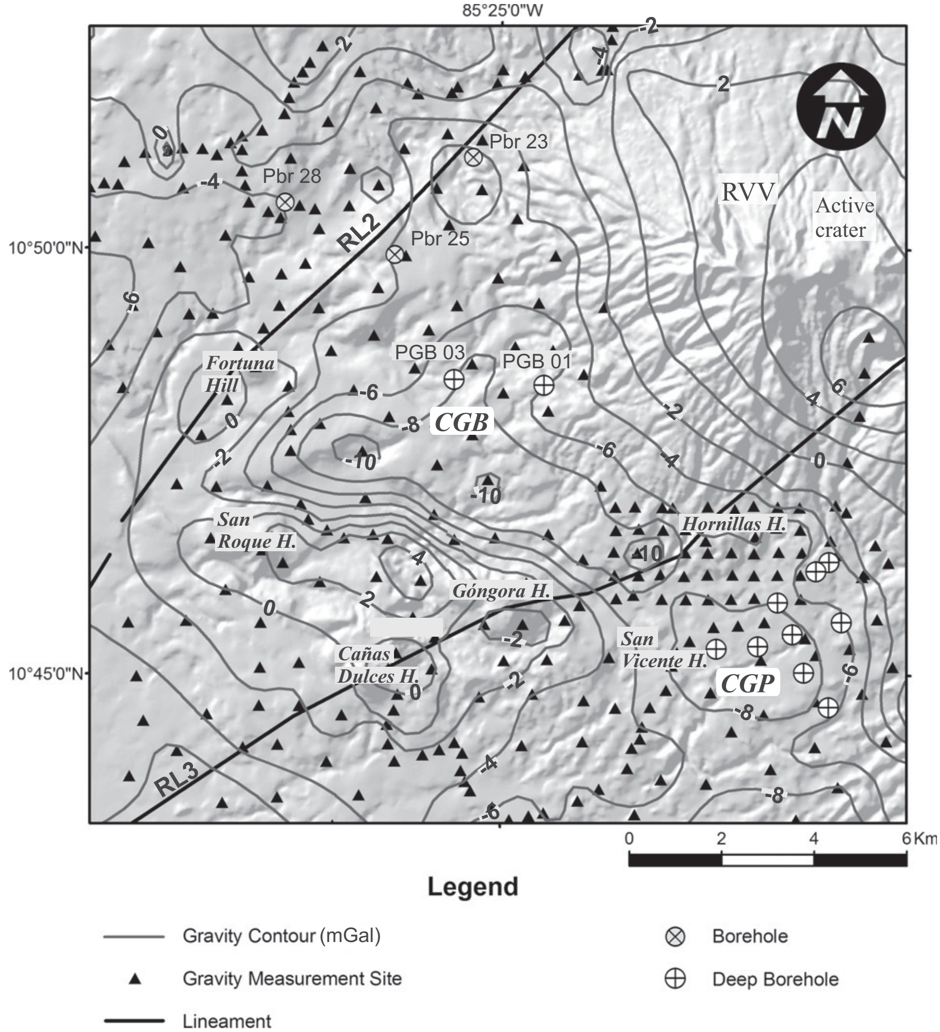

Figure 7. Bouguer gravity anomaly map of the study area reduced to a density of 2.3 g/cm^3. RVV—Rincón de la Vieja; CGP—Las Pailas geothermal field; CGB—Borinquen geothermal field; RL—regional lineament.

and a landslide scar generated by a sectorial collapse of the volcanic edifice. The trace of RL16 begins in the crater of Santa María, continues along the Salitral riverbed with several manifestations of thermal activity, and culminates on the western side of the Fortuna dome (Fig. 5). RL17 is defined by the alignment of the San Roque and Hornillas domes and the course of the Dos Quebradas Creek. LL12 is observed locally and can be traced from the San Vincente dome through Góngora Joven as far as the south of the San Roque dome and a sector of the Tizate riverbed. Another local lineament (LL13) can be identified to the north of the study area starting from RL2, and it is clearly defined by the 90° kink of several N-S riverbeds located on the northern flanks of Rincón de la Vieja (Fig. 5). RL14, RL18, and RL19 (Fig. 4) are located on the volcanoes Orosi and Miravalles.

Field Data

In contrast to the great quantity of morphotectonic lineaments generated using remote sensing, field structural data are scarce due to the burial of most of the area under material emitted by the Rincón de la Vieja–Santa María volcanoes and to the dense covering vegetation. Most of the structural features identified in the field correspond to faults, fractures, and joints (Fig. 6), generally subvertical and closed, with lengths between 1 and 25 m. We identified 377 such structures (Fig. 5) and for each one measured their corresponding strike, dip angle, and relative motion when marked by stratigraphic discontinuities (Data Repository Table DR2 [see footnote 1]). However, very few kinematic indicators were observed on the fault planes.

NE-SW– and NW-SE–oriented fracture systems predominate in the Holocene conglomerates and andesitic lavas, in which N-S– and E-W–oriented fractures are less abundant. In the Pliocene–Pleistocene sequence of the Pital Formation (Figs. 2 and 5), fractures run generally either NE-SW and E-W or—albeit to a lesser extent—NW-SE and N-S in direction. Along the Tizate River, NE-SW faults form a graben with an offset of ~10 m, while in the Tibio Creek, the Pital Formation is cut by a N-S–oriented fault with apparent dextral displacement. In the Bagaces Group, due to the wider range of ages covered by these rocks, there is a great amount of variability in the direction of fractures with N-S, NE-SW, NW-SE, and E-W orientations.

Symmetric rose diagrams obtained from field data confirm that two directions of faulting (NE-SW and E-W) predominate in the study area and its surroundings and correlate with regional and local morphological lineaments. The presence of fault offsets and scarps along the RL15 (E-W) and RL1 (NE-SW) lineaments (Figs. 4 and 5) in the northwest of the Fortuna dome confirms their tectonic nature. In the Borinquen sector (Gata Creek), a NE-SW system predominates, forming an angle of ~15° with respect to the LL6 lineament. To the south of Góngora, there is a correspondence between field data and the LR3 (NE-SW), LL12 (E-W), and LL10 (N-S) lineaments (Fig. 5). In the northeastern sector of Góngora, measurements of structural features reveal the influence of the LR17 (E-W) lineament. The field data obtained from east of Mount San Vicente show NE-SW trends, parallel to the LL2 and LR3 lineaments (Figs. 4 and 5).

Thermal Anomalies

Locations of thermal anomalies, which in the study area are mostly caused by the transport of hot fluids through fractures and faults, also show good correspondence with morphological lineaments and field structural data. In the study area, our field survey included various manifestations of thermal activity such as fumaroles, hot rock, thermal springs, fossil hydrothermal alteration zones, and craters, the distribution of which is shown in Figure 5. On the RL1 trace, we mapped intense hydrothermal alteration, having found some isolated dacitic and rhyolitic lavas belonging to the Cañas Dulces Formation toward its northeastern end. The Fortuna dome (1.31 ± 0.08 Ma), which also belongs to the Cañas Dulces Formation, lies on the RL2 trace (Fig. 5), along which there are numerous manifestations of thermal activity. The structural nature of the other lineaments (e.g., LL9, LL10, and LL11) is also indicated by the domes and manifestations of thermal activity that occur along them.

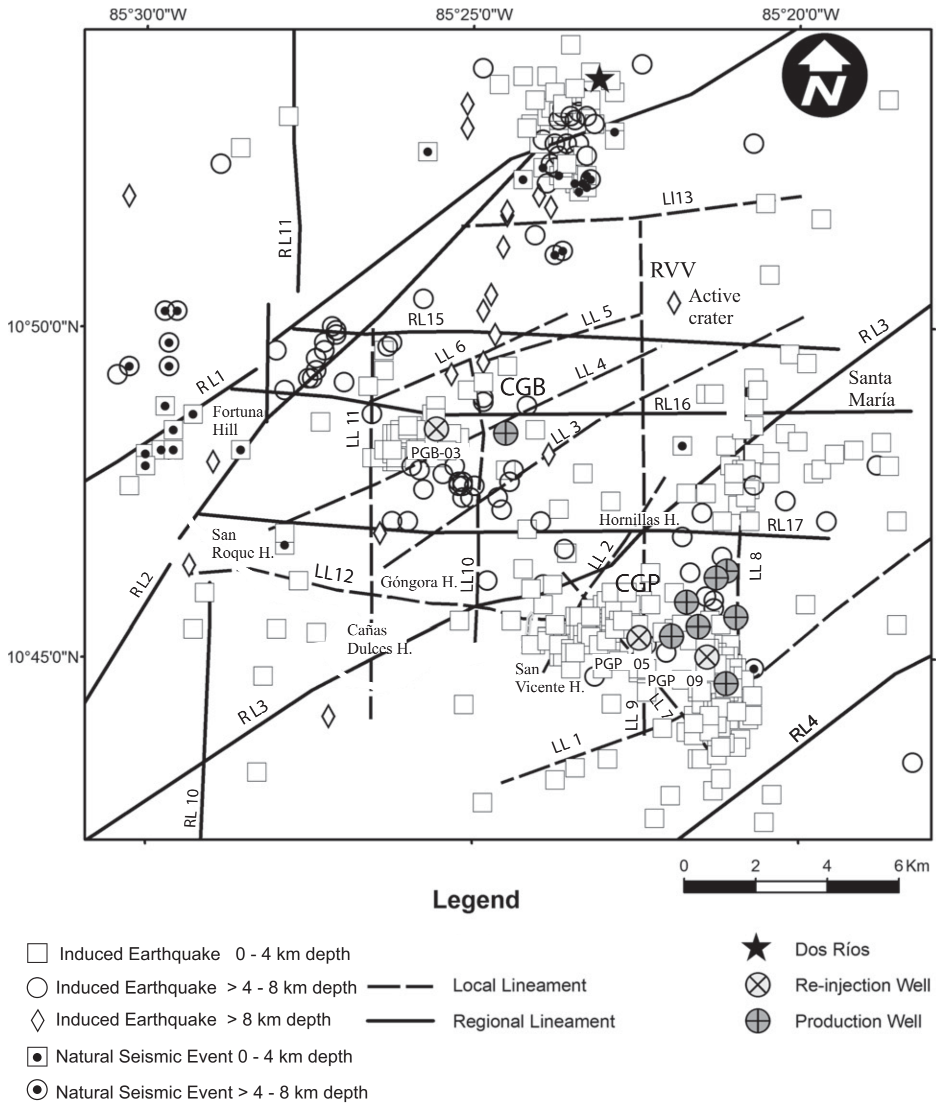

Figure 8. Spatial distribution of seismic events (natural seismicity and seismicity induced by re-injection of geothermal fluids into deep wells). The seismic events are grouped into three different families according to their depth. RVV—Rincón de la Vieja; CGP—Las Pailas geothermal field; CGB—Borinquen geothermal field; RL—regional lineament; LL—local lineament.

Structural Gravimetry

Over the previous two decades, the ICE has conducted several structural gravimetric surveys on the Pacific slopes of the Rincón de la Vieja volcano (ICE, 1993, personal commun.; GeothermEx, 2001, personal commun.). We used the results obtained in these studies as an additional correlation for the morphostructural features identified in the study area and its surroundings, and to define possible caldera structures. The Bouguer anomaly map (Fig. 7) suggests the existence of a relative minimum, from –10 to –6 mGal, that is roughly triangular in shape. One side is oriented NW-SE and extends for 13.5 km from Borinquen to Las Pailas geothermal field, another side is oriented NE toward borehole PBr 23, and the third and largest side runs from this borehole to Las Pailas geothermal field. Toward the southeast, this relative minimum is limited by the RL3 lineament but is limited to the northwest by RL2. To the south, it is bounded by a maximum gravity gradient, reaching values in the order of 4 mGal, probably as a response to the intrusive bodies constituting the Góngora, La Torre, Cañas Dulces, and San Roque domes (Fig. 7). To the west, the gradient is less pronounced, reaching values of 0 mGal, and is limited by RL2. However, this triangular shape does not correspond to the real distribution of the low-density body that is the origin of this gravity anomaly, since toward the northeast, from where available data are scarce, it is likely to be a positive effect caused by the Rincón de la Vieja–Santa María volcanic complex. In fact, two boreholes, PGB 01 and PGB 03, located toward the center of gravity minimum, were drilled 1350 m into the Liberia Formation (Fig. 7), which has a contrastingly lower density than the surrounding rocks. To the southeast of RL3, there is another gravimetric minimum, but less pronounced than the previous one. This was interpreted by Molina (2000) as a small caldera structure (San Vicente caldera) that hosts the Las Pailas geothermal field (Fig. 7).

Location of Natural and Induced Seismicity

Finally, we also took into account in our structural analysis the location of the seismic events recorded by the ICE Seismological and Arenal-Miravalles Volcanological Observatory (OSIVAM) monitoring network installed in the geothermal fields and surrounding areas. We computed natural events, as well as those induced by the re-injection of geothermal fluids into deep wells. We divided the seismicity events registered in the study area into three families according to their depths (Fig. 8). Earthquakes at depths of less than or equal to 4 km were the most numerous and in general are produced by the mobilization of geothermal fluids and concentrate in swarms around re-injection wells. In the Las Pailas geothermal field, there were two main clusters of seismic events located in the vicinity of the re-injector wells (Fig. 8). However, a smaller cluster was also present in the north of Las Pailas geothermal field, along the LL8 lineament (Fig. 8). Induced seismicity at this depth in the Las Pailas geothermal field area (Fig. 8) seems to find a barrier near the RL3 structure that prevents its propagation any further northwest. This barrier may correspond to the structural limit between the depression indicated by the gravity minimum and the San Vicente caldera. In the Borinquen geothermal field, earthquakes were concentrated in two areas, one around the re-injector well PGB 03 with a NE-SW trend, and the other ~9 km N-NE in a tectonically active area located at the intersection between the RL1 and RL2 lineaments. Earthquakes at depths of over 4 km but less than or equal to 8 km are scarce in the Las Pailas geothermal field and tend to concentrate between structures LL3 and LL4. The seismic events induced by re-injection in well PGB 03 were concentrated toward the N-NE at the intersection between structures RL1 and RL2, as well as 4 km west on the RL2 lineament (Fig. 8). Earthquakes at depths of over 8 km are

Geological Society of America Bulletin, published online on 23 June 2014 as doi:10.1130/B31012.1

rare and mostly occurred as a result of the reinjection tests conducted in the Borinquen wells in November 2005. Most trend N-NE toward the intersection of the RL1 and RL2 structures (Fig. 8). In addition, several natural seismic events, such as those that occurred on 2 July and 3 August 2005, with local magnitudes of 6.6 and 6.3, respectively, are also significant. The first occurred off the Pacific coast, and the second occurred in Lake Nicaragua. On 7 August 2005, an earthquake with a local magnitude of 3.9 was noted in Buenos Aires de Upala (14 km northeast of the Borinquen geothermal field, outside the study area). Two seismic swarms were recorded during this event around the study area, one near the town of Dos Ríos and the other 8 km west of the Borinquen geothermal field, corresponding to tectonic activity on the RL1 structure (Fig. 8).

DISCUSSION

Based on morphological features and the existence of a large ignimbritic plateau (Santa Rosa Plateau) on the Pacific side of the Rincón de la Vieja–Santa María and Miravalles volcanoes, previous studies (Chiesa, 1991; Kempter, 1997; Deering et al., 2007) have proposed the existence of collapse caldera structures in the vicinity of these volcanoes that would account for these voluminous explosive eruptions. However, none of these studies has documented precisely the limits of these calderas or their corresponding eruptive products.

Caldera limits are not always well defined, since, depending on their age, they may be partially eroded, hidden under postcaldera products, or even affected by postcaldera tectonics. In addition, preserved morphological limits do not coincide well with the original structural limits of the caldera, since they are immediately enlarged by landslides on the newly formed, unstable caldera walls (Lipman, 1997), and by subsequent erosion. Likewise, what appear to be volcanic depressions may have formed by processes other than true caldera collapse, such as erosion, landsliding, or tectonics. An additional difficulty in defining collapse calderas is the identification of the caldera-forming products and the corresponding eruption sequence, which are not always that evident. Therefore, if we are to define a volcanic depression as a true caldera formed by the collapse of the roof of a magma chamber after massive emptying during a volcanic eruption, it is essential to identify its structural limits and/or the caldera-forming products, as well as the mechanisms that caused the caldera to collapse.

One of the problems arising from previous studies in this area is that the postulated caldera structures have received a variety of names and have been assigned to different ages with different limits, and neither the numbers of caldera events recognized in the area nor their position and areal extent are known precisely. This places limits on any geothermal exploration in the area since good geological knowledge is an essential prerequisite for any such survey. In this study, we concentrated on the area occupied by the geothermal fields of Borinquen and Las Pailas, on the southern and western slopes of the Rincón de la Vieja–Santa María volcanic complex, where two main caldera structures, Cañas Dulces and Guachipelin, were proposed by previous studies (Chiesa, 1991; Kempter, 1997; Zamora et al., 2004; Vogel et al., 2004; Deering et al., 2007). In light of the data presented herein, we now discuss whether or not the stratigraphy, structure, and volcanology of the area are compatible with the existence of one or more caldera structures, and, if so, we consider the structural limits and age of such volcanic depressions.

Stratigraphy of Caldera-Forming Products

One aspect on which previous studies coincide is that the Liberia Formation is the main stratigraphic unit outcropping in the area and could represent a caldera-forming eruption. In fact, numerous previous works (Kempter, 1997; Zamora et al., 2004; Deering et al., 2007) associated the Liberia Formation with the Guachipelin caldera but disagreed as to its position and age and whether this caldera is a single or a multiple collapse structure. As well, Kempter (1997) has proposed the existence of a previous caldera (Cañas Dulces), partially destroyed by the formation of the Guachipelin caldera, of which only the southern morphological border, defined by the Cañas Dulces domes, is now visible.

Our stratigraphic reconstruction, based on field work and, in particular, on the stratigraphic logging of the cores obtained from deep geothermal boreholes, clearly suggests that the Liberia Formation corresponds to a caldera-forming eruption. There are considerable differences in thickness of over 1000 m between the area close to the Borinquen geothermal field—coinciding with the Cañas Dulces caldera postulated by Kempter (1997)—and that outside it (Fig. 9). This caldera-forming unit rests directly on the precaldera basement corresponding to the Bagaces Group. Accordingly (and based upon the corresponding stratigraphic correlations and field mapping), we have a minimum bulk volume of ~40 km^3 for the extracaldera part of the Liberia Formation, which could be greater, since part of the deposits were emplaced into the sea, and some ash was lost into the atmosphere. The average intracaldera thickness of the Liberia Formation—which mostly corresponds to the Liberia ignimbrite—is 1350 m, as determined by boreholes PGB 01 and PGB 03 (Fig. 9). In order to correctly establish the intracaldera volume of the caldera-forming unit, it is first necessary to determine the caldera size by identifying its structural borders.

Structural Limits of the Caldera

Morphologically, the caldera responsible for the eruption of the Liberia Formation is located in the southwestern sector of the Rincón de la Vieja–Santa María volcanic axis. Its southern and southwestern boundaries are well defined by the products of the Bagaces Group and form arched walls and steep slopes that rise more than 100 m from their bases to a maximum altitude of 500 m above sea level (asl) in the south and 300 m asl in the southwest. Inside the morphological caldera—and partially defining an arcuate structure—stand the domes of the Cañas Dulces caldera (Fig. 2). The rest of the theoretical caldera border is probably hidden below the products of the Rincón de la Vieja and Santa María volcanoes. These morphological limits correspond to those proposed by Kempter (1997) for the Cañas Dulces caldera (even though he did not associate this caldera with the Liberia Formation). However, due to this morphological and structural (see following) correspondence, we propose here the name "Cañas Dulces" for the caldera identified in this study as the eruption source of the Liberia Formation.

The hypothetical Cañas Dulces caldera has a visible southwestern topographical border formed by precaldera rocks belonging to the Bagaces Group, which are identifiable as an arc-shaped band extending from the RL1 structure in the west to LL1 in the southeast of the Las Pailas geothermal field area (Fig. 10). This is the morphological limit that was first identified and used by Kempter (1997) to hypothesize the existence of this caldera. Nevertheless, it does not correspond to the structural limit of the caldera, which we believe corresponds to the lineation formed by the Cañas Dulces dacitic domes. Given the ages and stratigraphic relationships of these domes with the surrounding rocks, we suggest that they were emplaced immediately after the formation of the caldera through the same fault system that controlled the caldera collapse. The presence of postcaldera domes emplaced along the faults that control the caldera collapse is a common feature in calc-alkaline calderas worldwide (see Geyer and Marti, 2008).

The remaining Cañas Dulces caldera borders have never been identified, neither morphologically nor structurally. However, from the data presented here, we suggest that the north-

Geological Society of America Bulletin, published online on 23 June 2014 as doi:10.1130/B31012.1

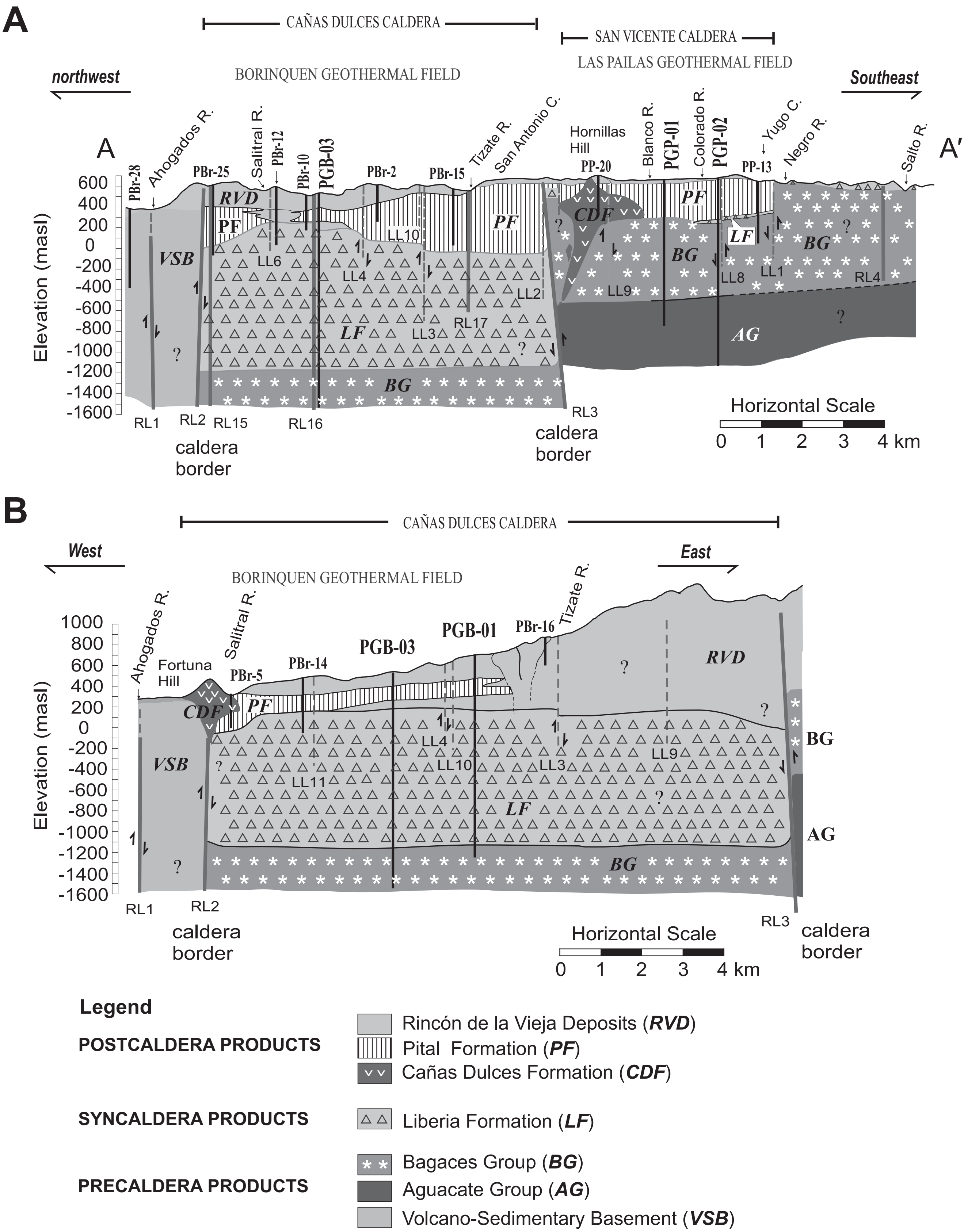

Figure 9. (A) Cross section from PBr 28 to Salto River and from PBr 25 to Liberia River. (B) Cross section from PBR 5 to PGB 01 (see Fig. 10 for location). RL—regional lineament; LL—local lineament.

Geological Society of America Bulletin, published online on 23 June 2014 as doi:10.1130/B31012.1

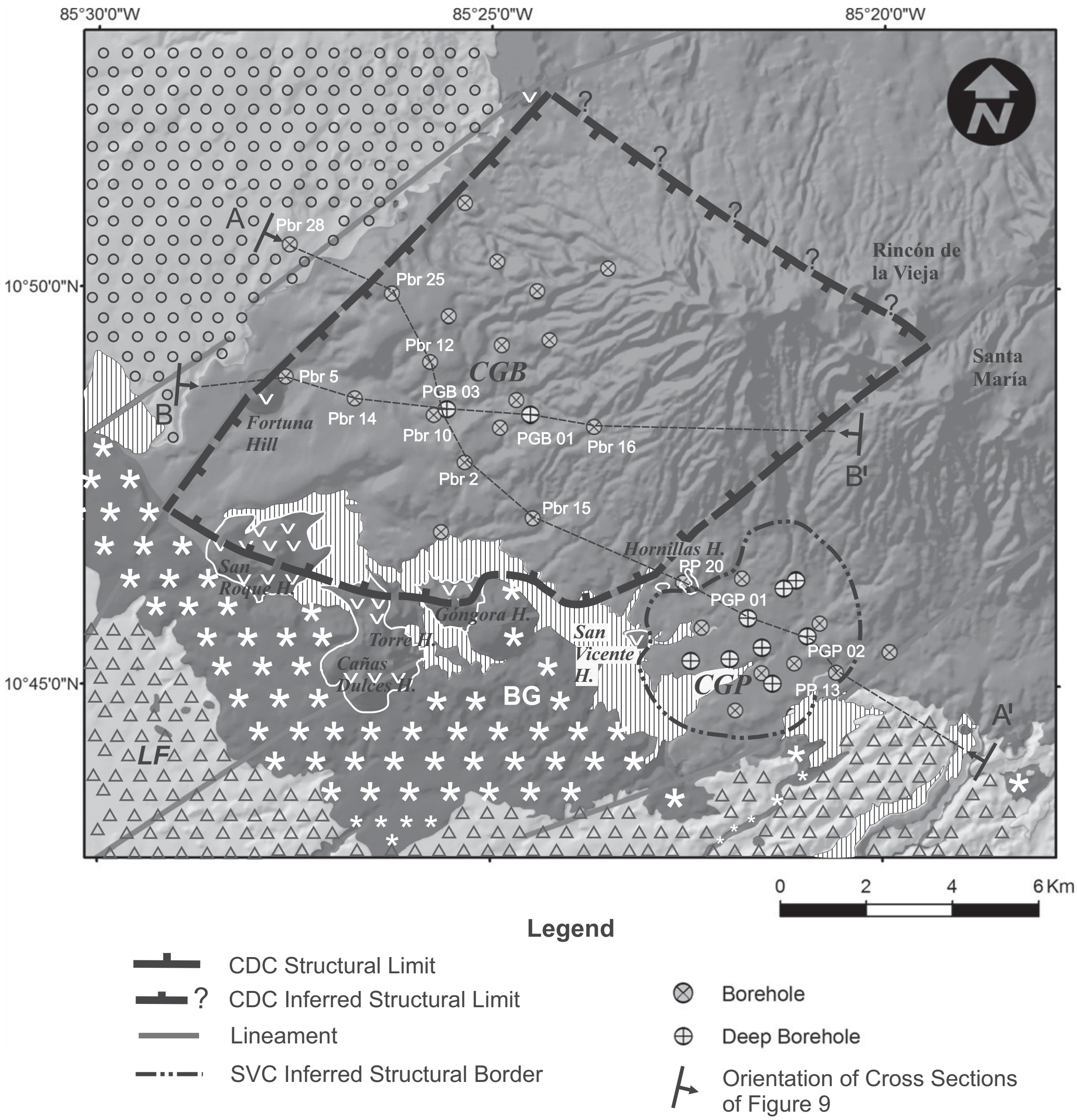

Figure 10. Inferred structural limits of the Cañas Dulces caldera (CDC; see text for more details). CGP—Las Pailas geothermal field; CGB—Borinquen geothermal field; LF—Liberia Formation; SVC—San Vicente caldera; BG—Bagaces Group.

western and southeastern structural limits are defined by lineaments RL2 and RL3, respectively, indicating that caldera subsidence was strongly controlled by preexisting fault systems. This is confirmed by the fact that the maximum thickness of the intracaldera succession (Liberia Formation) is constrained between these two limits. Moreover, the top of these successions deepens toward the RL2 and RL3 structures (Fig. 9), suggesting that these major tectonic lineaments acted as normal faults controlling the caldera collapse and the subsequent tectonic subsidence of the caldera depression. At the northwestern limit of the caldera, near the RL2 structure, borehole PBr 25 was the final borehole to include intracaldera rocks; despite being even deeper, borehole PBr 28 did not reach any intravolcanic rocks because it was drilled outside the limits of the caldera (Figs. 9A and 10).

The southeastern border of the Cañas Dulces caldera is marked by the San Vicente and Hornillas domes, which are located in an area influenced by the regional structure RL3 that cuts through the precaldera sequence and separates the volcanic edifices of Rincón de la Vieja and Santa María (Fig. 10). In this sector, there are two gravity minimums separated by the RL3 lineament; one corresponds to the southeastern border of the main gravity minimum, and the other corresponds to the San Vicente caldera (Molina, 2000). This small caldera originated during a later episode occurring adjacent to the Cañas Dulces caldera, as is indicated by the fact that here the Liberia Formation reaches a maximum thickness of 39 m (borehole PGP 02), similar to that of the extracaldera outcrops in this area (Fig. 9A).

The northeastern border of the Cañas Dulces caldera is buried below postcaldera deposits, which prevent the gravity minimum generated by the low density of the Liberia Formation from being expressed. However, it is plausible that this border could run from the northeastern end of the RL2 lineament near the outcropping dacitic-rhyolitic lava domes of Cañas Dulces (Fig. 10) to the RL3 structure crossing underneath the center of the Rincón de la Vieja volcano. The exact trace of the northern border of the caldera cannot be defined since today there is no clear morphological or structural expression on the surface. The only structural lineament identified in this area is LL5, which runs E-W and is defined by the alignment of the six craters of Rincón de la Vieja volcano and a landslide scar. It is possible that the easternmost sector of this lineament could have played some role as part of the northern caldera border; nevertheless, it is unlikely that the rest of the LL5 lineament played any part, as this would be incompatible with the presence of Cañas Dulces domes to the north of this lineament. However, the presence of these domes also prevents us from putting the caldera limit north of their location.

These conclusions indicate that the Cañas Dulces caldera had a strong structural control, resulting in a roughly rectangular shape of ~12 × 10 km with a minimum surface area of around 120 km^2 (Fig. 10). Therefore, assuming a thickness in the order of 1350 m for the intracaldera Liberia Formation, and an average difference in altitude of 200 m between the top of the Liberia Formation and the topmost precaldera unit rocks forming the structural border of the caldera (Fig. 9), we obtain a minimum vertical collapse of 1550 m. This figure multiplied by the area of the caldera gives a minimum volume of 186 km^3 for the caldera depression. The volume of the Liberia Formation can be estimated by multiplying the total intracaldera thickness by the area of the structural caldera, which gives 162 km^3. By adding to this value the extracaldera volume (40 km^3) calculated earlier, we obtain a total bulk volume of 202 km^3 for the Liberia Formation, which fits well with the estimated volume of the caldera depression, considering that these values correspond to bulk rock volumes.

Our data provide no evidence of the existence of a larger caldera in the area presently covered by the Rincón de la Vieja and Santa María volcanoes (Guachipelin caldera *in* Kempter, 1997; Zamora et al., 2004; Vogel et al., 2004; Deering et al., 2007), which would include our Cañas Dulces caldera and the smaller San Vicente caldera of Molina (2000), and so we propose that these two calderas are the only such structures persisting in the area hosting the Borinquen and Las Pailas geothermal fields, respectively. Any other collapse caldera that could be related to the formation of previous ignimbrite deposits forming part of the Santa Rosa Plateau must have been mostly obliterated by the formation of the Cañas Dulces and San Vicente caldera, and today no morphological or structural trait of their existence remains.

Formation of the Cañas Dulces Caldera

Figure 11 summarizes the volcanic evolution of the Cañas Dulces caldera. The volcano-tectonic evolution of the area in which the Cañas Dulces caldera developed began during the Eocene–Oligocene as a result of the geodynamics of the Caribbean plate, which were responsible for the formation of the main tectonic trends (e.g., RL1, RL2, RL3, and RL4) analyzed in this study. These regional structural features were then used to favor the ascent and accumulation of magma in shallower levels in the crust, giving rise to the formation during the Miocene of the inner volcanic arc. Its evolution to the present day has generated new faulting systems, including the NW-SE–oriented fault to which the RL9 lineament belongs.

The oldest volcanic rocks recorded in the study area are predominantly thick andesitic lava flow sequences belonging to the Aguacate Group, described from the base of the drilling operations in the geothermal field of Las Pailas.

At 8.75 ± 0.87 Ma, the first explosive episodes of this volcanism started and formed sequences of andesitic ignimbrites that crop out on the rim of the Cañas Dulces caldera. Subsequently, the oceanic crust began its transformation into continental crust, giving rise to an intense episode of silicic explosive volcanism responsible for the formation of the broad Santa Rosa ignimbritic plateau (Bagaces Group) during the Miocene–Quaternary, which could be related to pre–Cañas Dulces caldera centers that today show no clear morphological or structural expression of their existence. However, the dacitic Góngora Viejo dome, dated at 7.96 ± 0.53 Ma and located on a volcano-tectonic boundary corresponding to the structure RL3 on the southern border of the Cañas Dulces caldera (but without being related to it), is possible evidence for these pre–Cañas Dulces calderas. However, its age suggests that it may be contemporary with one of the oldest Santa Rosa Plateau ignimbrites (the Carbonal pyroclastic flow deposit, outside the study area) dated at 7.8 ± 0.16 Ma (Gillot et al., 1994). The stratovolcano Alcantaro, corresponding to the upper part of the Bagaces Group, was established in an area now occupied by the Cañas Dulces caldera (Fig. 11A). This volcanic complex was controlled from its outset by the fault systems RL1 in the west and RL3 in the center (Fig. 10).

At ca. 1.43 Ma, the caldera collapse episode that destroyed the Alcantaro volcano took place. This led to the eruption of large volumes of rhyolitic-dacitic magmas and the massive emptying of the associated magma chamber, mainly through preexisting faults (RL2 in the northwest and RL3 in the southeast), followed by the collapse of its roof and the formation of the Cañas Dulces caldera (Fig. 11B). The caldera-forming eruption started with a short Plinian phase that generated relatively thin Plinian fallout deposits and several intra-Plinian pyroclastic surges, which then rapidly developed into massive proportions, emplacing different flow units that formed the Liberia ignimbrite. This caldera collapse episode was followed shortly afterwards by the extrusion of the remaining magma in the form of a series of dacitic and rhyolitic domes (1.41 Ma, Cañas Dulces Formation) along the faults that controlled the caldera collapse (Fig. 11C). Postcaldera activity was followed by the deposition of a caldera-fill succession formed of pyroclastic and epiclastic deposits (Pital Formation), during which the San Vicente caldera originated adjacent to the Cañas Dulces caldera on the eastern flanks of the Alcantaro volcano, activity that was related to the activity of the RL3 tectonic system.

As has occurred in many other silicic calderas (Geyer and Martí, 2008), the formation of the Cañas Dulces caldera—and subsequently that of the San Vicente caldera—greatly affected the installation of a new shallow magmatic system that culminated in the construction of the Rincón de la Vieja–Santa María stratovolcanos and the appearance of active geothermal systems inside the caldera depressions (Fig. 11D).

CONCLUSIONS

Using field geology, remote sensing, stratigraphic logging of cores from exploratory and exploited geothermal wells, radiometric dating, and structural geophysical data, we have been able to identify and construct a comprehensive model of the origin and evolution of the Cañas Dulces caldera. This collapse caldera was formed ca. 1.43 Ma in the northwestern sector of the internal magmatic arc of Costa Rica as a result of the massive eruption of rhyolitic-dacitic magma that gave rise to the formation of the Liberia ignimbrite and associated deposits. The caldera collapse was mostly controlled by preexisting faults and generated a caldera depression of 186 km^3 in volume, which was mostly in-filled with syncaldera products. The formation of the caldera caused the destruction of the shallow magmatic system and allowed

Geological Society of America Bulletin, published online on 23 June 2014 as doi:10.1130/B31012.1

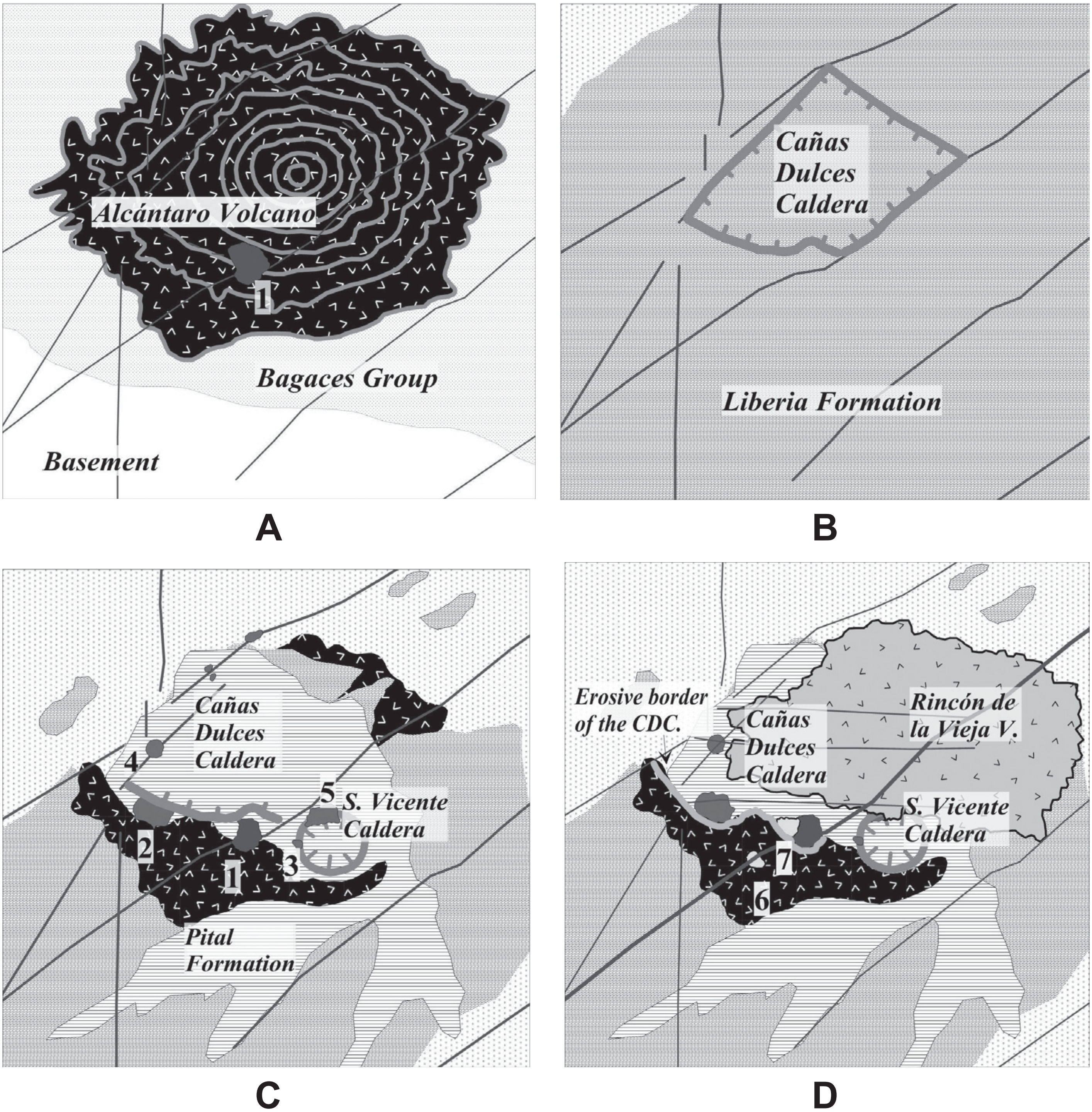

Figure 11. Schematic representation of the formation and evolution of the Cañas Dulces caldera (CDC). 1—Góngora Viejo Unit, 2—San Roque dome, 3—San Vicente dome, 4—Fortuna dome, 5—Hornillas dome, 6—Cañas Dulces dome, 7—Góngora Joven dome.

the intrusion of deeper magmas, which progressively formed a new shallow magmatic system inside the limits of the caldera. This new magmatic system was responsible for the construction of the Rincón de la Vieja–Santa María stratovolcanoes, which buried most of the caldera structure. The formation of the caldera and the installation of a new shallow magmatic system underneath have created very suitable conditions for a highly productive geothermal system inside the caldera. Its extent and dynamics are largely controlled by the structural limits of the caldera and the regional fault systems that favored caldera collapse. Therefore, understanding the caldera structure and its volcano-tectonic evolution constitutes the best guide for further exploration and exploitation of the geothermal resources of this area.

ACKNOWLEDGMENTS

We would like to wholeheartedly thank the Instituto Costarricense de Electricidad (ICE) for its support and help in undertaking this research and for giving us permission to publish the borehole and geophysical data. Martí and Aguirre were funded by Spanish Ministry of Science and Innovation (MICINN) grant CGL2010-22022-C02-02 and by Universidan Nacional Autonoma de México (UNAM) grant IN-112312. We thank Nancy Riggs and Luca Ferrari, editor and associated editor of *GSA Bulletin*, respectively, and two anonymous referees for their constructive reviews, which greatly improved the quality of this paper. The English text was revised and corrected by Michael Lockwood.

REFERENCES CITED

Astorga, A., Fernández, J.A., Barboza, G., Campos, L., Obando, J., Aguilar, A., and Obando, L.G., 1991, Cuencas sedimentarias de Costa Rica: Evolución geodinámica y potencial de hidrocarburos: Revista Geologica de América Central, v. 13, p. 25–59.

Bellon, H., and Tournon, J., 1978, Contributions de la géochronologie K/Ar á l'étude du magmatisme de Costa Rica, Amerique Centrale: Bulletin de la Société Géologique de France, v. 6, p. 955–959.

Carr, M., Chenser, C., and Gemmell, J., 1985, New analyses of lavas and bombs from Rincón de la Vieja volcano, Costa Rica: Bulletin of Volcanology, v. 15, p. 23–30.

Carr, M., Saginor, I., Alvarado, G.E., Bolge, L., Lindsay, F.N., Milidahis, K., Turrin, B.D., Feigenson, M.D., and Swisher, C.C., 2007, Element fluxes from the volcanic front of Nicaragua and Costa Rica: Geochemistry Geophysics Geosystems, v. 8, Q06001, doi:10.1029/2006GC001396.

Chiesa, S., 1991, El Flujo de pómez biotítica del Río Liberia, Guanacaste, Costa Rica: Revista Geologica de América Central, v. 13, p. 73–84.

Chiesa, S., Civelli, G., Gillot, P.Y., Mora, O., and Alvarado, G.E., 1992, Rocas piroclásticos asociadas con la formación de la caldera de Guayabo, cordillera de Guanacaste, Costa Rica: Revista Geologica de América Central, v. 14, p. 59–75.

Deering, C., Vogel, T.A., Patiño, L.C., and Alvarado, G.E., 2007, Origin of distinct silicic magma types from the Guachipelín caldera, NW Costa Rica: Evidence for magma mixing and protracted subvolcanic residence: Journal of Volcanology and Geothermal Research, v. 165, p. 103–126, doi:10.1016/j.jvolgeores.2007.05.004.

DeMets, C., 2001, A new estimate for present-day Cocos-Caribbean plate motion: Implications for slip along the Central American volcanic arc: Geophysical Research Letters, v. 28, p. 4043–4046, doi:10.1029/2001GL013518.

Denyer, P., and Alvarado, G.E., 2007, Mapa Geológico de Costa Rica: San José, Costa Rica, Librería Francesa, scale 1:400,000.

Denyer, P., Montero, W., and Alvarado, G., 2003, Atlas Tectónico de Costa Rica: Editorial Universidad de Costa Rica, San José, Costa Rica, 81 p.

Ferrari, L., Gardufio, V.H., Pasquaré, G., and Tibaldi, A., 1991, Geology of Los Azufres caldera, Mexico, and its relationships with regional tectonics: Journal of Volcanology and Geothermal Research, v. 47, p. 129–148, doi:10.1016/0377-0273(91)90105-9.

Geyer, A., and Marí, J., 2008, The new worldwide collapse caldera database (CCDB): A tool for studying and understanding caldera processes: Journal of Volcanology and Geothermal Research, v. 175, p. 334–354, doi:10.1016/j.jvolgeores.2008.03.017.

Gillot, P., Chiesa, S., and Alvarado, G.E., 1994, Chronostratigraphy of Upper Miocene–Quaternary volcanism in northern Costa Rica: Revista Geológica de América Central, v. 17, p. 45–53.

Gottsmann, J.H., and Martí, J., eds., 2008, Caldera Volcanism: Analysis, Modelling and Response, Developments in Volcanology 10: Amsterdam, Elsevier, 492 p.

Gudmundsson, A., 2011, Rock Fracturing in Geological Processes: Cambridge, UK, Cambridge University Press, 578 p.

Kempter, K.A., 1997, Geologic Evolution of the Rincón de la Vieja Volcano Complex, Northwestern Costa Rica [Ph.D. thesis]: Austin, Texas, University of Texas, 192 p.

Kussmaul, S., 2000, Estratigrafía de las rocas ígneas, *in* Denyer, P., and Kussmaul, S., eds., Geología de Costa Rica: San José, Costa Rica, Tecnológ, p. 63–86.

Laguna, J., 1984, Efectos de alteración hidrotermal y meteorización en vulcanitas del Grupo Aguacate, Costa Rica: Revista Geológica de América Central, v. 1, p. 1–17.

Lipman, P., 1997, Subsidence of ash-flow calderas: Relation to caldera size and magma-chamber geometry: Bulletin of Volcanology, v. 59, p. 198–218, doi:10.1007/s004450050186.

Melson, W., 1988, Major explosive eruption of Costa Rican volcanoes: Update for Costa Rican Volcanism Workshop, *in* Meeting held at Skyland, Shenandoah National Park, Virginia, 15–17 November 1988.

Meschede, M., and Frisch, W., 1998, A plate-tectonic model for the Mesozoic and early Cenozoic history of the Caribbean plate: Tectonophysics, v. 296, p. 269–291, doi:10.1016/S0040-1951(98)00157-7.

Mibei, G., 2012, Geology and hydrothermal alteration of Menegai geothermal field. Case study: Wells MW-04 and MW-05, *in* Geothermal Training in Iceland, Technical Report 2012, no. 21: Reykjavík, Iceland, United Nations University, p. 437–465, http://www.os.is/gogn/unu-gtp-report/UNU-GTP-2012-21.pdf.

Molina, F., 2000, Las Pailas geothermal area Rincón de la Vieja volcano, Costa Rica, *in* Geothermal Training in Iceland, Technical Report 2000, no. 13: Reykjavík, Iceland, United Nations University, p. 267–284, http://www.os.is/gogn/unu-gtp-report/UNU-GTP-2000-13.pdf.

Pindell, J., and Barrett, S.F., 1990, Geological evolution of the Caribbean region; a plate-tectonic perspective, *in* Dengo, G., and Case, J., eds., The Caribbean Region: Boulder, Colorado, Geological Society of America, Geology of North America, v. H, p. 405–432.

Pindell, J., and Kennan, L., 2009, Tectonic evolution of the Gulf of Mexico, Caribbean and northern South America in the mantle reference frame: An update, *in* James, K.H., Lorente, M.A., and Pindell, J.L., eds., The Origin and Evolution of the Caribbean Plate: Geological Society of London Special Publication 328, p. 1–55.

Price, N.J., and Cosgrove, J.W., 1990, Analysis of Geological Structures: Cambridge, UK, Cambridge University Press, 502 p.

Syracuse, E.M., Abers, G.A., Fischer, K., MacKenzie, L., Rychert, C., Protti, M., González, V., and Strauch, W., 2008, Seismic tomography and earthquake locations in the Nicaraguan and Costa Rican upper mantle: Geochemistry Geophysics Geosystems, v. 9, Q07S08, doi:10.1029/2008GC001963.

Tamanyu, S., and Wood, C.P., 2003, Characterization of geothermal systems in volcano-tectonic depressions: Japan and New Zealand: Bulletin of the Geological Survey of Japan, v. 54, p. 117–129.

Vogel, T., Patiño, L.C., Alvarado, G.E., and Gans, P.B., 2004, Silicic ignimbrites within the Costa Rican volcanic front: Evidence for the formation of continental crust: Earth and Planetary Science Letters, v. 226, p. 149–159, doi:10.1016/j.epsl.2004.07.013.

Wood, C.P., 1995, Calderas and geothermal systems in the Taupo volcanic zone, New Zealand, *in* Proceedings, World Geothermal Congress 19: Florence, Italy, p. 1331–1336.

Zamora, N., Méndez, J., Barahona, M., and Sjöbohm, L., 2004, Volcano estratigrafía asociada al campo de domos de Cañas Dulces, Guanacaste, Costa Rica: Revista Geológica de América Central, v. 30, p. 41–58.

Science Editor: Nancy Riggs
Associate Editor: Luca Ferrari

Manuscript Received 14 October 2013
Revised Manuscript Received 10 April 2014
Manuscript Accepted 7 May 2014

Printed in the USA

Anexo

B

The Borinquen geothermal system (Cañas Dulces caldera, Costa Rica)

Publicado en:

Geothermics

Autores del artículo:

Fernando Molina[a]

Joan Martí[b]

a) Área de Geociencias, Centro de Servicios Recursos Geotérmicos, Instituto Costarricense de Electricidad, Guanacaste, Costa Rica.

b) Institute of Earth Sciences Jaume Almera, (CSIC), Lluis Sole Sabaris, s/n 08028 Barcelona, Spain.

Molina, F., y Martí, J. (2016) The Borinquen geothermal system (Cañas Dulces caldera, Costa Rica). *Geothermics,* 64, pp. 410-425.

Geothermics 64 (2016) 410–425

Contents lists available at ScienceDirect

Geothermics

journal homepage: www.elsevier.com/locate/geothermics

The Borinquen geothermal system (Cañas Dulces caldera, Costa Rica)

F. Molina[a], J. Martí[b,*]

[a] Área de Geociencias, Centro de Servicios Recursos Geotérmicos, Instituto Costarricense de Electricidad, Guanacaste, Costa Rica
[b] Institute of Earth Sciences Jaume Almera, CSIC, Lluis Sole Sabaris, s/n, 08028 Barcelona, Spain

ARTICLE INFO

Article history:
Received 13 April 2016
Received in revised form 2 July 2016
Accepted 6 July 2016

Keywords:
Geothermal
Borinquen
Costa Rica
Caldera structure
Post-caldera volcanism
Exploration

ABSTRACT

The geotectonic location of Costa Rica has allowed the development of an active volcanic arc, geological context associated with hydrothermal systems with geothermal potential. In the northwest of the country, on the Pacific slope of the Rincon de la Vieja volcano, inside the Cañas Dulces caldera, the presence of thermal manifestations motivated the development of geoscientific studies that culminated with the drilling of 4 geothermal exploration wells to depths of 2078–2594 m, as part of the research that seeks to corroborate the existence of a commercially geothermal reservoir. A date has explored an area of 31 km^2 known as Borinquen where information on lithostratigraphy, mineralogy, electric resistivity and thermal gradients, as well as on the geochemical and isotopic composition of the fluids derived from the meteoric water, surface hydrothermal manifestation and exploration wells, was obtained. The distribution of the secondary mineral assemblages observed in the exploration wells suggests an increase in temperature with depth, which is confirmed by the distribution of the thermal gradient. The geoelectric structure hints at the existence of a cap rock and a geothermal reservoir, and the geochemistry and isotopic composition of the samples obtained from the exploration wells reveal the existence of neutral sodium chloride fluids with high enthalpy. This suggests exploitation could be economically viable, particularly in light of comparisons with similar reservoirs already being exploited in the neighbouring calderas of San Vicente and Guayabo. Taking into account all the available information, we provide a conceptual model of the Borinquen geothermal area that explains the main elements of its high enthalpy geothermal system – heat source, distribution of the thermal anomaly, recharge zone, reservoir, cap rock, main flow paths and flow directions. This will be useful as a guide for the exploration and future development and exploitation of this geothermal resource.

1. Introduction

Subduction occurs off the Pacific coast of Costa Rica as the Cocos plate slips beneath the Caribbean plate, is the origin of the notable tectonic and volcanic activity that characterises this region, and the formation of an internal magmatic arc that extends parallel to the Middle America Trench (Fig. 1). This geological environment provides Costa Rica with a great geothermal potential. Magma in multiple dykes and plutonic intrusions is the source of the necessary heat, while the rocks have a high fracture density – related to the tectonic activity (Curewitz and Karson, 1997) and decompression cooling (Norton, 1984) – and are ideal for storing the fluids that constitute the main energy transport mechanism. These fluids mainly may be meteoric water (Giggenbach, 1992; Curewitz and Karson, 1997), sea-water (Mottl, 1983), magmatic water (Giggenbach, 1992) or mixtures thereof.

Geothermal explorations undertaken by the Costa Rican Electricity Institute (ICE) have detected several areas with geothermal potential, one of the most important of which is located on the Pacific side of the Rincón de la Vieja volcano (Fig. 1), inside the Cañas Dulces caldera (Molina et al., 2014). It is well known that collapse calderas offer ideal sites for the development of internal geothermal reservoirs (see Gottsmann and Martí, 2008, and references therein). In the Cañas Dulces caldera and surrounding areas the existence of important thermal anomalies is revealed by the presence of abundant fumaroles, silicified rocks, soils and thermal springs, mainly in the sectors of Las Pailas and Borinquen. Since 2011, the geothermal resources of Las Pailas have been harnessed by a 35-MWe plant and drilling is currently being carried out as a prelude to the installation of a second, 55-MWe unit.

Exploration in the Borinquen sector, which included several geological, geophysical and geochemical studies and the drilling of four exploration wells to a depth of nearly 2500 m, got underway in 1974 and has continued intermittently ever since. To date, results provide evidence of a hydrothermal system related to the installation of magmatic intrusions during the volcanic evolution of the

* Corresponding author.
E-mail address: joan.marti@ictja.csic.es (J. Martí).

http://dx.doi.org/10.1016/j.geothermics.2016.07.001
0375-6505/

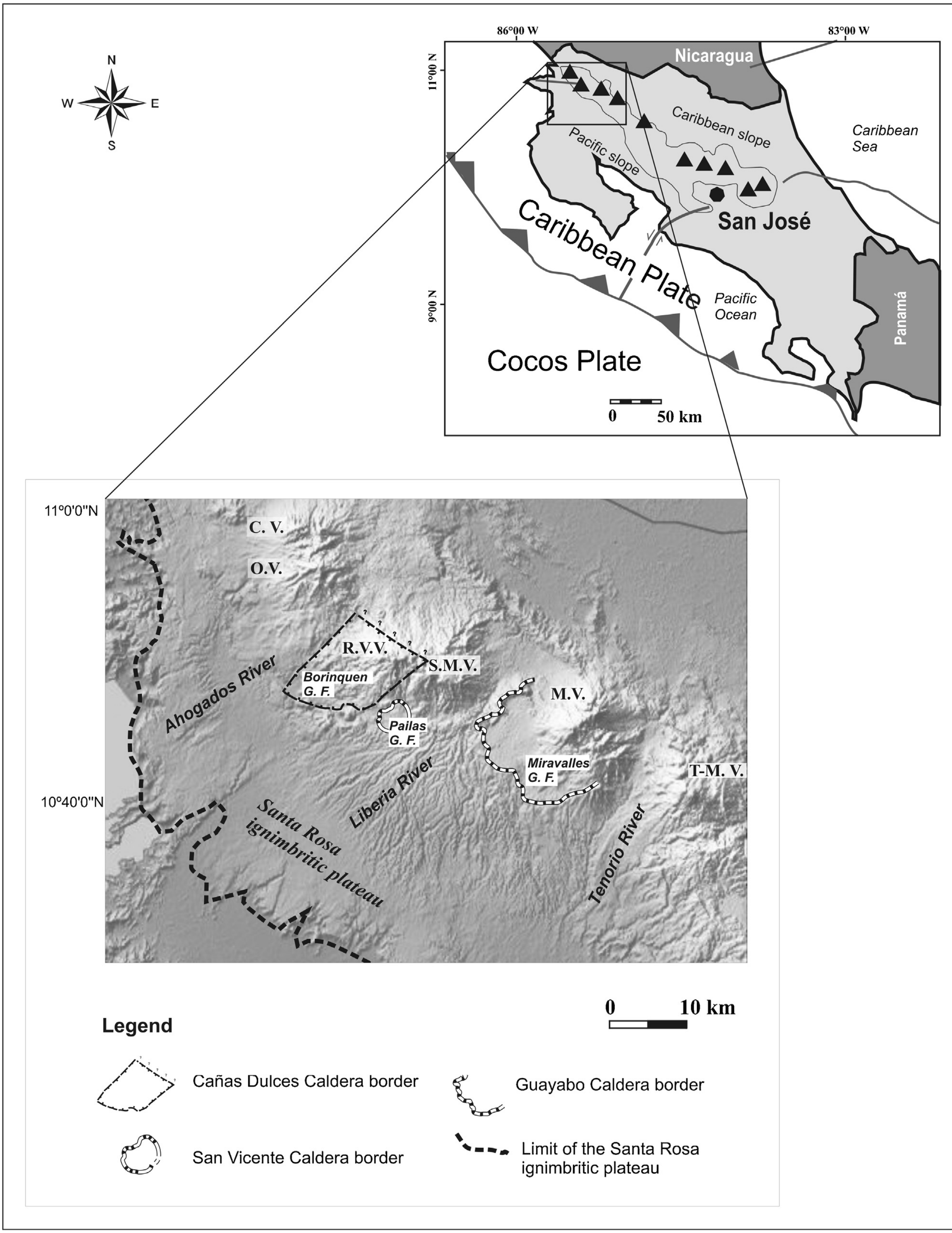

Fig. 1. Volcano-tectonic setting of Costa Rica showing the Cocos and Caribbean plates, the Mesoamerican trench, the internal magmatic arc and the location of the study area with the most important volcanic feature at the NW of Costa Rica. Nomenclature: C.V.—Cacao Volcano, O.V.—Orosí Volcano, R.V.V.—Rincón de la Vieja Volcano, S.M.V.—Santa María Volcano, M.V.—Miravalles Volcano, T.M.V.—Tenorio-Montezuma Volcano, Borinquen G.F.—Borinquen Geothermal Field, Pailas G.F.—Pailas Geothermal Field and Miravalles G.F.—Miravalles Geothermal Field.

area and the presence of a high enthalpy, commercially exploitable geothermal resource.

As a guide for further prospecting and potential exploitation, the following represents a conceptual model of the Borinquen geothermal system. First, we present and analyse existing geological, geochemical and geophysical information in an attempt to confirm the existence of the main elements of a geothermal system located no deeper then 3 km below the ground surface and at a temperature of at least 220 °C. We also define the secondary mineralogical associations and interpret them in terms of the conditions prevailing when these minerals were precipitated, and examine the evolution of the system. As well, we determine the geoelectric structure of the medium, the distribution of the thermal gradient, the geological structure and the main hydrogeological elements responsible for the circulation of hot fluids. Finally, we analyse the chemical and isotopic composition of these fluids and define their origin and thermodynamic evolution as a means of clarifying the hydrological and hydrogeological processes that take place in this hydrothermal system.

2. Geological setting

The internal magmatic arc of Costa Rica (Fig. 1) has developed on the oceanic crust of the Caribbean plate and runs parallel to the Middle America Trench in a southeast-northwest direction. The most important feature in its northwestern sector is the Guanacaste volcanic range consisting of four andesitic central edifices (Orosí-Cacao, Rincón de la Vieja-Santa María, Miravalles and Tenorio-Montezuma). Rising to a maximum height of 2028 m a.s.l. (Miravalles), this cordillera separates the Caribbean and Pacific watersheds. Before the construction of this chain of andesitic stratovolcanoes, intense episodes of explosive silicic volcanism, some associated with caldera collapse events, generated what Chiesa et al. (1992) refer to as the 'Santa Rosa Plateau ignimbrite'. One of these caldera structures corresponds to the Cañas Dulces Caldera, which covers an area of 120 km^2 and hosts the Rincón de la Vieja-Santa María active volcanic complex.

The Cañas Dulces caldera (CDC) has recently been studied by Molina et al. (2014) who,based on a revision of extensive deep boreholes and geophysical data obtained by the Instituto Costarricense de Electricidad (ICE) since 1970, combined with new geological work and radiometric dating, describe its stratigraphy, structure, and volcanic evolution. According to Molina et al. (2014) CDC resulted from the massive eruption 1.43 ± 0.09 Ma ago of about 200 km3 of rhyolitic magma that was largely responsible for the formation of the Liberia ignimbrite. The caldera was formed under strong structural control dominated by two parallel NE-SW regional faults and was followed by the construction of the Rincón de la Vieja-Santa María volcanic complex on one of the caldera's structural borders. The formation of this caldera and of a new shallow magmatic system facilitated the installation of the highly productive geothermal system inside the caldera, which the main subject of this study.

Evidence of the volcanic activity that has continued inside this caldera up to the present day is the construction of the active Rincón de la Vieja volcano (1895 m a.s.l.). The stratigraphy of the interior of the CDC has been established by Molina et al. (2014) from a lithostratigraphic analysis of cores and cuttings from 27 gradient wells drilled to depths of 91–670 m and four deep (2078–2594 m) geothermal boreholes. This stratigraphy is composed (from base to top) of the following units (Fig. 2b):

The Bagaces group, consisting of sequences of andesitic lavas, crystal tuffs and lithic tuffs, with a predominance of explosive products. In PGB 01 (Fig. 2a) it first occurs at a depth of −1150 m a.s.l. and reaches a maximum thickness of 749 m (without reaching the base). Its age ranges from 8.75 to 1.43 Ma. These rocks are very permeable and a total loss of drilling fluid often occurs (i.e. when the drilling system loses fluid at a flow rate of 50 L/s).

The Liberia Formation is mainly constituted of massive pyroclastic flow deposits, dacitic to rhyolitic in composition, characterised by corroded quartz and biotite phenocrysts. It usually occurs below 250 m a.s.l. and has a maximum thickness of 1692 m (PGB 02, Fig. 2b) inside the caldera. According to Molina et al. (2014), this formation corresponds to the products of the eruption that generated the CDC caldera about 1.43 Ma ago.

The Pital Formation includes dacitic pyroclastic sequences interbedded with minor epiclastic, lacustrine deposits and andesitic lavas, which constitute the post-caldera infill of the CDC. It was deposited 1.43–0.8 Ma ago, has a maximum thickness of 445 m (PGB 05, Fig. 2b), and always appears below −550 m.

The uppermost stratigraphic unit corresponds to the deposits from the Rincón de la Vieja volcano, which mainly consist of andesitic lava flows with subordinated pyroclastic deposits ranging in age from 1.14 ± 0.03 Ma ago (Carr et al., 2007) to the present. They outcrop at the surface with a maximum thickness of 450 m (PGB 05, Fig. 2b).

The intra-caldera stratigraphic correlations established by wells and boreholes show displacements at the top of the Liberia Formation of about 73 m (between PGB 02 and PGB 03) 300 m (between PGB 02 and PGB 05), thereby providing evidence of two structural features located on the Gata creek (EG1) and Salitral River (EG2) (Fig. 2a and b).

3. Methodology

This study was centred on the western sector of the CDC and focused on four main types of analysis: (1) secondary mineralogy, in order to establish a zonation pattern in the mineralogy of alteration with depth; (2) geophysical data aimed at reconstructing the geoelectric structure of the medium; (3) geothermal gradients used to determine the spatial distribution on the surface, the depth of the heat anomaly and the preferential paths of the hot fluids; and (4) geochemistry and the isotopic composition of meteoric and geothermal water to elucidate hydrological and hydrogeological processes.

During the drilling of the geothermal wells, cuttings collected every 3 m were analysed using a binocular stereoscope; additionally, thin sections were made every 9 m and studied with a polarised microscope to describe, identify and quantify secondary minerals. X-ray diffraction analysis was also performed every 50 m to identify phyllosilicates (used as geothermometers). Similar processes were applied to the rock cores extracted, particularly, from permeable zones. This was carried out to corroborate lithostratigraphic units, define mineralogical associations correlated with the temperature, and establish the various alteration zones of the geothermal field.

Using the apparent resistivity data obtained from Magnetotelluric (MT) and Time Domain Electromagnetic (TDEM) surveys conducted by the ICE, a three-dimensional inverse model of resistivity was created (Honda, 2012, written communication) and used to generate maps relating resistivity depth to the mineralogy of alteration. This enabled us to explain the geoelectric structure of the geothermal system and to locate the cap rock layer, the potential reservoir and the geoelectric lineaments that could be linked to the movement of the geothermal fluids.

To date, a total of 27 thermal gradient wells have been drilled with continuous core recovery, which have been used in stratigraphic correlations, the study of alteration mineralogy and to obtain temperature profiles. However, to ensure that the data was reliable, only profiles with depths of 300 m or more were selected, given that the first meter of the thermal profiles are affected by

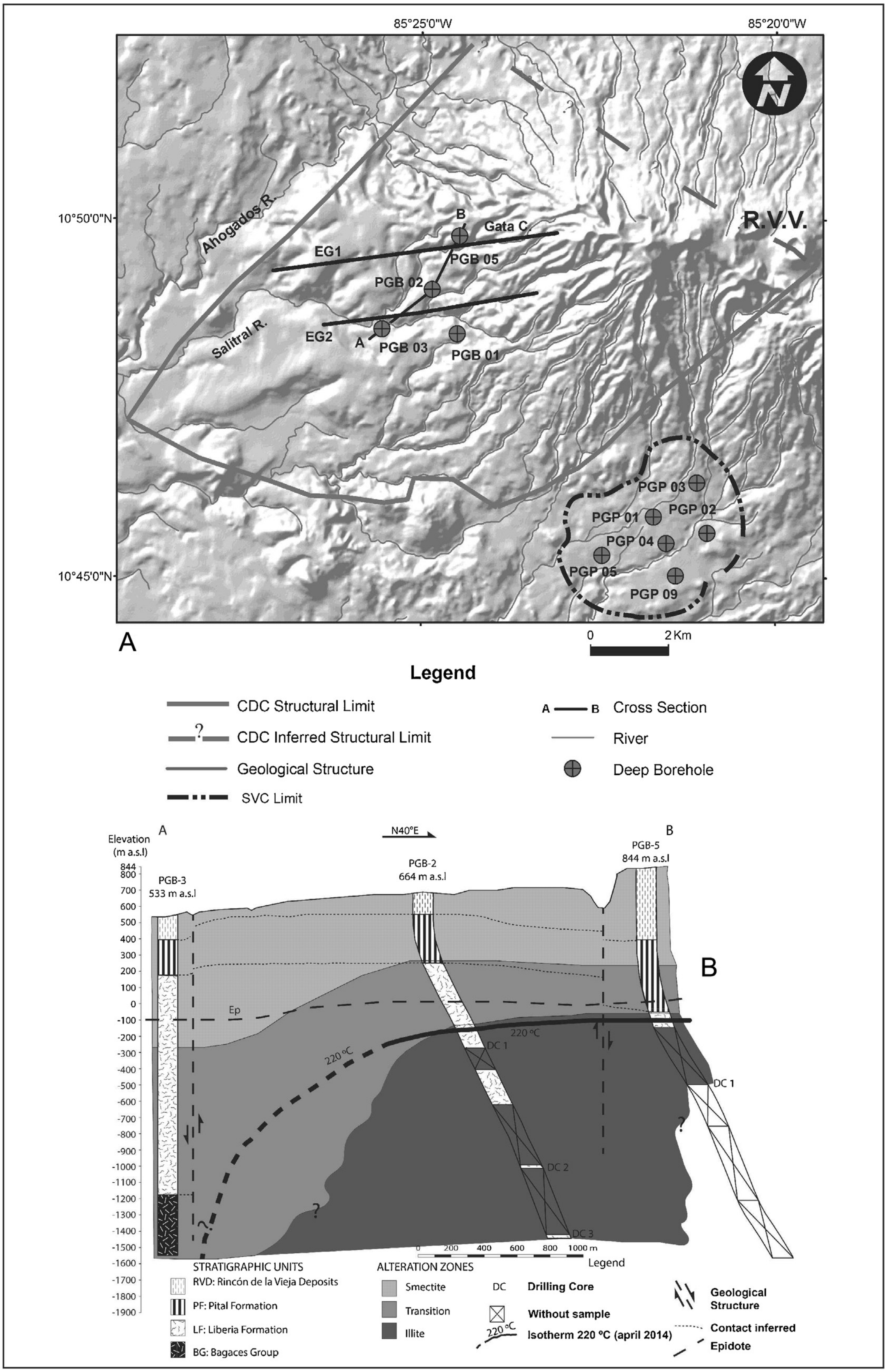

Fig. 2. (a) Cañas Dulces caldera with the distribution of the deep wells, geological structures and profile lines. (b) Profile between wells PGB-03, PGB-02 and PGB-05 showing the distribution of the mineralogical alteration zones with depths, the 220 °C isotherm and the isoline of epidote occurrence.

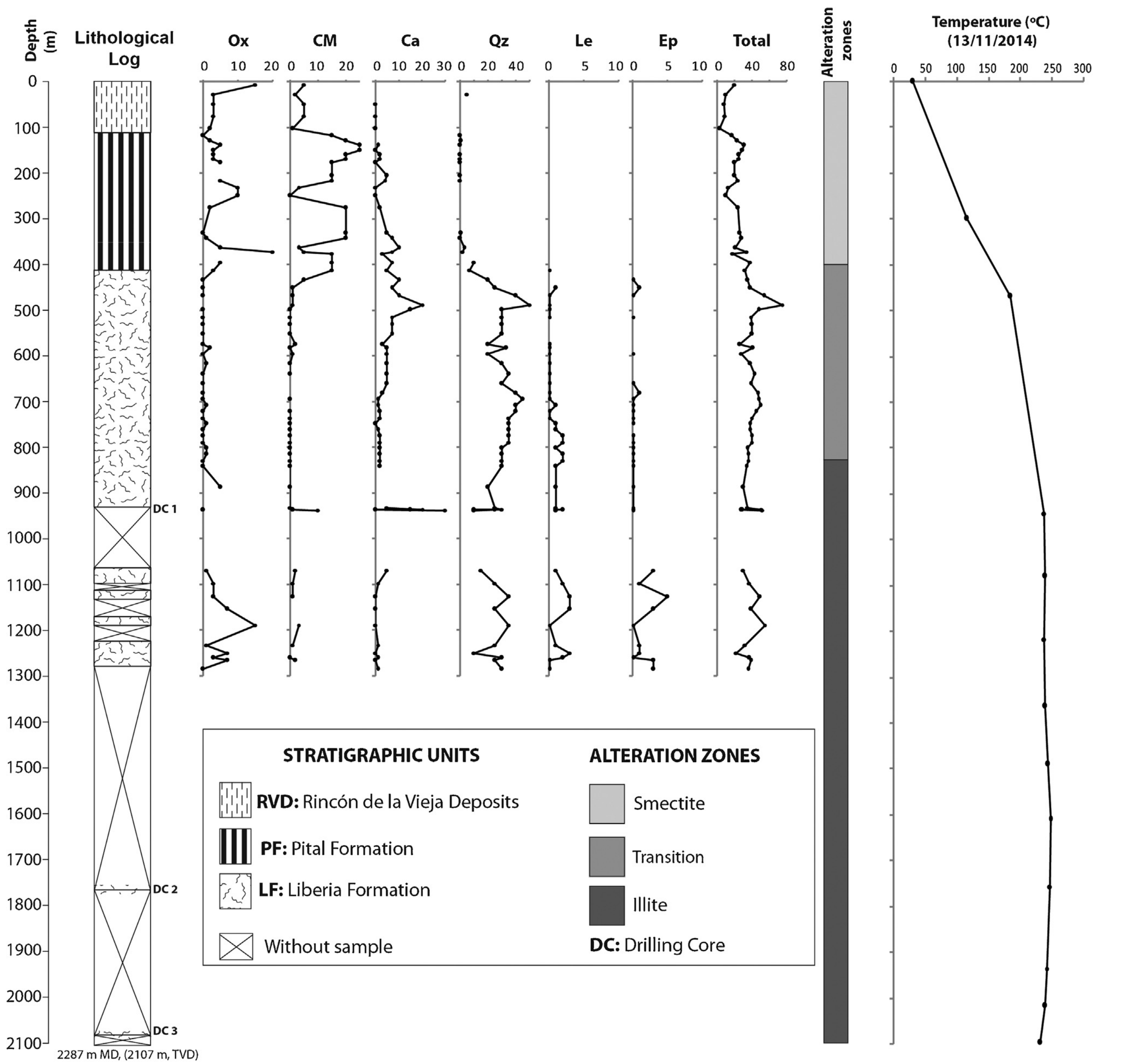

Fig. 3. Lithological column of geothermal well Borinquen 2 (PGB-2), showing the distribution of the main alteration minerals, the alteration zones and the static temperature profile.

the water table, which creates uncertainty when estimating the thermal gradient. Even wells with depths over 300 m were discarded from the analysis if disturbance due to the presence of hot or cold lateral aquifers occurred. With the information obtained from 17 selected profiles (see Fig. 7 for location), we calculated the rate of temperature change with depth, which we then interpolated to obtain equal geothermal gradient curves and a model of the distribution of the thermal anomaly over an area of 31 km^2.

The most consistent data matching the samples taken during the dry season on both sides of Rincón de la Vieja volcano (Pacific and Caribbean) were selected for a fluid geochemistry study. Sixteen samples from hydrothermal manifestations and four from the Borinquen geothermal wells were analysed and the results plotted onto a Piper ternary diagram. In addition, the Cl/B ratio of mature waters was compared as a further criteria for establishing the parental relationship of fluids. Likewise, in order to determine the origin of the geothermal fluids, the stable isotopic compositions (δ18 O and δD) of the meteoric springs and hydrothermal samples obtained from the discharge of geothermal wells from Pailas and Borinquen were also analysed.

4. Mineralogy of alteration

Mineralogical associations produced by hydrothermal alteration of the host rock are the result of physical-chemical changes in primary minerals and rock components provoked by a reaction with hydrothermal fluids trying to restore chemical and thermal equilibrium. Therefore, they provide invaluable information regarding the nature of the hydrothermal fluids and the thermodynamic conditions of mineral reactions. However, the degree and intensity of hydrothermal alteration will vary due to factors whose importance will fluctuate from one site to another in accordance with the geological setting. Browne (1978) identified six main factors: temperature, pressure, rock type, permeability, fluid composition and duration of the activity. In this context, temperature is a catalyst for chemical reactions and, according to Arnórsson (2000), for every 10 °C increase in temperature, the reaction ratio will rise 2–3 times; this means that in the event of an increase of 100 °C, common in high enthalpy geothermal environments, the increase in the reaction ratio will be between 2^{10} and 3^{10} (1024–59,049) times. Moreover, the permeability permits the movement of fluids and, depending on their origin, may generate an increase in the surface of exposure. Fluid composition regulates anion and cation exchange between the aqueous solution and the host rock, in which the pH is crucial. Therefore, the interpretation of mineralogical associations provides information on the degree and type of hydrothermal alteration, temperature, permeability, and the reducing or oxidising nature of the system during the precipitation of secondary minerals. This information is necessary for determining the thermodynamic conditions of the hydrothermal system and, above all, of the cap rock and geothermal reservoir.

A variety of secondary minerals are generated in active hydrothermal systems; however, alone, they are not very useful for determining the temperature and permeability of the system. Therefore, mineralogical associations that provide information on conditions in the system must be specifically selected. In the geothermal wells in Borinquen, calcite and quartz are both widely distributed and are stable over a wide temperature range. They are not good geothermometers but, because they tend to deposit more regularly in open areas of mineralization and in boiling areas, or in areas with pressure changes, they are useful for locating and identifying the limits of the cap rock above permeable zones. One of the minerals with temperature ranges and commonly used as a geothermometer in hydrothermal systems is epidote (Browne, 1978, 1993; Reyes, 2000). Reyes (2000) states that it occurs incipiently from 180 °C, but then changes its morphology and abundance as temperatures rise to over 280 °C. However, wherever it occurs continuously and is well crystallised in our geological environment, it is associated with temperatures of 220 °C or above, and behaves similarly to leucoxene.

On the other hand, secondary minerals sometimes reflect diagenetic conditions that differ from those related to the hydrothermalism associated with the geothermal reservoir. Therefore, we also analysed minerals more susceptible to thermal changes such as phyllosilicates (determined by X-ray diffractometry), which modify their lattice structure to equilibrate with the system temperature. According to Browne (1978), montmorillonite occurs at approximately 140 °C, interlayer illite/smectite at 140–about 210 °C, and illite at even higher temperatures. In geothermal fields in New Zealand interlayering of montmorillonite and illite occurs above 100 °C and reaches up to 200 °C (Browne, 1993). In the Miravalles Geothermal Field (Costa Rica), the temperature range of the montmorillonite/illite interlayer lies in the range 150–220 °C (Sánchez and Vallejos, 2000).

Currently, the Borinquen geothermal field only has four geothermal wells, which rules out any well-supported analysis relating the temperature and illite percentage. However, the available data (diffractometric analysis and profiles of static temperature) is similar in behaviour to data from the neighbouring Miravalles geothermal field (Sánchez and Vallejos, 2000), probably due to the common features of their geological environments. This information has allowed us to establish an initial relationship between zones of hydrothermal alteration with temperature (Table 1). These include:

4.1. Smectite zone

Characterised by high intensity alteration that sometimes reaches 100%, the smectite zone typically has low temperature minerals, mainly iron oxides and clay minerals. X-ray analysis has identified the clay minerals as members of the smectite group, which, as depth increases, appear together with chlorite. The percentages of quartz (Qz) and calcite (Ca) are usually low, and high temperature mineralogy is absent (Fig. 3). This zone has thicknesses ranging from 350 m in PGB 01 to 801 m in PGB 03, and correlates with a temperature less than or equal to 150 °C (Table 1, Figs. 2b and 3).

4.2. Transition zone

The alteration intensity is high in the uppermost part of this zone, but tends to decrease with depth as iron oxides and clay minerals decrease in prevalence. This zone is defined by the presence in variable proportions of interstratified layers of illite/smectite, smaller amounts of illite/smectite with chlorite, and, sporadically, corrensite. In general terms, the percentages of illite gradually increase and occasionally reach 100% in narrow and isolated parts of the system, a reflection of unstable thermal conditions caused by lateral flows in specific areas that do not give rise to a commercial high enthalpy reservoir. Quartz and calcite are present throughout this zone and here reach their highest percentages. Leucoxene (Le) and epidote (Ep) are present in incipient form but only in low percentages (Fig. 3). This area exhibits thicknesses ranging from 296 m in PGB 05 to 1282 m in the PGB 03 (Table 1, Figs. 2b and 3) and is correlated with temperatures of over 150 °C but less than 220 °C.

4.3. Illite zone

Interstratified layers of illite/smectite, along with chlorite, appear at the top of this layer. Illite percentages range from 95 to 100% and epidote and leucoxene occur more constantly than in the previous zone. The percentage of clay minerals and oxides decreases in comparison with other zones. With depth, phyllosilicates evolve into illite and chlorite (a mineral that tends to fix cations in the crystal lattice), the latter eventually dominating, and the abundance and size of crystals of epidote and leucoxene increase (Fig. 3). This zone exhibits a thickness of 1278 m in the PGB-02, although none of the boreholes reached its base. In the south-west of the explored area (PGB 03), this zone is absent (Table 1, Figs. 2B and 3). This geothermometer mineral is related to temperatures of ≥220 °C and in well PGB 01 was measured at a maximum temperature of 277 °C.

The order of occurrence of the alteration zones follows a normal pattern of increasing temperature with depth, where alteration minerals mark reservoir conditions of temperature starting from the illite zone at depths ranging from −60 to −165 m. The isoline indicating the permanent existence of epidote, related in this geological setting to temperatures of about 220 °C, appears slightly above the illite zones in the northeast and the 220 °C isotherm (Fig. 2b), thereby indicating a thermodynamic equilibrium between the rock and the geothermal fluid. By contrast, towards the southwest (PGB 03), epidote appears at a similar depth but the isotherm and the illite zone deepen, thereby demonstrating that this sector has cooled over time and is further from the current heat source; the epidote thus is a relic of higher temperatures.

5. Magnetotellurics

Magnetotelluric (MT) surveys use natural variations in electric and magnetic fields to explore variations in resistivity in the Earth's crust (Tikhonov, 1950). This method has been successfully used in high enthalpy volcanic geothermal fields such as Nesjavellir in Iceland (Arnason et al., 2000) and Ngatamariki in the Taupo Volcanic Zone in New Zealand (Urzúa, 2008). As has been observed in Iceland, a typical resistivity pattern consists of a layer of low resistivity on the outer margins of the reservoir, underlain by a

Table 1
Distribution and thickness of the alteration zones per well and relationship to temperature. Nomenclature: Thick.—thickness in meters, Temperature in degrees Celsius, NP—not present.

Zone	Well								Temperature (°C)
	01		02		03		05		
	Depth (m)	Thick. (m)	Depth (m)	Thick. (m)	Depth (m)	Thick. (m)	Depth (m)	Thick. (m)	
Smectite	0–350	350	0–412	412	0–801	801	0–608	608	T ≤ 150
Transition	350–807	457	412–829	417	801–2083	1282	608–904	296	150 < T < 220
Illite	807–2065	1258	829–2107	1278	NP		904–1342	438	T ≥ 220

core of higher resistivity in its inner part (Arnason et al., 2000). This geoelectric structure resembles that seen in the geothermal fields of Costa Rica, which reflects the products of rock alteration and the presence of hydrothermal fluids, and helps determine the dimensions of the geothermal reservoir. Moreover, one of the main advantages of MT is the ability to define geoelectrical anomalies in depth, that might be associated with geological structures affecting the geothermal reservoir, which is of paramount importance in the exploration and development of geothermal fields. Based on the 3D-inversion model of resistivity (Honda, 2012, written communication) and using the apparent resistivity in the explored area, we identified four layers that correlate with the mineralogy of alteration: (1) a shallow layer with resistivities between 4 and 75 ohm-m; (2) a layer with values below 10 ohm-m; (3) a deep layer with intermediate values between 10 and 40 ohm-m; and (4) the deepest layer with values above 40 ohm-m.

The wide range of resistivity values shown by the surface layer is due to the existence of fresh rock and little temperature alteration, with different degrees of compaction and moisture content. This layer extends for 100 m. The second layer starts to appear very clearly at a depth of −150 m (500 m map, Fig. 4) and extends to a depth of −800 m, and reveals the abundance of smectite. These two layers form the largest part of the cap rock in this geothermal system.

The area with intermediate resistivities (10–40 ohm-m) is heterogeneous with respect to depth and extends from −900 m to −1100 m. As this area deepens, resistivity values move toward the peripheral areas, while in the central part resistivity values are over 40 ohm-m (1350 m map, Fig. 4). This area of higher resistivity is related to the hottest parts of the system in which the rock matrix is much less conductive than the fluid saturation due to the presence of low conductivity alteration products such as illite, chlorite, illite/smectite and epidote.

The distribution of the resistivity also distinguishes eight resistive lineaments (RL) that might be associated with fractured zones along faults, which act as pathways for hydrothermal fluids, or zones with permeability changes that form hydrogeological barriers (Fig. 4). The resistive lineaments RL1 (NE-SW), RL2 and RL3 (NW-SE) are marked by abrupt changes in the resistive gradient, lineaments RL4 and LR5 (ENE-WSW) have less pronounced gradients, and lineaments LR6, LR 7 (E-W) and LR8 (NE-SW) are marked by inflections in the isoresistivity curves.

6. Thermal anomaly

Good evidence for the existence of a hydrothermal system is the presence of thermal anomalies since the greater the amount of natural heat at the bottom of the system, the greater the upward fluid flow and the greater the heat download to the surface that gives rise to thermal activity.

Thermal manifestations in the study area include fumaroles, silicified rocks, hot soils and thermal springs. The temperatures of these anomalies range from ambient temperature to the boiling point of water (24–97 °C) and their pH vary from acidic to neutral (2.4–7.57), which in some cases can lead to the generation of sinter and travertine deposits. The fumaroles are located at different points in the study area at 560–900 m a.s.l. (Fig. 5), for example around the headwaters of the Colorado River (thermal manifestations of Las Pailas, MLP), at the source of the Zanja Tapada creek (thermal manifestations of Las Hornillas, MLH), and in the Salitral River and Gata creek (thermal manifestations of Borinquen, MB). They are characterised by constant gas emissions at temperatures of 97 °C and argillic alteration around their vents. Sometimes, gas emissions is not constant but soils and rocks register temperatures up to 88 °C, with intense clay alteration and the presence of silica and sulphur. In the MLP there are three lagoons with diameters of 35–90 m and temperatures of 86 °C, which correspond to small craters produced by phreatic explosions. Hot springs occur throughout the area at temperatures of 31–91 °C and usually consist of surface water heated by steam that has little residence time. These thermal manifestations provide useful hydrogeological and structural observations. Fossil manifestations are found farther from the volcanic edifice and help delimit the boundaries of the hydrothermal system.

However, as the fluids flow away from the heat source and the residence time increases, thermodynamic and chemical processes induce a fluid-rock equilibrium and generate self-sealing. This forces the fluid temperature to decrease, the pH to increase and the composition to become more sodium-chlorided, while the system tends to a chemical equilibrium. When a structure or fracture zone intercepts this type of fluid and reaches the surface, it is called a geothermal reservoir outlet (‘outflow’) and, according to Giggenbach (1988), the fluid is classified as ‘mature water’. Therefore, it is crucial to analyse the chemical and isotopic composition (see next section) as it provides valuable information on the fluids during their stay in the subsurface, which, together with the samples extracted from wells and meteoric springs, helps explain hydrological and hydrogeological processes operating in the area and elucidate the origin, temperature and composition of the fluids that form the geothermal system.

7. Hydrogeochemistry

We analysed a total of 16 samples from hydrothermal manifestations and four from the Borinquen geothermal wells. Based on the concentration of SO^4, Cl and HCO^3 anions, and using the Piper ternary diagram, we distinguished three types of waters (Fig. 6a, Table 2):

Sulphated waters have pH values of 2.40–5.43 and temperatures of 57–97 °C. This kind of water originates from fumaroles (or from nearby) located at 560–900 m a.s.l. and consist of immature waters that have not had enough residence time to reach chemical equilibrium with the rock. They originate from groundwater with high oxygen content, and react with H_2S of magmatic origin, then oxidise and form SO_4. In the context of the hydrothermal system, they are associated with areas of fluid rise (upflow) and do not come into direct contact with a high enthalpy geothermal reservoir.

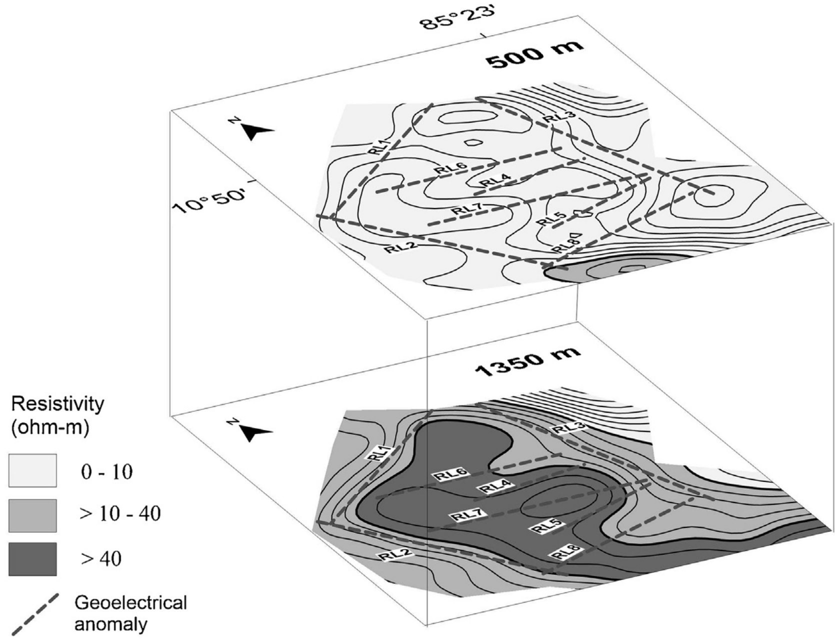

Fig. 4. Distribution of resistivity at depths of 500 m and 1350 m related to mineral alteration zones and resistive lineaments, obtained from the 3D-inverse model and the distribution of alteration mineralogy.

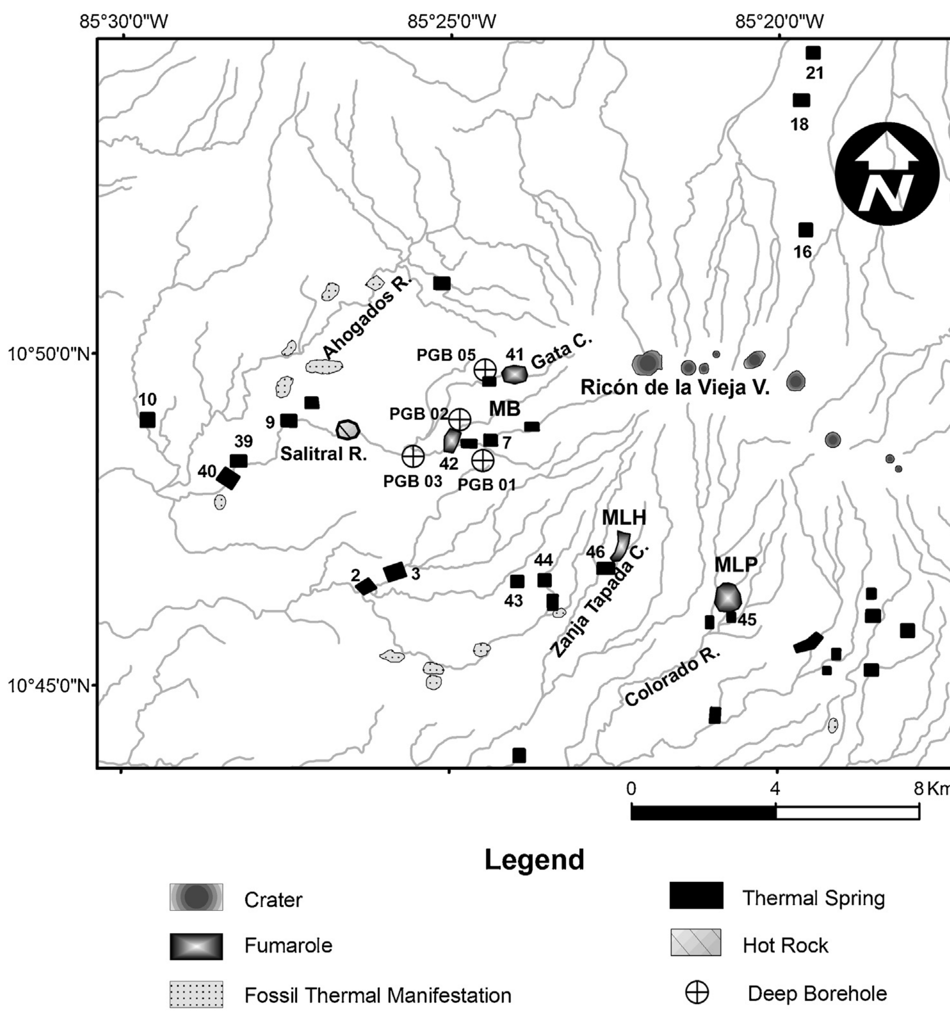

Fig. 5. Distribution of the main thermal manifestations. MLP: Las Pailas thermal manifestations, MLH: Las Hornillas thermal manifestations; and MB: Borinquen thermal manifestations. Numbers link the location of the thermal manifestations with chemical analysis samples.

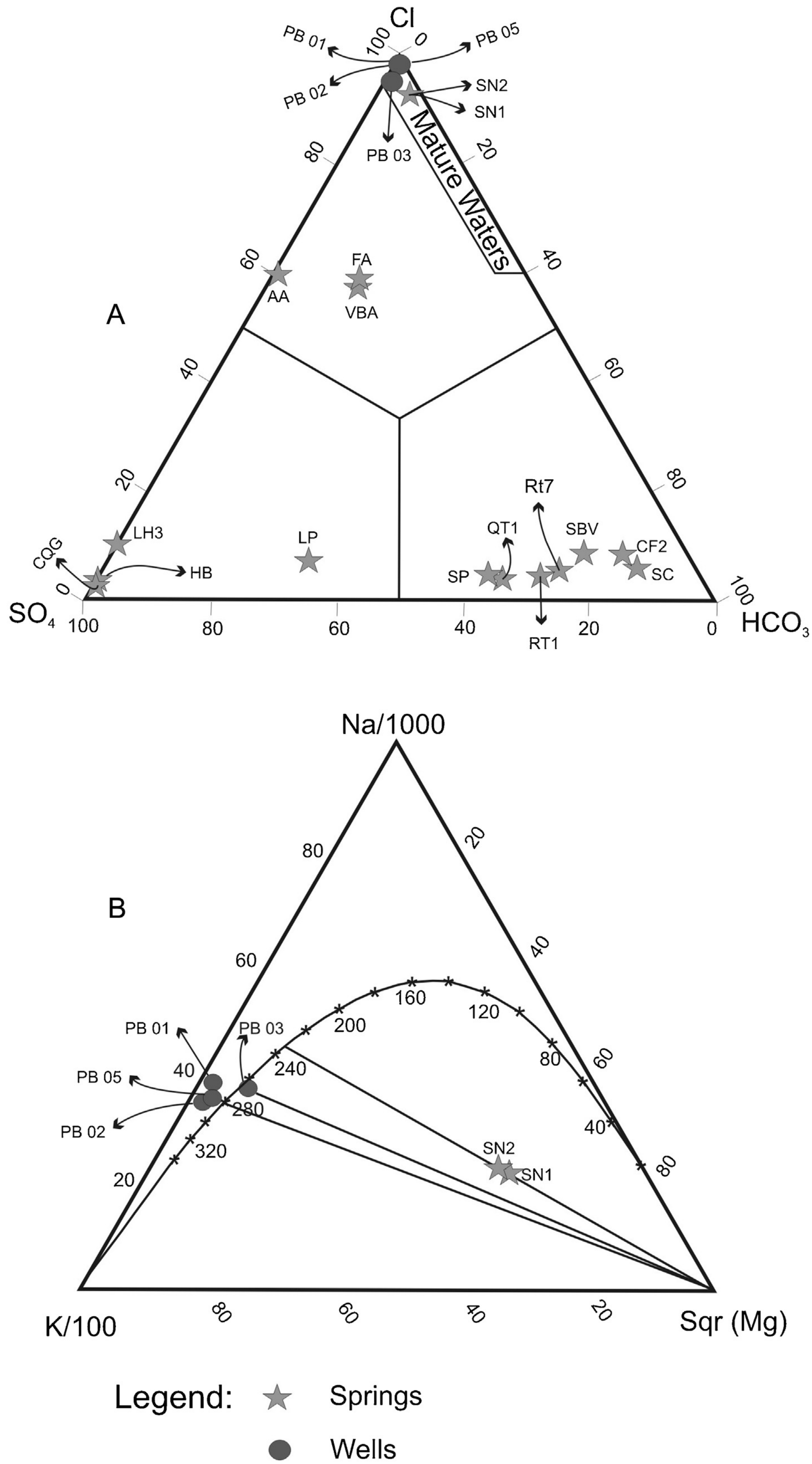

Fig. 6. (a) Piper diagram with the relative concentration of the anions SO_4, Cl and HCO_3 of 16 samples from thermal springs and the Borinquen geothermal wells. (b) Diagram Na-K-Mg with the full Giggenbach equilibrium curve (1988) used as a geothermometer to define the temperature equilibrium of the samples of sodium-chlorinated water from deep wells in Borinquen and hydrothermal manifestations in Salitral North.

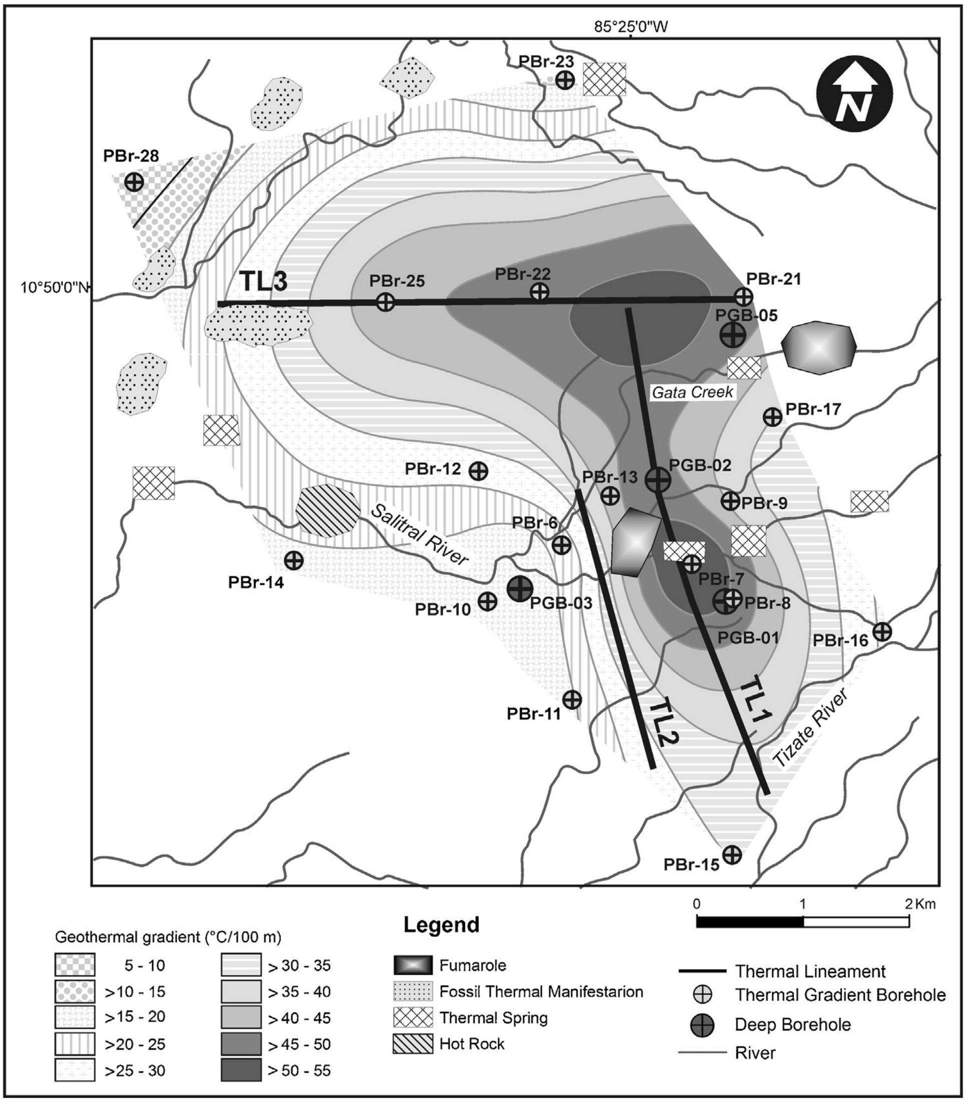

Fig. 7. Distribution of the gradient and thermal lineaments drawn using the temperature profiles of 17 thermal gradient boreholes.

Table 2
Chemical analysis of samples from hydrothermal manifestations and geothermal wells at Borinquen, with the respective classification of the type of water based on the concentration of SO_4, Cl and HCO_3 anions. Nomenclature: Temp—Temperature, Lab. Com—conductivity measured in laboratory, ND—not determined.

Location		Sample	Height	Temp	pH	Lab. Con	Na^+	K^+	Ca^{+2}	Mg^{+2}	B	Cl^-	$SO_4^=$	HCO_3^-	STD	Type
	In Fig. 5		m asl	°C	Lab.	µS/cm²	mg/L	mg/L	mg/L	mg/L	mg/L	ppm	ppm	ppm	mg/L	
Tizate River	3	RT 7	350	35	6.9	444	39.8	9.8	28.3	15.0		9.2	48.0	206.0	381	HCO_3
Tizate River	2	RT 1	330	40	7.1	447	42.0	8.1	27.5	14.8		6.3	56.0	201.0	387	HCO_3
Buena Vista Spa	7	SBV	630	47	7.6	332	28.3	4.8	27.8	7.9		10.0	26.0	153.0	259	HCO_3
Fortuna Hill 2	9	CF2	363	39	7.1	155	9.2	4.5	12.9	4.8		4.0	7.2	73.0	153	HCO_3
Salitral Norte	39	SN 1	270	69	6.4	9180	1617.0	159.0	191.0	17.5	31	3035.0	67.0	280.0	5565	Cl
Salitral Norte	40	SN2	259	73	6.4	9420	1663.0	164.0	195.0	16.7	31	2960.0	68.0	265.0	5675	Cl
Santa Clara Spring	10	SC	276	31	6.0	532	35.0	6.0	47.0	21.0		12.0	25.0	300.0	423	HCO_3
Gata Creek Fumarole	41	CQG	900	97	2.8	1525	116.0	31.0	27.0	5.9		10.1	495.0	0.0		SO_4
Borinquen Hotel	42	HB	560	96	3.0	1250	19.0	12.0	55.0	22.0		6.8	422.0	ND	958	SO_4
Sitio Pilón	43	SP	622	50	6.0	2070	113.0	35.0	106.0	65.0		21.0	270.0	624.0	7134	HCO_3
Tibio Creek	44	QT1	620	35	5.0	1252	95.0	28.6	47.0	55.0		18.1	217.0	561.0	966	HCO_3
PGB-01	PGB 01	PB 01	699		7.7	18,535	3681.0	628.0	162.0	< 0.1	63	6445.0	40.5	5.7	12,460	Cl
PGB-02	PGB 02	PB 02	699		7.8	21,500	4188.0	818.0	177.0	< 0.1	69	7276.0	30.5	8.8	14,540	Cl
PGB-03	PGB 03	PB 03	533		7.2	7370	1229.0	189.0	221.6	0.1	29	2307.0	111.0	44.0	4530	Cl
PGB-05	PGB 05	PB 05	844		7.6	17,238	3386.0	593.0	166.0	0.1	57	5810.0	46.0	9.0	11,400	Cl
Agroecológico Hostel	16	AA	740	36	4.0	1550	61.4	9.0	142.0	49.3		314.0	284.0	1.0	1202	Cl
Araya Family	18	FA	435	56	6.5	5880	361.0	122.0	433.0	310.0		1374.0	866.0	578.0	4861	Cl
El Volcancito B. Aires	21	VBA	410	61	6.4	6100	331.0	128.0	400.0	330.0		1396.0	916.0	599.0	5102	Cl
Las Pailas	45	LP	763	57	5.4	154	5.4	1.8	11.8	5.4		3.3	38.0	25.0	162	SO_4
Las Hornillas	46	LH3	770	93	2.4	2570	31.9	11.0	50.6	19.0		62.0	757.0	ND	1526	SO_4

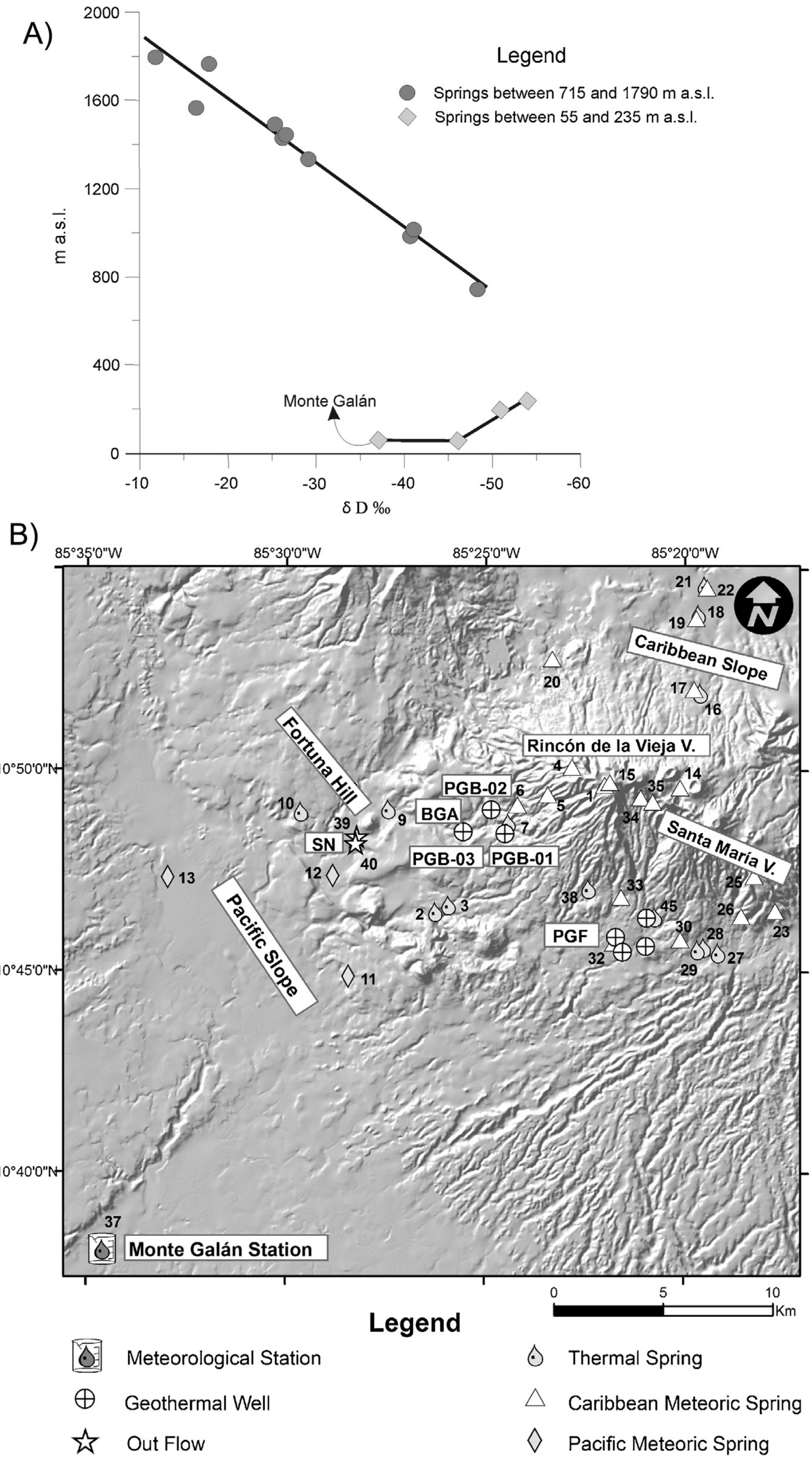

Fig. 8. (a) Distribution of deuterium with respect to height on the Pacific slope at 55–1790 m a.s.l. (b) Spatial distribution of samples of meteoric water, geothermal wells and the Monte Galan station used to analysis the stable isotopes δ D and δ O18°.

Bicarbonate waters come from hot springs located at 276–630 m a.s.l.; they are slightly acidic-to-neutral (pH 5.0–7.57) with temperatures of 30.5–50 °C. These waters originate in shallow aquifers with little residence time in the subsurface (Mg concentrations of 4.8–65 mg/L). They are heated or mixed with steam condensation, and are supposedly unrelated to a geothermal reservoir. They become slightly acidic if they have a small proportion of H_2S.

Chloride waters are slightly acidic-to-neutral (pH 4.01–6.43) with temperatures of 36.6–73.0 °C. They originate from hot springs located at 259–270 m a.s.l. on the Pacific side of the cordillera, and at about 410–740 m a.s.l. on the Caribbean slope. Samples taken from the springs Salitral Norte SN 1 and SN 2 (39 and 40 Fig. 5), and from the geothermal wells PGB 01, PGB 02, PGB 03 and PGB 05 (PB 01 PB 02 PB 03 and PB 05), occupy a similar position in the Piper diagram in the field of mature water (Fig. 6a). Furthermore, their concentrations of Na, K and Mg (Fig. 6b) suggest that the waters from spring SN have reached equilibrium with the rock at a temperature of nearly 235 °C. This indicates that they have a relationship with a high enthalpy reservoir. On the other hand, samples from the Borinquen geothermal wells have temperatures of the order of 280 °C, which is consistent with the maximum temperature measured directly in the PGB 01 (277 °C).

It is legitimate to assume that, once in the liquid phase, the concentrations of Cl and B are only affected by dilutions or concentrations and not by chemical equilibria given that (i) these elements are of magmatic origin and conservative and (ii) the fact that during the geological survey (Molina et al., 2014) and the geothermal drilling no evidence was found of sedimentary rocks of marine origin that could contribute B and Cl to the system. Thus, the Cl/B ratio suggests that the Salitral Norte spring (SN1, SN2 97.9 and 95.5) and samples obtained from the geothermal wells PGB 01, PGB 02 and PGB 05 (102.6, 105.6 and 101.9) are related, but unrelated to those from PGB 03 (79.6).

8. Thermal gradient

To identify and evaluate the magnitude and spatial distribution of the heat anomaly, we analysed the temperature profiles obtained from 17 wells at depths of 300–670 m in an area of about 31 km^2. Thermal gradient values varied from 6 °C/100 m (PBr-28 located in the NW) to 56 °C/100 m (PBr-7 located in the south). These results enabled us to model the areal distribution of the isotherms and to infer the thermal lineaments (TL) or preferential zones that regulate heat transfer (Table 3, Fig. 7).

The sector with the main thermal gradient is located around PBr-7, where the geothermal borehole PGB 01 reached a maximum temperature of 277 °C at a depth of 2570 m. At this point, the thermal anomaly seems to be related to the ascending heat plume as suggested by the surface thermal manifestations that reach boiling point. This sector shows a thermal lineament oriented NNW-SSE (TL 1), with a gradient that decreases rapidly towards the W of lineament TL2. This suggests that the media is less permeable in this sector, as shown by fact that well PGB 03 had a temperature of 189 °C at 1900 m and a low injectability index (1.5 l*Bar/S). Towards the central part of the explored area the isogradient curves become narrow, forming a bottleneck, thereby reflecting a change in the permeability of the medium.

The thermal anomaly extends northwards and widens to embrace a larger area oriented E-W (TL3). Northwards and westwards the thermal gradient decreases but the separation of isothermal curves suggests that heat transfer is good, probably due to greater permeability that facilitates fluid flow. A similar situation occurs southwards where the thermal gradient gradually decreases along TL 1.

Such a configuration permits us to hypothesise that the area is affected by a heat source in which the inherent secondary permeability of the rock and the E-W oriented structure facilitate the movement of geothermal fluids. Likewise, the heat plume detected close to PGB 01 represents an upflow of the geothermal system. The heat source of both zones seems to be related to the active Rincón de la Vieja volcano rather than to a residual magma chamber in the Cañas Dulces caldera. However, this latter site could be the source of the thermal anomaly around PGB 03.

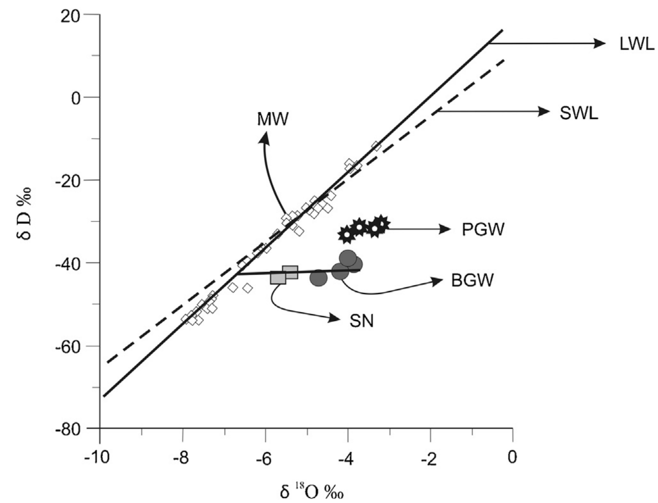

Fig. 9. Correlation of δ D and δ O18° in samples from Las Pailas and Borinquen geothermal wells (PGW and BGW), thermal springs (Salitral Norte SN) and meteoric waters (MW). Also shown are the meteoric line calculated for Costa Rica (SWL) and the local meteoric line (LWL).

9. δ D and δ ^{18}O stable isotopes

To complement the hydrochemical study and acquire a wider knowledge of the fluids involved in the hydrothermal system, we also used data from the δ D and δ 18O stable isotopes taken from the geothermal wells of Borinquen and Las Pailas, fresh water sources and hot springs, as well as from the Monte Galán meteorological station, part of the Global Network of Isotopes in Precipitations (Lachniet and Patterson, 2002; Table 4).

The distribution of δ D in meteoric waters from the Pacific side at altitudes of 55–1790 m a.s.l. (Fig. 8a and b) shows two trends corresponding to the influence of two types of meteoric water. At 55–235 m a.s.l. the distribution of D is normal due to the local effect of altitude, i.e. higher values with lower altitudes. However, the opposite is observed at 715–1790 m a.s.l., where the D concentrations increase with altitude. At the Monte Galán meteorological station, located 6 km from the Pacific coast at an altitude of 60 m a.s.l., the values for δ D are similar to those recorded at 1150 m a.s.l.

To corroborate or discard the possible relationship between meteoric water and the fluids in the geothermal system, we also analysed the concentration of δ D and δ 18O by plotting fresh water sources in the same diagram as the surface water line (SWL, δ D = 7.6δ 18O + 10.5, (r2 = 0.96, n = 66)) defined for Costa Rica by Lachniet and Patterson (2002). However, as this line has little affinity with local data given that it was established for the whole country, the best-fit line was calculated using the least squares method and fresh water sources (δD = 9.16δ 18O + 17.95, r2 = 9.88, n = 18), which was then taken as the local meteoric line (LWL, Fig. 9).

When isotopic data from samples corresponding to hydrothermal waters (from hot springs and geothermal wells at Borinquen and Las Pailas) are added to the previous data, the Borinquen fluids are seen to be composed of lighter isotopes than those from Las Pailas geothermal reservoir. This suggests that, despite the fact that both geothermal systems are located on the same slope of the volcanic edifice at a distance of just 8.5 km from each other, the hydrothermal fluids from Borinquen and Las Pailas are derived from two different – and independent – geothermal reservoirs. Moreover, samples from wells PGB 01 and PGB 02 and from the hot springs of Salitral Norte (SN1 and SN2) have a genetic relationship, as both are associated with the same dissolution line, thereby confirming that both these thermal waters come from the same geothermal reservoir located in the Borinquen area, composed of

Table 3
Summary of the perforations used to determine the distribution of the thermal gradient in Borinquen. Nomenclature: Temp. Max—maximum temperature measured in the well, Thermal Grad.—Thermal Gradient.

Well Location Fig. 7	Elevation (m)	Depth (m)	Temp. (Max °C)	Thermal Grad. (°C/100)
PBr-6	545	360	93	21
PBr-7	602	320	198	56
PBr-8	704	510	202	49
PBr-9	770	405	135	39
PBr-10	512	340	67	16
PBr-11	605	340	58	19
PBr-12	589	560	148	27
PBr-13	605	380	130	43
PBr-14	472	550	118	19
PBr-15	551	540	123	30
PBr-16	859	510	121	24
PBr-17	785	420	111	35
PBr-21	845	527	144	48
PBr-22	691	300	76	48
PBr-23	560	505	89	14
PBr-25	580	670	207	43
PBr-28	414	640	61	6

Table 4
Data of stable isotopes δ D y δ 18O from the geothermal wells (Borinquen and Pailas), fresh water sources, hot springs, and the meteorological station of Monte Galán. Nomenclature: Temp.—Temperature, Sep. water—Separated water.

Sample Site	Location Fig. 8b	Code	Height (m asl)	Temp. (°C)	$\delta\,^{18}$O (‰)	δ D (‰)
Tizate River Spring	1	NRT	1790	15	−3.29	−11.73
Tizate River Thermal 1	2	RT1	330	40	−7.83	−53.22
Tizate River Thermal 7	3	RT7	550	35	−7.91	−53.43
Gata Creek Spring	4	NQG	1330	17	−5.33	−29.11
Pacayal Creek Spring	5	NQP	1015	18	−6.56	−41.07
Borinquen Hotel Spring	6	NHB	745	25	−7.31	−48.27
Spa Buena Vista Thermal	7	TSBV	630	47	−7.69	−52.08
Fortuna Hill 2 Thermal	9	TCF2	363	39	−7.39	−50.71
Santa Clara Thermal	10	NSC	276	31	−7.32	−49.17
Buena Vista Spring	11	NBV	235	21	−7.66	−54.00
Atravezado Hill1	12	AT1	195	21	−7.37	−50.95
Vado La Esperanza 1	13	VE1	55	26	−6.43	−46.13
Jilgueros Lagoon	14	LJ	1560	19	−3.96	−16.34
Azul River Spring	15	NRA	1760	16	−3.96	−17.86
Agroecológico Hostel Thermal	16	TAA	740	36	−4.78	−26.74
Agroecológico Hostel Aqueduct	17	AAT	748	28	−4.65	−25.94
Araya Family Thermal	18	TFA	435	56	−4.83	−26.45
Los Araya Spring	19	NLA	475	25	−5.19	−32.34
Dos Ríos Aqueduct Spring	20	ADR	600	22	−4.81	−26.68
El Volcancito B. Aires	21	VBA	410	61	−4.84	−28.15
Araya Spring	22	NPA	440	25	−4.42	−23.70
Salto River Spring	23	NRS	980	20	−6.51	−40.65
Salto River Thermal (left side)	24	TRS	730	33	−6.15	−36.71
Zopilote River Spring	25	NRZ	1320	17	−4.80	−25.75
Pailas – Santa María Cold Water	26	PSM	916	20	−6.44	−40.10
Negro River (tributary) Thermal	27	TRN	760	38	−5.73	−32.86
Santa María Thermal	28	TSM	767	38	−5.23	−28.43
Azufrales Thermal	29	TAZ	698	44	−5.47	−29.50
Yugo Creek Spring	30	NQY	785	23	−6.21	−37.48
Guachipelin Hostel Aqueduct Spring	32	NAG	595	27	−7.51	−50.27
Quebrada Agua Escondida Creek	33	PAE	785	21	−5.43	−30.84
Blanco River (right side) Spring	34	NRB	1440	18	−4.81	−26.55
Colorado River Spring	35	NRC	1485	17	−4.67	−25.37
Monte Galán	37	MG	60		−37.00	−6.00
Hornillas Rincón de la Vieja 4	38	LH4	751	88	−7.30	−50.90
Salitral Norte 1	39	SN1	270	69	−5.41	−42.68
Salitral Norte 2	40	SN2	259	73	−5.68	−43.95
Las Pailas	45	LP	763	57	−6.01	−36.90
PGB-01 FP 2000 m	PGB-01		669		−3.87	−40.40
PGB-01	PGB-01		669		−4.70	−43.50
PGB-01 FP 1000 m	PGB-01		669		−4.18	−42.20
PGB-02	PGB-02		664		−3.98	−39.53
PGP-02					−3.21	−30.79
PGP-01 Sep. water					−3.31	−31.39
PGP-03					−3.71	−31.66
PGP-04					−4.01	−33.40

16.4 of magmatic water and 83.6 of meteoric water (Fig. 9). In other words, this geothermal reservoir is recharged by 83.6% meteoric water with an isotopic composition of δ 18O = −6.75 and δ D = −43.4 (Fig. 9), corresponding to an altitude close to 950 m (Fig. 8a). This isotopic composition may be attributable to the water from the western slopes of Rincón de la Vieja and south of Orosi Cacao, which are both drained by the Ahogados river whose course in this area is controlled by a regional structure (Molina et al., 2014).

10. Discussion

We explored an area of 31 km^2 inside the Cañas Dulces caldera to determine whether or not the Borinquen hydrothermal system possessed a high enthalpy geothermal reservoir of economic interest. Any such reservoir would have to be located at a depth of less than 3000 m and near a heat source, lie within a rock with good permeability, contain fluids at a temperature of at least 220 °C, and have a cap rock. Currently, the main limiting factor is that the distribution of the geothermal wells only covers a surface area of 4.5 km^2. However, the available complementary information is sufficient to extrapolate for the explored area.

During the drilling of the four wells in the Borinquen area we were able to check that the order of appearance of the alteration zones follows a normal pattern − that is, with an increase of temperature with depth − and that the minerals inside the thermal anomaly indicate conditions of high enthalpy starting at depths varying from −60 to −165 m, indicted by the beginning of the illite zone. This is reflected by the geoelectric structure of the system in which resistivity increases from a depth of −100 m onwards. This thickness constitutes the bulk of the cap rock that includes the deposits from the Rincón de la Vieja volcano, the Pital Formation and part of the Liberia Formation. Moreover, below the cap rock the presence of high temperature minerals increases, thereby indicating the existence of a nearby heat source. However, towards the SW (PGB 03) the illite zone is not present and the thermal anomaly deepens, which suggests that the current heat source is remote and that there is no geothermal reservoir at the explored depth.

According to the alteration mineralogy, the distribution of the thermal gradient indicates the presence of an active heat source, with two separate sectors with higher heat flow, in the vicinity of the explored area. Close to PBr-7, the thermal anomaly seems to be related to an ascending heat plume, whose thermal manifestations on the surface reach boiling point, which reveals the presence of an upflow. Nevertheless, westwards, the thermal gradient decreases rapidly, indicating the existence of a hydrological barrier that hinders the movement of hot fluids. On the other hand, northwards the thermal anomaly extends in an E-W direction and the distribution of the isogradients indicates good heat flow, probably due to the greater permeability of the host rock.

However, the magnitude of an accessible geothermal system depends entirely on the extent of the permeable zones and, consequently, one of the major problems in the study area is the massive and poorly permeable intra-caldera Liberia ignimbrite that, with a thickness of over 1000 m, acts as a barrier to the circulation of fluids. Therefore, the permeability of the system must be related in the first instance to tectonic structure and, to a lesser extent, to lithological contacts and variations in the thickness of the permeable materials. This implies that, to develop the high enthalpy geothermal resource, geothermal boreholes will have to be deepened and the main faults affecting the pre- and syn-caldera products – i.e. the preferential paths for the circulation of geothermal fluids – will have to be identified.

In general terms, the hydrothermal system of the Cañas Dulces caldera is limited by the master faults that controlled the collapse (F2 and F3, Fig. 10) and the regional structure F1, as defined by Molina et al. (2014). However, in the area we explored inside the caldera it is not easy to identify the faults that affect the geothermal reservoir, despite some evidence (e.g. geological structures and resistive and thermal lineaments) of structural discontinuities that do not necessarily affect the geothermal system. The distribution of the thermal gradient also provides evidence of this and, for example, in the N and NW of the studied area, the thermal gradient progressively decreases and shows hydraulic communication, and so it is possible that the structural systems (F1 and F2) are more permeable in that zone. Similar behaviour occurs towards the south, where fault F3 may increase the permeability. The E-W thermal lineament TL3, aligned with the craters of Rincón de la Vieja volcano – as shown by magnetotelluric data (LR6) – and located close to the geological structure EG1 with an orientation ENE-WSW, plays an important role in the hydrothermal system as it distributes the heat flow from it source close to the active volcano. Moreover, N-S thermal lineaments TL1 and TL2 influence hydrothermal circulation (Fig. 10): while TL1 distributes the heat flow northwards, TL2 works as a hydrogeological barrier that prevents the movement of hot fluids and therefore the continuity of the geothermal reservoir towards the SW. Lastly, the geological structure EG2 combined with TL1 could be sufficiently permeable to generate the ascent of the heat plume in the southern sector of the study area.

By contrast, to determine the origin of the geothermal fluids it is crucial to identify the provenance of the recharge water. The geographical characteristics of Costa Rica and of the study area in the NW of the country mean that Rincón de la Vieja is affected by rain from two oceanic slopes (the Caribbean watershed is more humid than the considerably drier Pacific side). This explains the exposed D distribution with altitude on the Pacific side (Fig. 8a): meteoric waters at 55–235 m a.s.l. originate from precipitations on the Pacific slope, those at 715–1790 m a.s.l. derive from precipitation on the Caribbean slope, while those at 235–715 m a.s.l. have D concentrations reflecting the mixture of waters from both sides. However, this latter elevation interval may decrease as no meteoric analysis exists for 235–715 m a.s.l.

SO_4, Cl and HCO_3 concentrations allowed us to identify three water types. Waters from the geothermal sources (Salitral Norte SN1 and SN2) are classified as mature waters that have reached their equilibrium with the host rock at nearly 235 °C, which suggests links to a high enthalpy reservoir. Samples obtained from wells PGB 01, PGB 02 and PGB 05 have temperatures of 280 °C; the lower temperatures from the SN sources, obtained with the geothermometer Na-K-Mg, may be due to re-equilibrium occurring during the ascent process. On the other hand, the relationship Cl/B suggests that waters originating from the SN sources and wells PGB 01, PGB 02 and PGB 05 could have a genetic link, which is confirmed by the $\delta\,^{18}$O and δ D concentrations in samples from SN and wells PGB 01 and PGB 02 through a dilution line. This also confirms that the manifestations located along the trace F2 are the discharge of the high enthalpy geothermal reservoir of Borinquen, that consisting of 16.4% of andesitic (magmatic) water from the Rincón de la Vieja volcano and 83.6% of meteoric water, with an isotopic composition of $\delta\,^{18}$O = −6.75 and δ D = −43.4, corresponding to an altitude of about 950 m a.s.l. and therefore originating from rain on the Caribbean slope.

11. Conclusions

The hydrothermal system located in the western sector of the Cañas Dulces Caldera contains elements that prove the existence of a commercially exploitable, high enthalpy geothermal reservoir. The heat source is located to the E, and is related to the Rincón de la Vieja volcano, which radiates heat and magmatic fluids. Meteoric water originating chiefly from the Caribbean slope of the cordillera

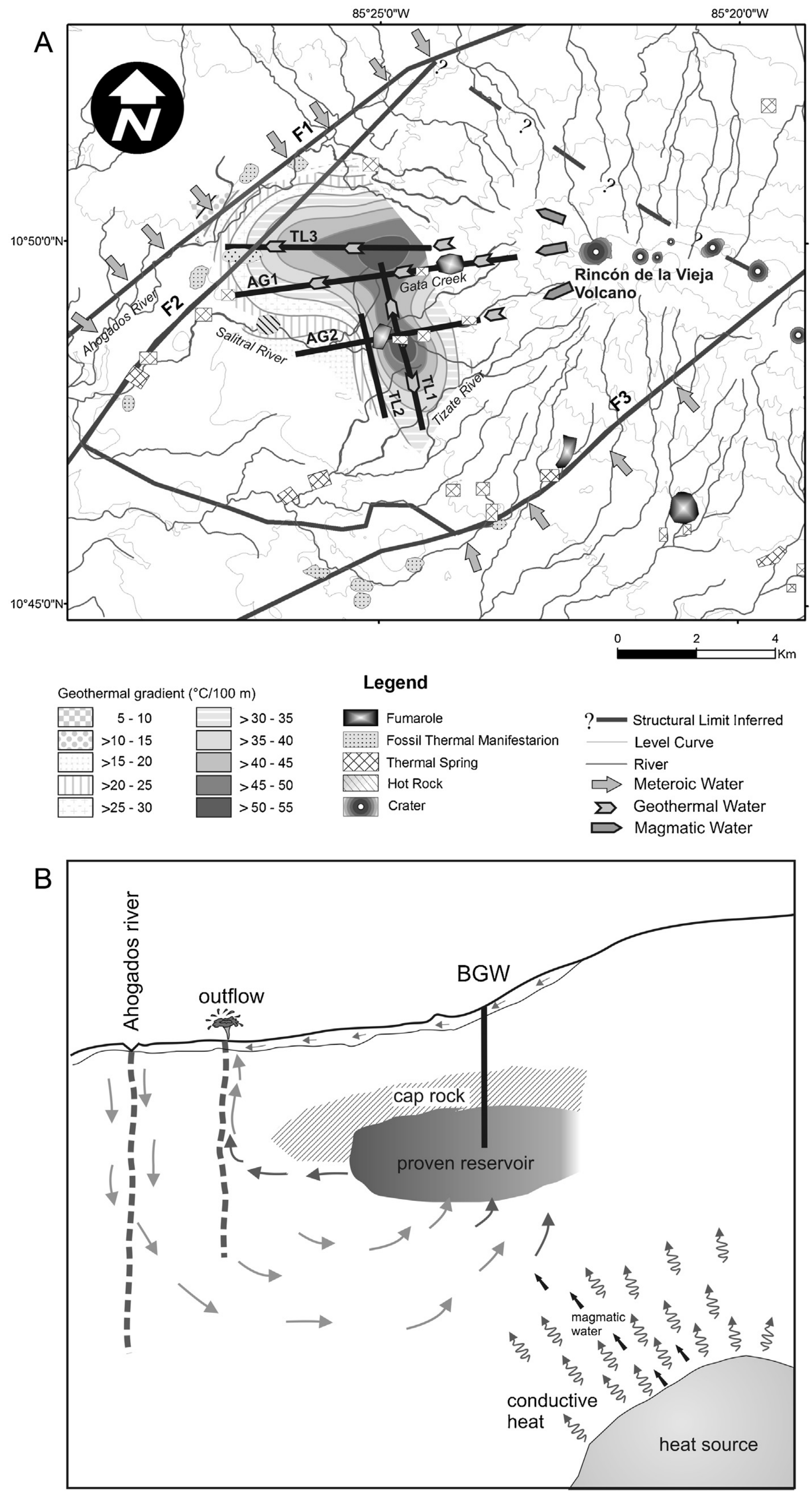

Fig. 10. Conceptual model of the Borinquen geothermal system showing the main components of a geothermal commercial reservoir: (a) thermal anomaly, recharge area, main flow paths and flow directions; (b) heat source, cap rock, proven presence of reservoir and movement of the fluid.

drains the NW and W slopes of Rincón de la Vieja and the SE slope of Cacao volcano; this water is the main recharge source that makes use of the system's permeability due to structures F1 and F2, through which water infiltrates and flows westwards. Similarly, in the foothills south of Rincón de la Vieja, the meteoric water uses the F3 structure to infiltrate and move towards the NW. In both cases, water reaches depths where it can come into contact with hot rock and mix with magmatic fluids. Subsequently, heated fluids ascend and are stored in the rocks of the Bagaces and Liberia formations, being halted by the base of the cap rock (at a depth of −10 to −165 m), which prevents them from continuing their migration to the surface. They thus form a sodium-chlorinated reservoir (~6000 ppm), with neutral pH at a temperature of about 235 °C (that can reach 280 °C). This reservoir consists of 83.6% meteoric water and 16.4% andesitic fluids that move naturally eastwards, as revealed by geothermal wells and outflows (SN), but possibly also drain naturally southwards despite no outflow being detected in this latter sector.

Acknowledgements

We would like to thank the Instituto Costarricense de Electricidad (ICE) for its support and help in undertaking this research, and for giving us permission to publish the data. Thanks are also due to Leyner Chavarría, Ronald Ramírez and Eduardo Vega for their support and fruitful discussions. English text has been corrected by Michael Lockwood.

References

Arnórsson, S. (Ed.), 2000. Isotopic and Chemical Techniques in Geothermal Exploration, Development and Use: Chemical Reactions and Chemical Equilibria 3. International Atomic Energy Agency, Vienna, 351 p.
Arnason, K., Karlsdottir, R., Eysteinsson, H., Flovenz, O., Gudlaugsson, S., 2000. The resistivity structure of high-temperature geothermal systems in Iceland. In: Proceedings WGC, Kyushu, Japan, pp. 923–928.
Browne, P., 1978. Hydrothermal alteration in active geothermal systems. Annu. Rev. Earth Planet. Sci. 6, 229–250.
Browne, P., 1993. Proceedings, Eighteenth Workshop on Geothermal Reservoir Engineering Stanford University , Stanford, California, January, pp. 26–28 (SGP-TR-145).
Carr, M., Saginor, I., Alvarado, G.E., Bolge, L., Lindsay, F.N., Milidahis, K., Turrin, B.D., Feigenson, M.D., Swisher, C.C., 2007. Element fluxes from the volcanic front of Nicaragua and Costa Rica. Geochem. Geophys. Geosyst. 8, Q06001, http://dx.doi.org/10.1029/2006gc001396.
Chiesa, S., Civelli, G., Gillot, P.Y., Mora, O., Alvarado, G.E., 1992. Rocas piroclásticos asociadas con la formación de la caldera de Guayabo, cordillera de Guanacaste Costa Rica. Rev. Geol. Am. Cent. 14, 59–75.
Curewitz, D., Karson, J., 1997. Structural settings of hydrothermal outflow: fracture permeability maintained by fault propagation and interaction. J. Volcanol. Geotherm. Res. 79, 149–168.
Giggenbach, W., 1988. Geothermal solute equilibria: derivation of Na-K-Ca-Mg geoindicators. Geochim. Cosmochim. Acta 52, 2749–2765.
Giggenbach, W., 1992. Isotopic shifts in waters from geothermal and volcanic systems along convergent plate boundaries and their origin. Earth Planet. Sci. Lett. 113, 495–510.
Gottsmann, J.H., Martí, J. (Eds.), 2008. Caldera Volcanism: Analysis, Modelling and Response, Developments in Volcanology, vol. 10. Elsevier, Amsterdam, p. 492.
Lachniet, M., Patterson, W., 2002. Stable isotopes values of Costa Rican surface water. J. Hydrol. 260, 135–150.
Molina, F., Martí, J., Aguirre, G., Vega, E., Chavarría, L., 2014. Stratigraphy and structure of the Cañas Dulces caldera (Costa Rica). Geol. Soc. Am. Bull., http://dx.doi.org/10.1130/B31012.1 (published online 23 June 2014).
Mottl, M., 1983. Metabasalts, axial hot springs, and the structure of hydrothermal systems at mid-ocean ridges. Geol. Soc. Am. Bull. 94, 161–180.
Norton, D., 1984. Theory of hydrothermal systems. Rev. Earth Planet. Sci. 12, 155–177.
Reyes, A., 2000. Petrology and Mineral Alteration in Hydrothermal Systems: From Diagenesis to Volcanic Catastrophes. Report 18. United Nations University, Reykjavík, Iceland.
Sánchez, E., Vallejos, O., 2000. Practical uses of clay minerals at the miravalles geothermal field, Costa Rica. In: Proceedings WGC, Kyushu, Japan, pp. 1623–1628.
Tikhonov, A., 1950. The determination of electrical properties of deep layer of the Earth's crust. Dokl. Akad. Nauk SSR 73, 295–297.
Urzúa, L., 2008. Integration of a Preliminary One-dimensional MT Analysis with Geology and Geochemistry in a Conceptual Model of the Ngatamariki [M.Sc. Thesis]. University of Auckland, Auckland, New Zealand, 128 p.

Anexo

C

Proposal of an initial development strategy for the Borinquen geothermal zone (Cañas Dulces, Costa Rica).

Aceptado para revisión en:

Renewable Energy

Autores del artículo:

Fernando Molina[1]

Joan Martí[2, a]

1) Área de Geociencias, Centro de Servicios Recursos Geotérmicos, Instituto Costarricense de Electricidad, Guanacaste, Costa Rica.

2) Group of Volcanology, Institute of Earth Sciences Jaume Almera, CSIC, Lluis Sole Sabaris, s/n, 08028 Barcelona, Spain.

a) now at the Institut des Sciences de la Terre d'Orleans (ISTO, CNRS), Université d'Orleans, Campus Géosciences, 1A rue de la Férolerie, F45071, Orleans Cedex 2.

Elsevier Editorial System(tm) for Renewable Energy
Manuscript Draft

Manuscript Number:

Title: Proposal for an initial development strategy for the Borinquen Geothermal Zone (Cañas Dulces, Costa Rica)

Article Type: Research Paper

Keywords: Geothermal energy, Costa Rica, collapse caldera, Borinquen, development strategy

Corresponding Author: Professor Joan Marti, Prof

Corresponding Author's Institution: CSIC

First Author: Fernando Molina

Order of Authors: Fernando Molina; Joan Marti, Prof

Abstract: The uncertainty regarding the dimensions and exact location of the geothermal resource, along with the cost of any project for exploiting it, are usually two factors that hinder the wider use of high enthalpy geothermal energy to generate electricity. In the second half of 2018, the Costa Rican Institute of Electricity (ICE) will begin to develop the Borinquen geothermal zone (drilling) with the intention of generating 50 MWe from the reservoir. In order to reduce the investment risk in this phase, we combine available geological, geophysical and thermal gradient data to identify the most appropriate locations for drilling rigs, to define the high enthalpy geothermal resource, and to identify the areas to be used as poles of production and for the reinjection of geothermal fluids. In addition, we use the USGS Heat in Place volumetric method and the Monte Carlo simulator to evaluate the geothermal potential and to estimate the electrical energy that will be produced in the area designated as a production zone. This information enables us to calculate the number of wells required to produce 50 MWe. Finally, we propose a preliminary viable development strategy as the basis for the sustainable exploitation of the Borinquen geothermal field.

Suggested Reviewers: Jim Cole
jim.cole@caterbury.ac.nz
expert on caldera geothermal systems

Jose Luis Macias
jlmv63@gmail.com
expert on Mexican calderas and geothermal exploration

Enrico Barbier
barbier@igg.cnr.it
expert on geothermal resources in volcanic systems

MINISTERIO
DE ECONOMÍA
Y COMPETITIVIDAD

CSIC ICTJA
INSTITUT OF EARTH SCIENCES JAUME ALMERA (ICTJA)

Barcelona, April 12, 2017

Dear Renewable Energy Editor,

Please find enclosed the the manuscript entitled "**Proposal for an initial development strategy for the Borinquen Geothermal Zone (Cañas Dulces, Costa Rica)"**, by Fernando Molina and Joan Martí, to be submitted for publication to Renewable Energy.

This manuscript includes new, unpublished material concerning a proposal for a preliminary viable development strategy for the sustainable exploitation of the Borinquen geothermal field (Cañas Dulces, Costa Rica). This work is part of the PhD Thesis of the first authors. In the second half of 2018, the Costa Rican Institute of Electricity (ICE) will begin to develop the Borinquen geothermal zone (drilling) with the intention of generating 50 MWe from the reservoir. In order to reduce the investment risk in this phase, we use a conceptual model of this high enthalpy geothermal reservoir that we developed in a previous study (Molina and Martí, 2016, Geothermics) to generate suitability scenarios for choosing the most appropriate locations for drilling rigs, to define the high enthalpy geothermal resource, and to identify the areas to be used as poles of production and for the reinjection of geothermal fluids. In addition, we also evaluate the geothermal potential and estimate the electrical energy that will be produced in the area designated as a production zone.

We declare that there is not conflict of interests among the authors or with third parties.

We hope you will find this manuscript of interest and suitable to be published in your journal

Sincerely yours

Joan Marti

C/ SOLÉ I SABARÍS, S/N
08028 BARCELONA SPAIN
TEL.: +34 93 409 54 10
FAX.: +34 93 411 00 12

***Highlights**

The cost of any project for exploiting a geothermal resource is always subjected to the uncertainty regarding the its dimensions and exact location.

Exploitation of high enthalpy geothermal energy to generate electricity in Costa Rica

Combining geological, geophysical and thermal gradient data to generate suitability models for choosing the most appropriate exploitations locations

Statistical and probabilistic basis to evaluate the geothermal potential and to estimate the electrical energy

Proposal for an initial development strategy for the Borinquen Geothermal Zone (Cañas Dulces, Costa Rica)

Fernando Molina[1], Joan Martí[2,a]

1.- Área de Geociencias, Centro de Servicios Recursos Geotérmicos, Instituto Costarricense de Electricidad, Guanacaste, Costa Rica.

2.- Group of Volcanology, Institute of Earth Sciences *Jaume Almera*, CSIC, Lluís Solé Sabarís, s/n, 08028 Barcelona, Spain.

a.- Now at: Institut des Sciences de la Terre d'Orléans (ISTO, CNRS), Université d'Orleans, Campus Géosciences, 1A rue de la Férolerie, F45071, Orleans Cedex 2.

Contact author: Joan Martí (joan.marti@ictja.csic.es)

Submitted for publication to: Renewable Energy (Elsevier)

Abstract

The uncertainty regarding the dimensions and exact location of the geothermal resource, along with the cost of any project for exploiting it, are usually two factors that hinder the wider use of high enthalpy geothermal energy to generate electricity. In the second half of 2018, the Costa Rican Institute of Electricity (ICE) will begin to develop the Borinquen geothermal zone (drilling) with the intention of generating 50 MWe from the reservoir. In order to reduce the investment risk in this phase, we combine available geological, geophysical and thermal gradient data to identify the most appropriate locations for drilling rigs, to define the high enthalpy geothermal resource, and to identify the areas to be used as poles of production and for the reinjection of geothermal fluids. In addition, we use the USGS Heat in Place volumetric method and the Monte Carlo simulator to evaluate the geothermal potential and to estimate the electrical energy that will be produced in the area designated as a production zone. This information enables us to calculate the number of wells required to produce 50 MWe. Finally, we propose a preliminary viable development strategy as the basis for the sustainable exploitation of the Borinquen geothermal field.

Keywords: Geothermal energy, Costa Rica, collapse caldera, Borinquen, development strategy

Introduction

Costa Rica's electricity grid uses six sources of clean energy. In 2015 energy production was 75% HEP, 13% geothermal, 10% wind, 1% thermal and 1% biomass and solar. Given that any energy matrix must be robust and reliable, geothermal energy is used as a basic energy resource since it is not dependent on climatic phenomena and is stable 24 hours a day, 365 days a year (except during maintenance periods).

Despite the advances made in electricity generation, Costa Rica still faces the challenge of phasing out its use of fossil fuels in energy production. The country is aware that its high enthalpy geothermal resource, in use since 1994, satisfies its environmental and economic policies since it is clean, autochthonous and sustainable, and has low environmental impact. Currently, Costa Rica has two geothermal fields: Miravalles 163.5 MWe and Pailas 41.6 MWe [1]. In addition, the development of a second 55-MWe unit in the Pailas geothermal field was begun in 2014, and a 50-MWe unit in the Borinquen geothermal zone, located in the Cañas Dulces Caldera [2] on the slopes of the Rincón de la Vieja volcano, is planned for the second half of 2018 (Fig. 1).

However, it is well known that during the development of this type of project, there is no guarantee of the existence of a viable geothermal resource and so drilling has to take place to ensure that the resource exists. According to Gehringer and Loksha [3], more than 50% of the total investment in such geothermal projects is linked to exploration and drilling. The drilling of a 2000-m well will cost the Instituto Costarricense de Electricidad (ICE) somewhere between US $ 2.5 million and US $ 4 million, depending on whether the well is vertical or directional. Thus, bearing in mind the two factors mentioned above (uncertainty and cost), the development of a geothermal project is a high investment risk, which is one of the main obstacles preventing the greater use of this energy worldwide. Therefore, in order to reduce the risk associated with the development of geothermal projects, it is essential to conduct systematic geoscientific research beforehand to obtain the necessary knowledge for selecting prospective areas and for locating drilling targets efficiently.

Here we propose a development strategy for the Borinquen geothermal zone, in which a weighted aptitude model is applied to zone the high enthalpy geothermal resource. This, together with the conceptual model developed by Molina and Martí [4], allows us to identify areas that could be devoted to production, damping and the reinjection of geothermal fluids. In addition, the USGS *Heat in Place* method enables us to estimate the energy potential of the explored area, the size of the plant that needs to be installed, and the pads and wells required to initiate the generation of electricity. We propose a strategy that will permit the sustainable exploitation of the geothermal resource and prolong the useful life of the geothermal field, thereby guaranteeing that the necessary investment will be economically viable.

Geological setting and general characteristics of the Borinquen geothermal system

The Borinquen geothermal area is located in the western sector of the Cañas Dulces caldera, which forms part of the Guanacuaste volcanic range along with the more recent andesitic stratovolcanoes of Orosí-Cacao, Rincón de la Vieja-Santa María, Miravalles and Tenorio-Montezuma. Cañas Dulces is a collapse caldera structure of volcano-tectonic origin formed about 1.43 Ma that covers an area of 120 km^2 [2]. This caldera was built by a massive eruption of about 200 km^3 of rhyolitic magma that was largely responsible for the formation of the Liberia ignimbrite. It was formed under strong structural control dominated by two parallel NE-SW regional faults. After its formation, volcanic activity has continued inside the caldera up to the present day with the construction of the active Rincón de la Vieja volcano (1895 m a.s.l.).

The stratigraphy of Cañas Dulces was established by Molina et al. [2] and consists of the following formation (from base to top): the Bagaces group, forming the basement of the caldera and consisting of sequences of andesitic lavas, crystal tuffs and lithic tuffs; the Liberia Formation that corresponds mostly to the caldera infill but also to an extensive ignimbrite sheet outside the caldera mainly composed of a massive pyroclastic flow of dacitic to rhyolitic deposits; the Pital Formation that includes dacitic pyroclastic sequences interbedded with minor epiclastic, lacustrine deposits and andesitic lavas, which constitute the post-caldera infill; and the Rincón de la Vieja volcano succession, which chiefly consists of andesitic lava flows with subordinated pyroclastic deposits

Geological, geochemistry and geophysical studies, along with gradient wells and geothermal perforations, have been carried out in the caldera. This information allows us i) to establish a relationship between the zones of alteration of the hydrothermal system, temperature and electrical response (apparent resistivity, Table 1), ii) define the initial parameters that characterise this reservoir, and iii) propose a conceptual model of the Borinquen geothermal system [4] (Fig. 2). This model provides a synthesis of the main hydrogeological and geothermal elements: it locates the heat source in the east (related to the Rincón de la Vieja volcano, which radiates heat and magmatic fluids) and the main recharge zone in the north-west, the sector in which the meteoric water that drains through the Ahogados river basin infiltrates and moves eastwards through the tectonic network until it reaches the depths at which it comes into contact with hot rock and mixes with magmatic fluids. These hydrothermal fluids ascend and are stored in the rocks of the Bagaces and Liberia formations until they hit the seal layer, which prevents them from migrating to the surface. Here they form a chloridated sodium reservoir composed of 83.6% meteoric water and 16.4 andesitic water – with neutral pH and temperatures that can reach 280°C – that moves naturally westwards and possibly southwards [4].

To date, four geothermal wells have been drilled in the Borinquen geothermal area. In 2004 –2005 the Borinquen Geothermal Project wells 01 and 03 (PGB 01 and PGB 03) were drilled vertically. However, results were not encouraging since the head pressure and total flow values measured in PGB 01 did not allow the resource to be exploited by a condensation plant. PGB 03, at a depth of 2082 m, reached a maximum temperature of 210°C and flowed at 30 l/s, thereby indicating that this perforation was located outside the area of the high enthalpy reservoir. Thus, a fresh analysis of the existing information aimed at designing new exploration campaigns was carried out, which culminated in the definition of new drilling targets. The campaign was resumed in 2012–2013 with the drilling of two directional wells, PGB 02 and PGB 05, the results of which were to change the future development of the Borinquen geothermal zone.

Methodology

A specific methodology was used to i) identify areas suitable for the installation of drilling platforms, ii) perform the zoning of the enthalpy geothermal resource, and iii) quantify the number of wells needed to start generating electricity with a 50-MWe plant (Fig. 3).

To select the areas offering favourable conditions for constructing and operating the drilling rigs, we analysed topographical, environmental and logistical questions. We applied a simple fitness model consisting of the following thematic layers: ‘Slopes’, ‘Water network’ (both derived from the digital elevation model), ‘Existing infrastructure’, and ‘Existing platforms’, which were binarised and combined to obtain the layer ‘Areas suitable for drilling rigs’.

Zoning of the high enthalpy geothermal resource was conducted using a weighted fitness model with information compiled and synthesized in three thematic layers: ‘Resistivity’, which helped to define the seal layer and areas with geothermal potential; ‘Thermal Gradient’, which allowed us to delimit the distribution of the thermal anomaly and the directions of the flow of heat and fluid; and ‘Structural’, which sought to define structures that are directly related to the hydrothermal system. The basic concept behind weighted adequacy modelling lies in evaluating each thematic layer in the context of a common goal and reclassifying them into a common unit of measure (adequacy), which allows their space relationship to be analysed logically; then, each layer is multiplied by its relative weight and finally all are summed, the highest value obtained being taken as the best-fitting model. This methodology generates different results for the geothermal resource distribution by changing thresholds and relative weights, thereby making it easier to evaluate and select scenarios.

The zoning of the geothermal resource was combined with the conceptual model produced by Molina and Martí [4] to define the most suitable areas for use as zones of production, damping and the reinjection of geothermal fluids, which are referred to as ‘Suitable for geothermal development’. To define the viable sectors for reinjection and production platforms, the ‘Suitable for geothermal development’ layer was combined with the ‘Areas suitable for drilling rigs’ layer. It is important to note, however, that it is likely that not all the sectors delimited in this operation will need to be used given that the quantity and distribution of platforms and wells devoted to production and reinjection, as well as the capacity of the plants to be installed, will depend on the amount of electric energy that can be potentially provided by the geothermal reservoir; this information forms the basis of the initial development strategy (Fig. 3).

To obtain a simple evaluation of the Borinquen geothermal resource and to estimate its potential electric power, we used the USGS’s volumetric method known as *Heat in Place* or ‘Stored Heat’ [5], [6], [7], [8]. This method provides a general, conservative rather than optimistic, estimate of the energy potential, which is valid during the early stages of a project. It evaluates the geothermal resource or recoverable amount of heat (RH) by determining the stored heat (SH) in a specific volume of rock. Given that all the heat stored in the rock cannot be extracted, SH is multiplied by a recovery factor (FR) that takes into account the geological conditions. The produced fluid is cooled from its natural state to a base temperature, which is the lowest temperature that can guarantee the commercial and technical viability of the geothermal power plant to be built. The maximum amount of geothermal energy (GE) that can be generated from the RH depends on the efficiency of the conversion of thermal energy into mechanical energy; to obtain the energy potential in MW (PP), the plant lifespan (PL) and the plant capacity or specific consumption factor (PCF) must be defined.

The geological environment is heterogeneous and so there is uncertainty regarding the reservoir parameters used as input values. To reduce this uncertainty, we combined the USGS *Heat in Place* method with simulations of the Montecarlo method [8], [9], which enabled us to evaluate the energy potential on a statistical and probabilistic basis.

Suitable areas for drilling pads

Certain factors make the exploitation of this area of geothermal interest difficult and costly: poor access, irregular topography, a water network with deep channels, and its importance for tourism since it is near Rincón de la Vieja National Park (it is an area of great scenic valuable and so there are also a number of administrative restrictions). However, a good development strategy must be flexible and efficient, and must allow adjustments and changes to be implemented during its execution to optimize resources and reduce any negative impact without losing sight of its objectives. Therefore, we propose developing the Borinquen geothermal zone using directional drilling, a technique that, due to its versatility, allows several wells to be drilled from the same pad, thereby reducing, for example, the land required, the surface area of the infrastructure, the access routes needed, the number of pipelines, the amount of waste, and all the respective maintenance. The immediate consequence is a reduction in costs and environmental impact. This solution, implemented with the drilling rigs used by ICE and combined with the experience gained during the development of the Las Pailas geothermal field, allows us to estimate that the appropriate area for constructing the drilling pads with six working areas would cover 25 600 m^2 (160 m x 160 m).

Slopes

The project is located on the flanks of a large stratovolcano. The terrain is very steep and irregular and there are very few flat areas of adequate size for constructing drilling rigs. As a starting point, a Digital Elevation Model (DEM) was used to create a binary map of slopes with a threshold of 15°. Areas with slopes equal to or less than this value were integrated into the study, all others were excluded (Figs. 3 and 4a). We decreased the cost-benefit ratio by reducing the threat of slope instability, i.e. slippage, by siting drilling platforms on low-gradient slopes, and by keeping land movement, slope construction and containment or reinforcement work to a minimum.

Water network

In order to mitigate the threat of contamination of surface water by sediments or other substances generated during the drilling process, a buffer distance of 100 m is proposed – to comply with the Forest Law of Costa Rica 7575 ([10] – to ensure that sites selected as drilling platforms are located at least this distance from rivers and streams (Fig. 4b).

Existing infrastructure

Tourism is one of the main economic activities conducted in the area of interest. In an attempt to keep geothermal development away from tourist centres and related infrastructures, a buffer area of 400 m was created to safeguard the coexistence of tourism and exploitation of the geothermal resource (Fig. 4c).

Existing platforms

There are four platforms currently operating in the Borinquen geothermal zone, each with a well. We proposed a minimum distance of 200 m between platforms to avoid interference between producing and/or reinjecting areas. In order to reach the drilling targets defined according to the geology of the area and the depth of the reservoir, the main factors to be considered in the basic design of a directional well are the depth of the start of the kick-off point (KOP) and the heading of the well, and/or the drilling angle. To guarantee a similar distance between the wells of different platforms, we must take into account the capacity of the ICE drilling equipment, which can drill horizontally for 800 m; thus, a buffer area of 900 m is required for each platform (Fig. 4d).

Taking into account all the available topographical, logistical and environmental information, as well as the existing geological and geophysical data, the model showed that the most suitable areas for building new drilling pads are concentrated in the north and west (Fig. 5). This result is in part due to the existing conditions in the south of the study area, where there are three drilling rigs and two important tourist complexes. However, to select the definitive sectors for the drilling rigs, this result must be analysed in combination with the suitable areas for the development of the geothermal resource and their energy potential.

Zoning of the high enthalpy geothermal resource

In order to zone the high enthalpy geothermal resource, we conducted a geospatial analysis by applying a weighted suitability model. The strength of this method is that it combines geoscientific data of diverse origin by reclassifying all the data with the same suitability. It then uses map algebra to generate maps that delimit areas of different geothermal potential. To assign the values of aptitude and weight to the information layers, we estimated the uncertainty of the data, as well as the behaviour of the information analysed in the geological environment and its nexus with the existence of a geothermal resource: the higher the weighted value assigned, the greater the coverage of the analysed phenomenon.

Resistivity

Given that the distribution of resistivity reflects (among other factors) the lithology, mineralogical alteration and presence of fluids in the subsoil, we used the electrical structure model defined by Molina and Martí [4] to define the thematic layer 'Resistivity' for the Borinquen geothermal zone. This relates the distribution of the resistivity, lithology, mineral alteration and temperature of the medium in relation to depth. The geoelectric structure consists in the outer margins of the reservoir of a low resistivity layer (0 and 10 ohm/m) with hydrothermal alteration minerals dominated by the smectite zone, with temperatures up to 170°C. This layer overlies a core of higher resistivity that increases towards the interior, which crosses first the transition zone formed by the mixture of illite-smectite until it reaches resistivities that are associated with the illite zone, with temperatures above 220°C. These temperatures are suitable for the commercial exploitation of a high enthalpy geothermal field (Table 1).

We used the three-dimensional resistivity inversion model generated by West [11] to delimit the depth range where the low resistivity layer is present. When examining the distribution of resistivity at different plants, we observed that at a depth of 500 m, the layer with values below 10 ohm/m extends throughout the whole study area (Fig. 6). At 1100 m, this layer tends to disappear and moves to the edges, where it reaches values of up to 40 ohm/m, and is related to the transition zone (Fig. 6). At 1750 m, the distribution and values with an apparent resistivity of up to 100 ohm/m suggest that this zone is more likely to be associated with a high enthalpy geothermal reservoir. Therefore, it was selected for geospatial analysis and was reclassified on the basis of the data in Table 2 (Figs. 6 and 7a).

Thermal gradient

In an active hydrothermal environment, the heat energy contained in the rock is transported by geothermal fluids through fractures interconnected by porous rock. Thus, the spatial distribution and magnitude of the thermal anomaly is directly related to the distribution of the heat, permeability and fluid in the medium. This means that the identification and analysis of the distribution of the thermal anomaly is needed to locate sectors that could contain a viable geothermal resource. In the study area, there are 17 wells with depths ranging from 300 to 670 m, distributed over an approximate surface area of 31 km^2, whose thermal profiles show conductive behaviour that is ideal for obtaining temperature change rate with depth. The thermal gradient values range from 6°C/100 m to 55°C/100 m. With this information, the spatial distribution of thermal isogradient curves, which constitutes the thematic layer of the same name integrated into the process, was reclassified based on the values in Table 2 (Figs. 3 and 7b). The reliability of the data, as well as its relationship with the existence of a geothermal resource, justifies the allocation of greater weight in the geospatial analysis.

Tectonic structures

In a collapse caldera system such as Cañas Dulces, the tectonic structures are responsible for a high percentage of the existing permeability and induce the circulation of the geothermal fluids. Therefore, we used the tectonic structures that affect the reservoir ([4]). However, TL 2 was eliminated (Fig. 3), as it is a hydrogeological barrier that limits the circulation of geothermal fluids. In hydrothermal systems where the rocks are hot, as in the case of the Borinquen geothermal system, there will be a high density of fractures close to the line of the main faults. However, they will decrease in number and size as they become more distant from these faults, to the point that the remaining permeability may be related to other geological processes (generally to porosity). Therefore, this thematic layer assigns higher fitness values in the vicinity of the tectonic line, which decrease with distance until they reach a background value (Table 2, Fig. 7c). Given that the geological environment is heterogeneous, that the reservoir is below 1000 m, and that most of the information regarding this layer was obtained indirectly, the lowest weight was assigned during the geospatial analysis.

Model results

The result of the zoning of the geothermal resource may lead to a series of different implications when defining the strategy for the development of the geothermal field. On the one hand, it facilitates the identification of sectors with greater or lesser geothermal potential, knowledge that is indispensable for selecting the areas that are suitable for development. On the other hand, it allows for the development of scenarios for geothermal resource extraction (Maximum, Most Likely and Minimum) that are essential for evaluating the energetic potential (see section below).

Using the thematic layers, the different suitability and weight values (see Table 2) were used to run the model. The results are summarised in Fig. 8. Sectors classified as having ‘Very good’ or ‘Good’ geothermal resource potential are more likely to contain a high enthalpy geothermal resource. In total, they cover 17.6 km^2, the maximum possible area with favourable characteristics for extracting the geothermal resource. However, we must also consider the distribution of the damping and reinjection zones if we are to propose an adequate model for the sustainable development of the geothermal field; otherwise the result obtained when calculating the electrical potential could cause an over-installation error. For this reason, the zoning result has to be analysed in conjunction with the conceptual model to identify the area of ‘Very good geothermal potential resource', which represents the best option for locating the production pole even if from a purely conceptual and logistic point of view the shape and distribution of this area are not the most viable choices. Therefore, this result was modified and complemented with part of the area 'Good geothermal resource potential' (9.85 km^2 surface area), which is defined as the most probable area (Figs. 8a,b). However, given that in the southern sector, PLB 01 is located between two important tourist complexes, which may negatively affect the exploitation of the geothermal resource in the future, we propose a third scenario in which PLB 01 and the surrounding production area are discarded, thereby obtaining a minimum area with an extension of 7.31 km^2 usable as a production pole (Fig. 8b).

In order to extend the useful life of the geothermal field, it is necessary to maintain the support pressure without permitting the reservoir to cool, thereby guaranteeing the stability of the resource over time. This can be achieved through knowledge of the hydrogeological processes occurring in the area, since the reinjection wells must be located at a safe distance from the production area in sectors in which the temperatures of the hydrothermal system are lower (but are still connected to the reservoir). Based on the above premises and the conceptual model, which indicates the direction of natural discharge of the geothermal fluids from east to west, and locates the main area of meteoric water recharge in the north-west and west, we selected the areas defined as 'Medium and Low geothermal resource potential' as reinjection zones. These areas have thermal gradients of between 25 and 35°C/100 m and are possibly affected by tectonic structures, which increase the permeability of the system and can be used as reinjection zones. Additionally, a distance of 1 km is delimited as a buffer zone separating the production and reinjection zones (Fig. 9).

Assessment of energy potential

The USGS *Heat in Place* volumetric method, together with the Monte Carlo simulator, were used to evaluate and estimate the electrical energy potential of the Borinquen Geothermal zone.

Perforations from which rock samples were collected were used as sites to carry out production tests, which ensured the calculation of realistic reservoir parameters. The probabilistic approach was applied to the type of parameter (linked to the geothermal reservoir) considered in the calculation, which introduced inherent uncertainty into the process. The Montecarlo simulator allowed us to iterate the possible range of conditions and to obtain a distribution of the probability of occurrence of energy storage and the resulting electrical capacity of the geothermal reservoir potential. To test for real results for different situations, we used three scenarios that considered three different sets of values (cases) for the most significant input variables relating to the geothermal reservoir: Minimum (the smallest size and lowest temperature of the reservoir; conservative case); Maximum (the maximum size and highest temperature of the reservoir; more liberal estimate); and the Most Likely (most probable conditions in the geothermal reservoir) (Table 3).

To assign the density values of the rocks, cores from intra-caldera pyroclastic flows and lavas, extracted from depths of over 1200 m (2.36–2.60 g/cm^3), were used. According to the literature, porosity (permeability) can reach up to 10% [7] and, bearing in mind that the specific heat does not vary significantly, the same value was thus assumed in all three cases. The density of the fluid was obtained by analysing the geothermal fluids obtained during the well production tests; in addition depth, pressure, temperature and sodium chloride (NaCl) content were also estimated [12]. Given that it was in the rock, the specific heat was assigned the same value in all cases. The surface area of the reservoir to be exploited was estimated during the zoning of the geothermal resource. The thickness and the temperature of the reservoir were deduced by examining thermohydraulic records (temperature and pressure profiles) and known permeable areas (Fig. 10). The recovery factor depends on the geological conditions (rock temperature, fracture volume, fracture spacing and fluid flow rate) and, after stimulation of permeability, may vary between 10 and 50% [5], [7]. The other parameters – reinjection temperature, conversion efficiency, load factor and plant life – are not values that vary significantly from one field or one geothermal power plant to another (Table 3).

The equations used to calculate the energy potential [7], [8] were:

$$SH=[(1-\phi)\cdot\rho_r\cdot C_r+\rho_w\cdot C_w]\cdot V\cdot(T_r-T_f)$$

$$RH=SH\cdot RF$$

$$PP=(RH\cdot CE)/(PL\cdot PCF)$$

SH Stored Heat (kJ)

Φ Rock porosity (%)

ρ_r Rock Density (kg/m3)

C_r Rock Heat Capacity (kJ/kg°C)

ρ_w Water Density (kg/m3)

C_w Water Heat Capacity (kJ/kg°C)

V Rock Volume (m3)

T_r Reservoir Temperature (°C)

T_f Rejection Temperature (°C)

RF Recovery Factor

RH Recoverable heat (kJ)

CE Conversion Efficiency (%)

PL Plant Life (years)

PCF Plant capacity Factor (%)

PP Power Potential (MWe)

The results of the geothermal potential obtained with the volumetric-Monte Carlo model for the three scenarios, Minimum (57 MWe), Most Likely (164 MWe) and Maximum (579 MWe), were estimated for maximum plant capacity with a useful life of 30 years, with simple flashing and reinjection at 165°C. In all three cases values were obtained that exceed the capacity of the proposed plant (50 MWe); nevertheless, these results should be regarded simply as a first approximation, since at this stage the uncertainty of factors such as area, thickness, permeability and reservoir temperature is still high.

Characteristics of geothermal wells

In order to complement the information necessary for defining an initial development strategy, wells PGB 01, PGB 02 and PGB 05 were evaluated between 2014 and 2015 (Table 4). According to the results obtained, and assuming a separation pressure of 6 bar and a simple flashing plant, there is currently a flow of 58.9 kg/s of steam and 155.1 kg/s of liquid (Table 4). With this information available we posit two possible scenarios: either the use of the three producing wells or the use of two, discarding PGB 01 since its location is not strategic; as well, it lies between two tourist areas, is further away from the reinjection zone, and is separated from the rest of the country by the river Salitral.

The average enthalpy of the three wells is 1245 kJ/kg, the current available power is 26.66 MWe, with an average of 8.85 MWe per well. The generation of this energy would produce 214 kg/s of brine, an average of 71.3 kg/s per well, which would have to be reinjected. If we discard PG 01, the average enthalpy is 1259 kJ/kg, the current available power would decrease by 21.73 MWe but the average per well would increase by 10.86 MWe. The generation of this energy would produce 171 kg/s of brine, an average of 85.5 kg/s per well (Table 4). This estimate is based on preliminary data and so the result in each case should be taken as an indication – rather than a definitive calculation – of the magnitude of the probable geothermal potential. More precise drilling would be required to obtain a more accurate result.

Discussion

During the development of a geothermal project, the initial stages (exploration and development) are generally judged to be the most risky. This is because at the end of these phases, significant investment has been made — but with no guarantee regarding the capacity of the geothermal reservoir to drive the power plant. This is why geological and geophysical studies must elucidate the main volcanological, structural and hydrogeological characteristics of the area in order to determine the existence, location and evaluation of the geothermal resource. Nevertheless, even if these stages are successful, the risk does not end there, as the geothermal resource must guarantee the smooth running of the plant for a minimum of 30 years. Therefore, the development of a geothermal zone also requires a strategy that will ensure the sustainable exploitation of the reservoir.

Starting from the basis that geothermal energy is renewable but that the medium (i.e. the geothermal fluid) enabling the heat energy to be extracted from the rocks is not sustainable, the development strategy must focus on achieving a balance that permit the sustainability of the resource. This means that the risk of pressure and temperature drops, or the exhaustion of the reservoir, must be minimised, a key factor in extending the useful life of the energy resource and making the project economically viable. Therefore, it is vital to understand the distribution of the elements constituting the hydrothermal system (conceptual model) and the zoning of the geothermal resource if the areas for the production, buffering and reinjection of geothermal fluids are to be delimited. However, it is also important to estimate the energy potential so that the size of the plant can be decided upon, and to define the number of production and reinjection wells needed — but without exceeding the productive capacity of the geothermal zone (as this would cause a loss of part of the investment).

In the conceptual model of the areas developed by Molina and Martí [4], the heat source is located in the east (Fig. 3). Given that the exploitation of the geothermal resource is based on using production wells to extract the fluid present inside the hot rock [7], the wells should be located in areas with the greatest potential, usually close to the heat source. In this case, we delimited an area of 9.85 km^2 as suitable for locating the extraction pole. Taking into account the logistical and environmental conditions, as well as the maximum horizontal extension and the separation between wells, we identified within this area four viable sectors for locating production platforms (Fig. 11).

On the other hand, to ensure the sustainability of the resource, the natural flow of fluids must be altered as little as possible and the reservoir support pressure maintained; thus, reinjection must be undertaken. However, geothermal systems are susceptible to changes in their natural state and so this process should avoid decompressing and/or cooling the reservoir. Thus, good knowledge of the hydrogeology of the region is essential to ensure that reinjection wells are sited strategically to respect the natural flow of the fluids, in areas of lower temperature that are still connected to the reservoir. This will guarantee that the differences in pressure and temperature in the reinjected fluids will obstruct initially the natural passage of the geothermal fluids at a safe distance from the extraction zone. However, when the production wells start extraction – thereby causing negative pressure in the reservoir – the reinjected fluids will migrate towards the exploitation zone with a residence period that enables the temperature to recover and prevents the reservoir from cooling. In this way, the original geothermal fluid is replaced by reinjected fluid and the geothermal energy (only the heat) is extracted without any loss of mass. Experiences in the Miravalles and Pailas geothermal zones reveal that about 15% of the extracted mass is lost in the process.

Therefore, when defining the suitable reinjection zones, we took into account the location of the main recharge area of the meteoric water and the direction of discharge of the geothermal fluids from the hydrothermal system in its natural state, which provided a location for the reinjection zone in the north and west of the study area. We created a buffer area with a minimum distance of 1 km between the outer boundary of the production zone and the inside of the reinjection zone (Fig. 9). This sector has a thermal gradient of over 35°C/100 m and so we assumed that the medium has sufficient energy to allow the reinjected brine to regain the necessary temperature before returning to the industrial process. Nevertheless, we recommend analysing the design of the strategy via a simulation using a minimum of five wells (producers and reinjectors) with a suitable spatial distribution in order to obtain more realistic information and evaluate the convenience of making changes. A relatively small area such as Borinquen is prone to require adjustments during the development stage. Part of the flexibility needed to adapt to possible changes is obtained by using directional drilling, which allows for different perforations to be performed from the same platform, by modifying the well design (KOP depth, drilling angle and/or well direction), or by varying the distance between production and/or reinjection zones or the estimated minimum separation distance between wells of 200 m if necessary.

If we assume a plant life of 30 years, all three of the cases we have analysed show that the zone has enough energy for a plant with a capacity of 50 MWe to be constructed. This is the value we use to conceptualize the development strategy and to calculate the number of wells required to extract and reinject the brine into the reservoir. However, to guarantee stable geothermal production 24 hours a day, 365 days a year, it is also necessary to have at least 30% backup energy. Therefore, the number of production wells needed to generate 50 MWe is calculated on the basis of 65 MWe, whereas the number of reinjection wells is estimated at 50 MWe. In addition, we take into account the success rate (85%) of the ICE's geothermal well drilling process.

Therefore, using the information obtained from the production tests of the existing perforations (Table 4), we propose two scenarios: 1) the use of three producing wells or 2) discarding PGB 01 and using just two wells. The first scenario employs PGB 01, PGB 02 and PGB 05 and, based on the thermodynamic conditions of these three existing wells, the average energy per perforated well will be 8.85 MWe. Therefore, if 65 MWe is required, 7.3 wells would be necessary. Furthermore, bearing mind the success rate, the number of wells required increases to 8.44 ≈ 9. Thus, as there are already three wells, six new production wells will need to be drilled. Moreover, assuming that i) each reinjector well drilled accepts 70 l/s (subject to verification), which corresponds to an injection rate of less than 2 l*Bar/s; ii) an average energy production per well of 8.85 MWe representing a total extracted mass of 71.33 kg/s; and iii) a reinjection of 403 kg/s required to produce 50 MWe, 6.5 ≈ 7 reinjector wells will need to be drilled (taking into account the success rate).

The second scenario, in which only wells PGB 02 and PGB 05 would be used, assumes an average energy per perforated well of 10.86 MWe. Therefore, to generate 65 MWe, six production wells would be needed (or 6.68 ≈ 7 if the success rate is taken into account), which implies that fives new wells will be needed in addition to the two already available wells. Assuming that each reinjector well drilled will accept 70 l/s and an average energy production per well of 10.86 MWe, a mass of 85.50 kg/s will have to be extracted. Thus, to produce 50 MWe, reinjection must be 394 kg/s, which represents the drilling of 6.47 ≈ 7 reinjector wells (taking into account the success rate).

Conclusions

The results obtained from our assessment of an exploitation strategy for the Borinquen geothermal systems reveal scenarios with positive outcomes. In all three considered scenarios, the Borinquen geothermal zone has sufficient extractable energy potential to install a geothermal power unit with a capacity of 50 MWe for a period of useful life of 30 years. Under scenario 1, the most conservative and viable from a development point of view, a volume of 7.31 km^3 of the geothermal reservoir (7.31 km^2 * 1 km) would be used as a production area. Only the existing PGB 02 and PGB 05 wells would be used and five new production wells and seven reinjection wells should be budgeted for. Although production drilling can be performed from existing platforms, we recommend that two further platforms – PLB 06 and PLB 09 – be constructed (Fig. 11). Thus, considering the layout of the four platforms and the two drilled wells, there are theoretically 22 options available for locating the next five production wells, which allows for a wide range of scenarios. However, even with such a large number of alternatives, at this stage it would not be wise to accelerate the drilling process by perforating more than one well at a time since the results of the drilling of all new wells must be used to select the location of the next one. Therefore, we propose drilling from the PLB 09 eastwards and then PLB 06 north-eastwards to gain greater knowledge of the geothermal zone (Fig. 11). With regard to the reinjection process, fewer wells will be necessary, although exactly how many will depend on the results of the first drilling. Using a similar analysis, three reinjection platforms (PLB 07, PLB 08 and PLB 10) should be constructed and a well drilled in each directed towards the reinjection zone (PLB 08 to NNW, PLB 07 to NW and PLB 10 to W). According to the results of drilling and numerical simulations, the calculations can be fine-tuned and the development strategy adjusted, so that the sites of the remaining wells can be selected with greater precision.

Acknowledgements

We would like to thank the Instituto Costarricense de Electricidad (ICE) for its support and help in undertaking this research and for giving us permission to publish the data. JM is grateful for the MECD (PRX16/00056) grant. Thanks are also due to Leyner Chavarría for his support and fruitful discussions. The English text was corrected by Michael Lockwood.

References

[1] DiPippo, R., Moya, P., 2013, Las Pailas geothermal binary power plant, Rincón de la Vieja, Costa Rica: Performance assessment of plant and alternatives. Geothermics 48, 1 – 15.

[2] Molina, F., Martí, J., Aguirre, G., Vega, E., Chavarría, L. 2014, Stratigraphy and structure of the Cañas Dulces caldera (Costa Rica). Geological Society of America Bulletin published online 23 June 2014; doi: 10.1130/B31012.1

[3] Gehringer, M,. Loksha V., 2012, Manual de geotermia: Cómo planificar la generación de electricidad. Banco Internacional para la Reconstruccion y el Desarrollo / Grupo del Banco Mundial, Washington D.C., EE. UU. 164 p..

[4] Molina , F., Martí, J., 2016, The Borinquen geothermal system (Cañas Dulces caldera, Costa Rica). Geothermics 64, 410–425 [5] Muffler, P. and Cataldi R., 1978, Methods for regional

assessment of geothermal resources. Geothermics 7, 53-89. http://dx.doi.org/10.1016/j.geothermics.2016.07.001

[6] Brook, C., Mariner, R., Mabey, D, Swanson, J, Guffanti, M., Muffler, L., 1979, Hydrothermal Convection Systems with Reservoir Temperatures > 90°C: in Assessment of Geothermal Resources of the United States 1978. p.18 -85

[7] Mendrinos, D., Karytsas, C., Georgilakis. P., 2008, Assessment of geothermal resources for power generation: Journal of Optoelectrics and Advanced Materials, v. 10, p. 1262 – 1267.

[8] Hiriart, G., 2011, Evaluación de la Energía Geotérmica en México. Informe para el Banco Interamericano de Desarrollo y la Comisión Reguladora de Energía. México, DF. 164 p.

[9] Garg, S., Combs, J., 2010, Appropriate use of USGS volumetric “Heat in Place” method and Monte Carlo calculations. Proceedings, Thirty-Fourth Workshop on Geothermal Reservoir Engineering. Stanford University, Stanford, California, SGP-TR-188

[10] Asamblea Legislativa, 1996, Ley Forestal (Ley No. 7575). San José, Costa Rica. Editorial Investigaciones Jurídicas. Diario La Gaceta # 72, 19 P. www.dse.go.cr.

[11]West JEC, 2011, Servicios de consultoría para la explotación racional y sostenible del campo geotérmico Las Pailas (volumen de tablas y figuras, reporte final). BCIE – ICE. San José, Costa Rica.

[12] Robert, W., Potter, II., Brown, D., 1977, The Volumetric Properties of Aqueous Sodium Chloride Solutions from 0° to 500°C at Pressures up to 2000 Bars Based on a Regression of Available Data in the Literature. Geological Survey Bulletin 1421-C

List of figures and tables

Figure 1: Location of the study area.

Figure 2: Conceptual model taken from Molina and Martí [4] synthesising the main hydrogeological and geothermal elements: movement of meteoric water and geothermal fluids, geological structures affecting the hydrothermal system, and distribution of the thermal gradient.

Figure 3: Flow chart of the proposed methodology for the development strategy of the Borinquen geothermal zone. DCM Decision Making Criteria; DEM Digital Elevation Model.

Figure 4: Thematic layers reclassified in a binary form to be used in the selection of areas suitable for locating drilling pads: a) areas with slopes less than or equal to 15%; b) 100 m protection area along both banks of all rivers and streams; c) buffer area of 400 m around existing infrastructures; d) buffer area of 900 m around the existing drilling platforms.

Figure 5: Distribution of areas suitable for locating drilling pads taking into account topographical, logistical and environmental criteria.

Figure 6: Resistivity distribution in relation to depth (modified from West [11]): a) layer at 500 m with values below 10 ohm/m; b) layer at 1100 m with values reaching 40 ohm/m; c) layer at 1750 m with values reaching 100 ohm/m.

Figure 7: Reclassification of thematic layers based on the values in Table 2 used in the zoning of the geothermal resource: a) resistivity, b) thermal gradient, c) structures.

Figure 8: Zoning model of the high enthalpy geothermal resource. a) Distribution of areas according to the potential of the high enthalpy geothermal resource. b) Delineation of three scenarios (Maximum, Minimum and Most likely) for the suitable development of the production area.

Figure 9: Distribution of the main areas suitable for the development of the high enthalpy geothermal resource.

Figure 10: Geological and thermohydraulic characteristics of the Borinquen 05 Geothermal Well (lithological column, zones of alteration, zones of loss of circulation of drilling fluid, static temperature profiles and pressure).

Figure 11: Final map of the development strategy for the Borinquen Geothermal Zone, showing the recommended distribution of production well platforms.

Table 1. Relationship between the zones of alteration, resistivity, depth and temperature for the hydrothermal system in the Borinquen geothermal zone.

Table 2. Value of suitability and weight assigned to the thematic layers of the selected geothermal resource-zoning scenario.

Table 3. Values used in the calculation of the electric potential using the USGS *Heat in Place* method and the Monte Carlo simulator.

Table 4. Thermohydraulic characteristics of the Borinquen wells (the estimates of vapour and liquid flow are based on six absolute pressure rods).

Figure 1

Click here to download high resolution image

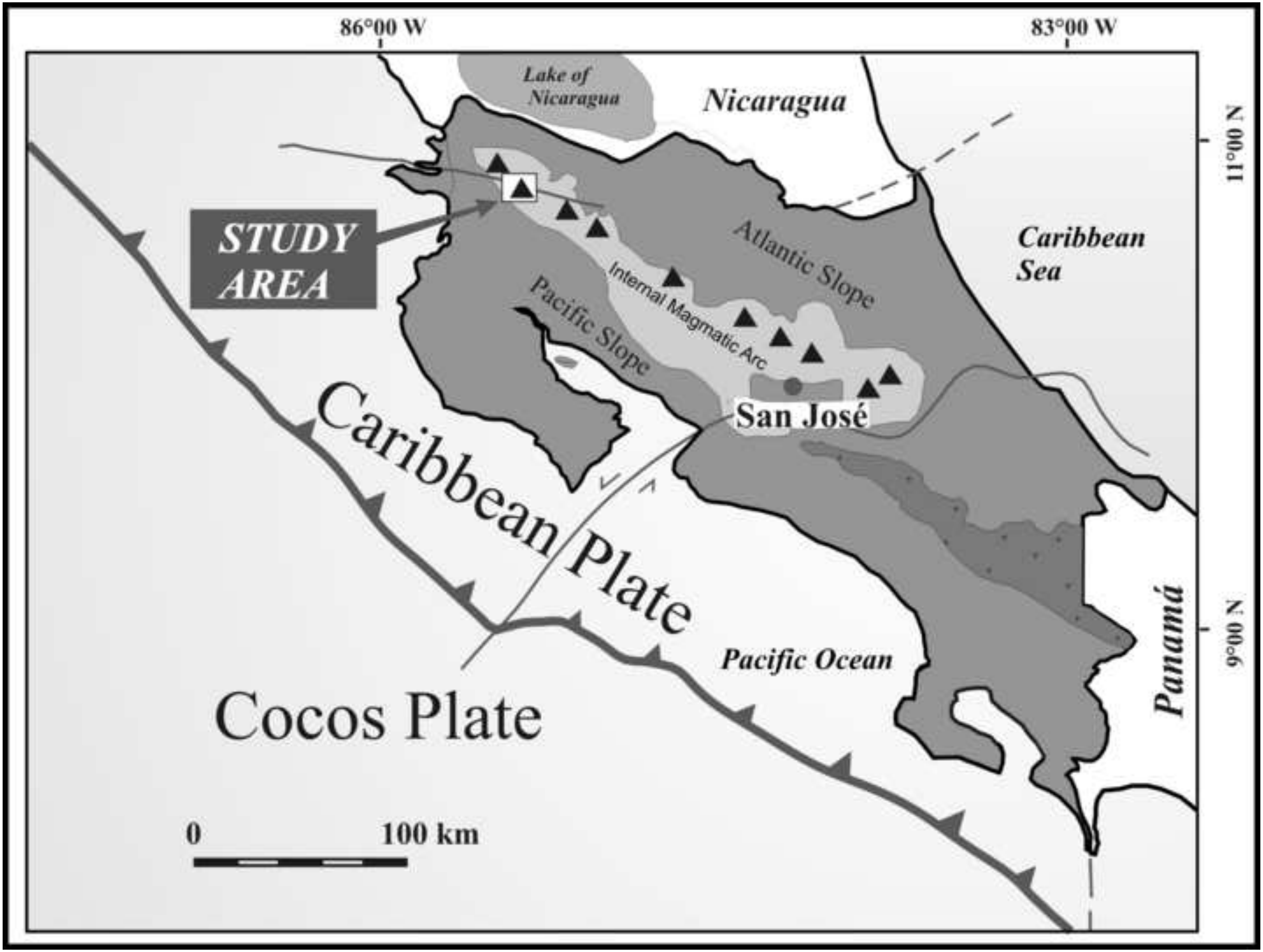

Figure 2
Click here to download high resolution image

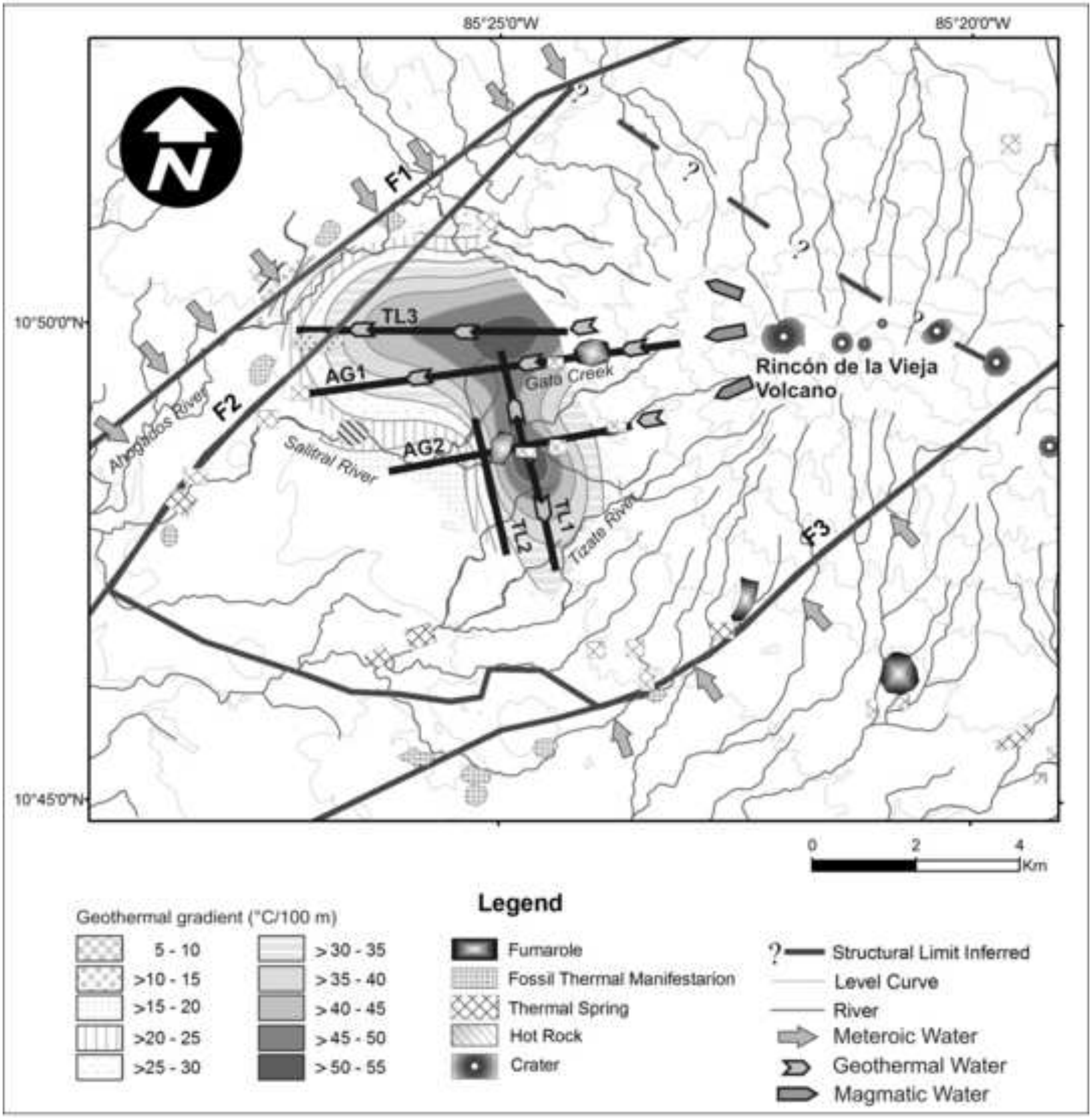

Figure 3

Click here to download high resolution image

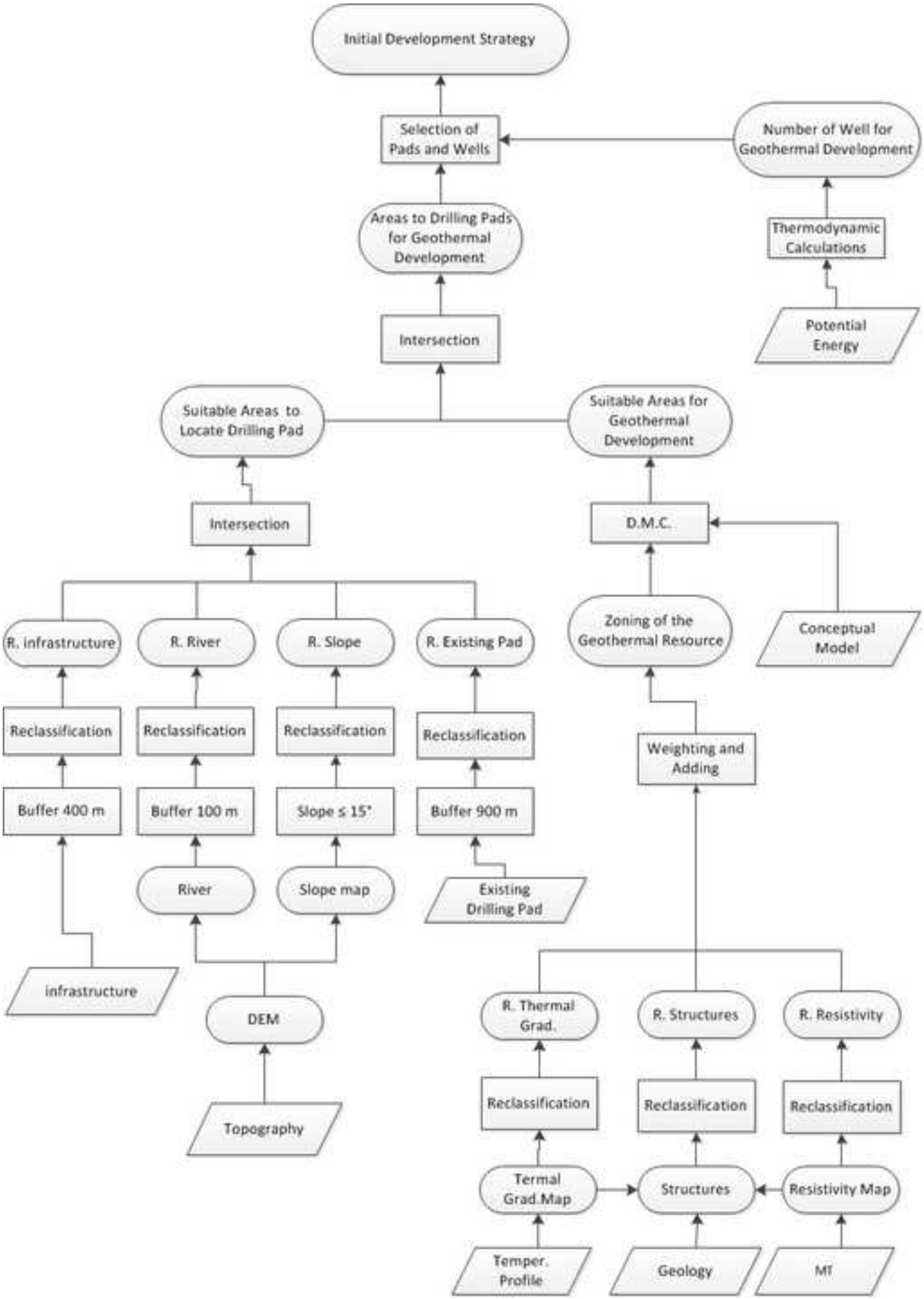

Figure 4
Click here to download high resolution image

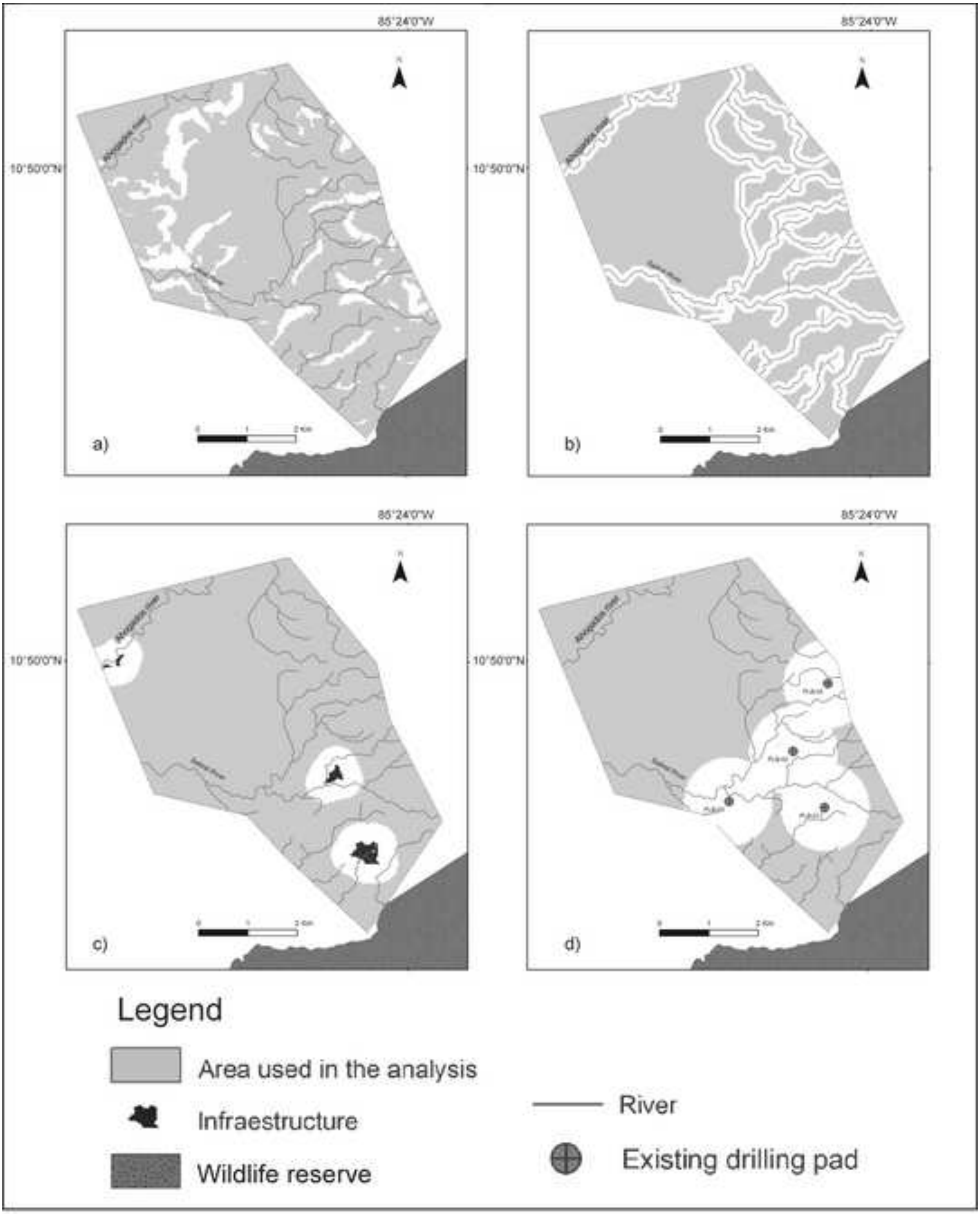

Figure 5

Click here to download high resolution image

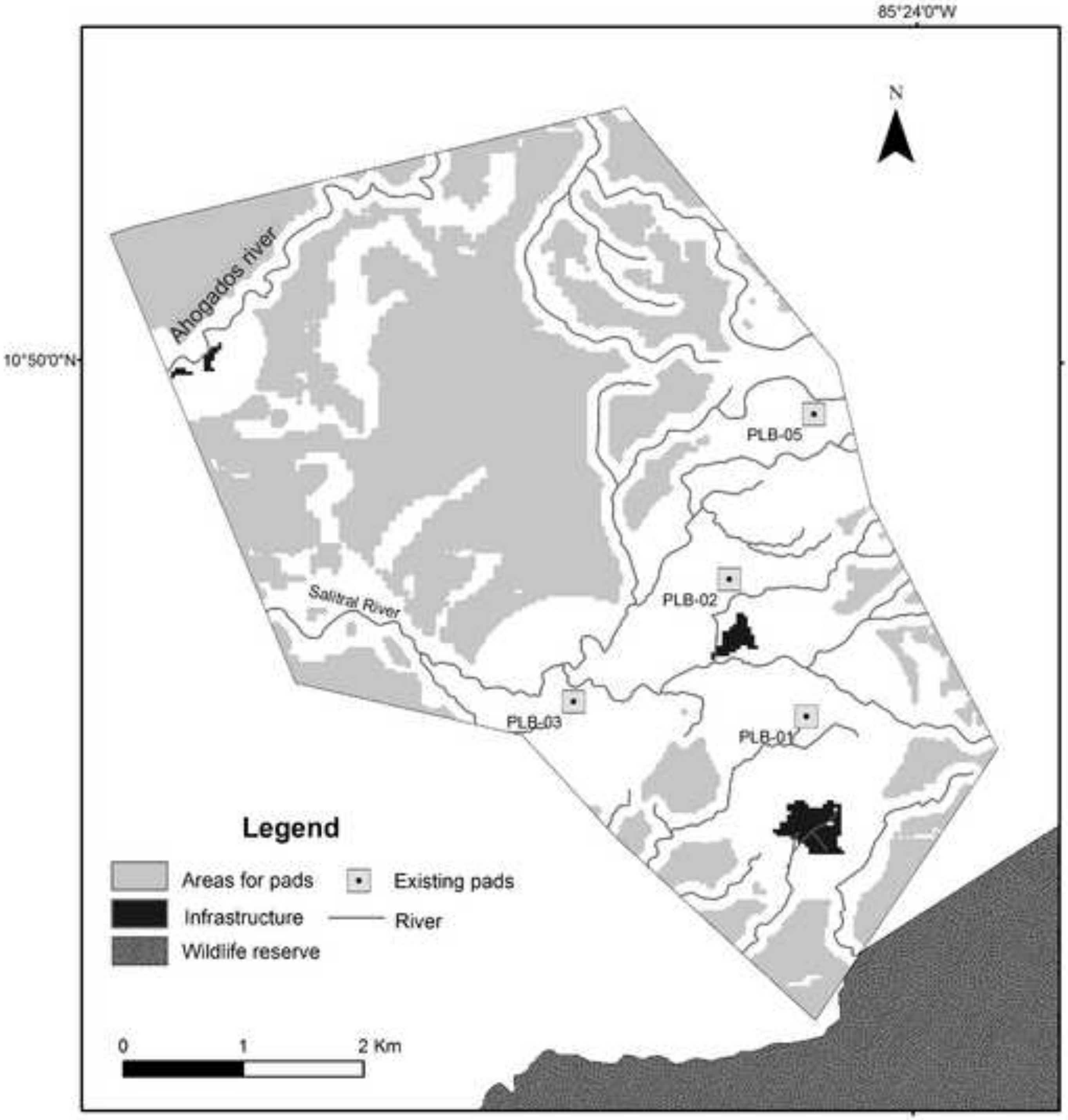

Figure 6

Click here to download high resolution image

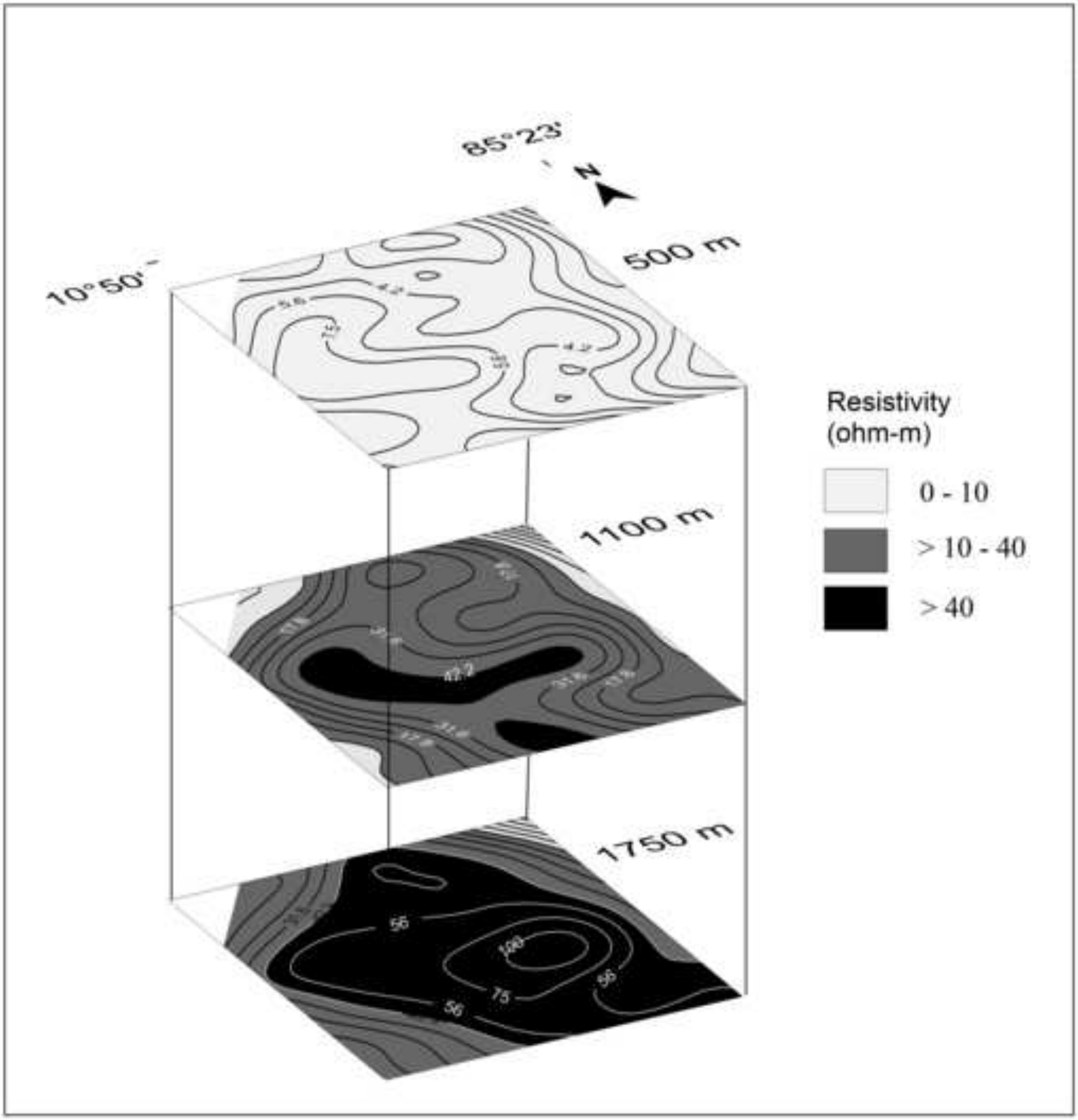

Figure 7

Click here to download high resolution image

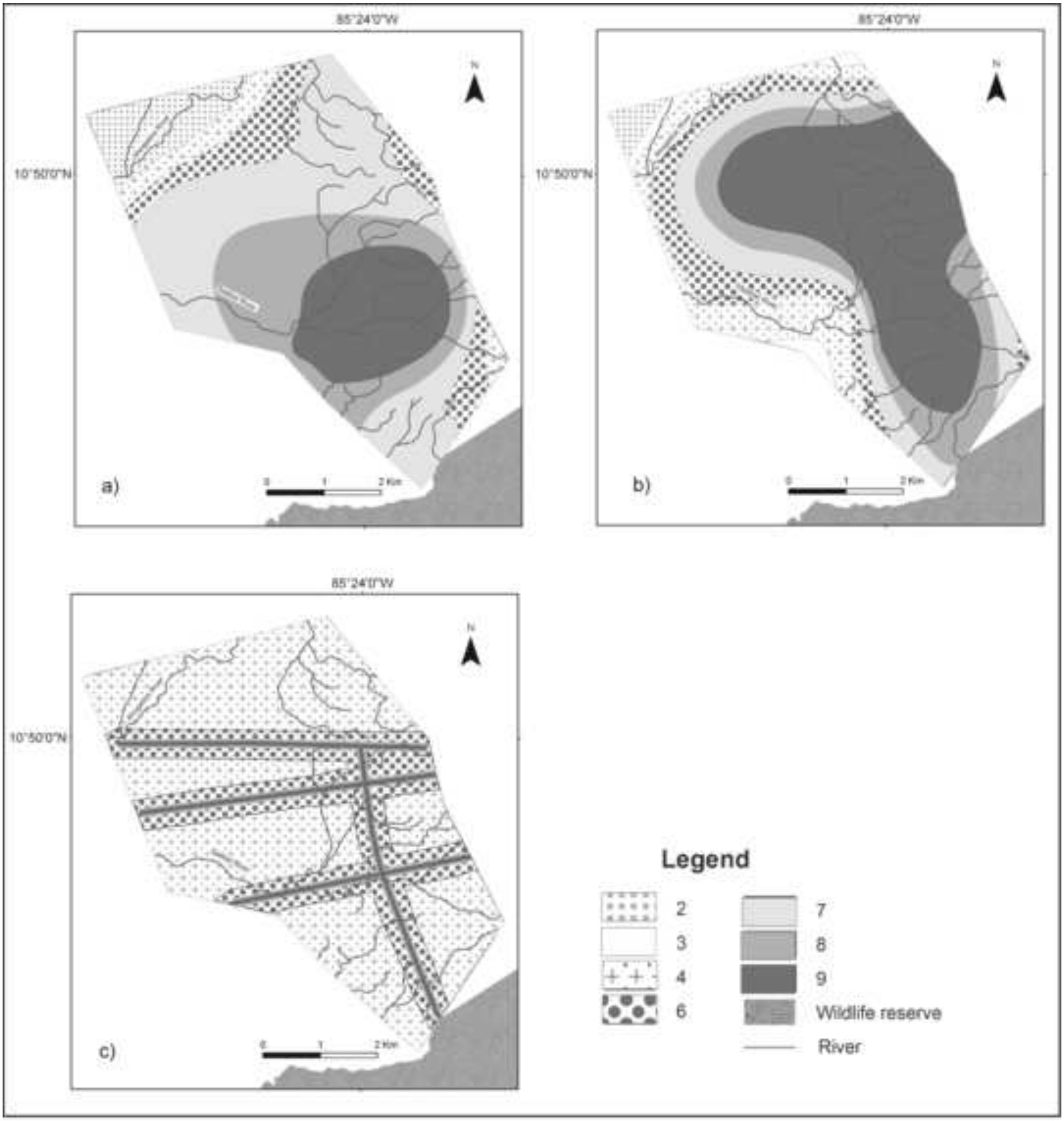

Figure 8a
Click here to download high resolution image

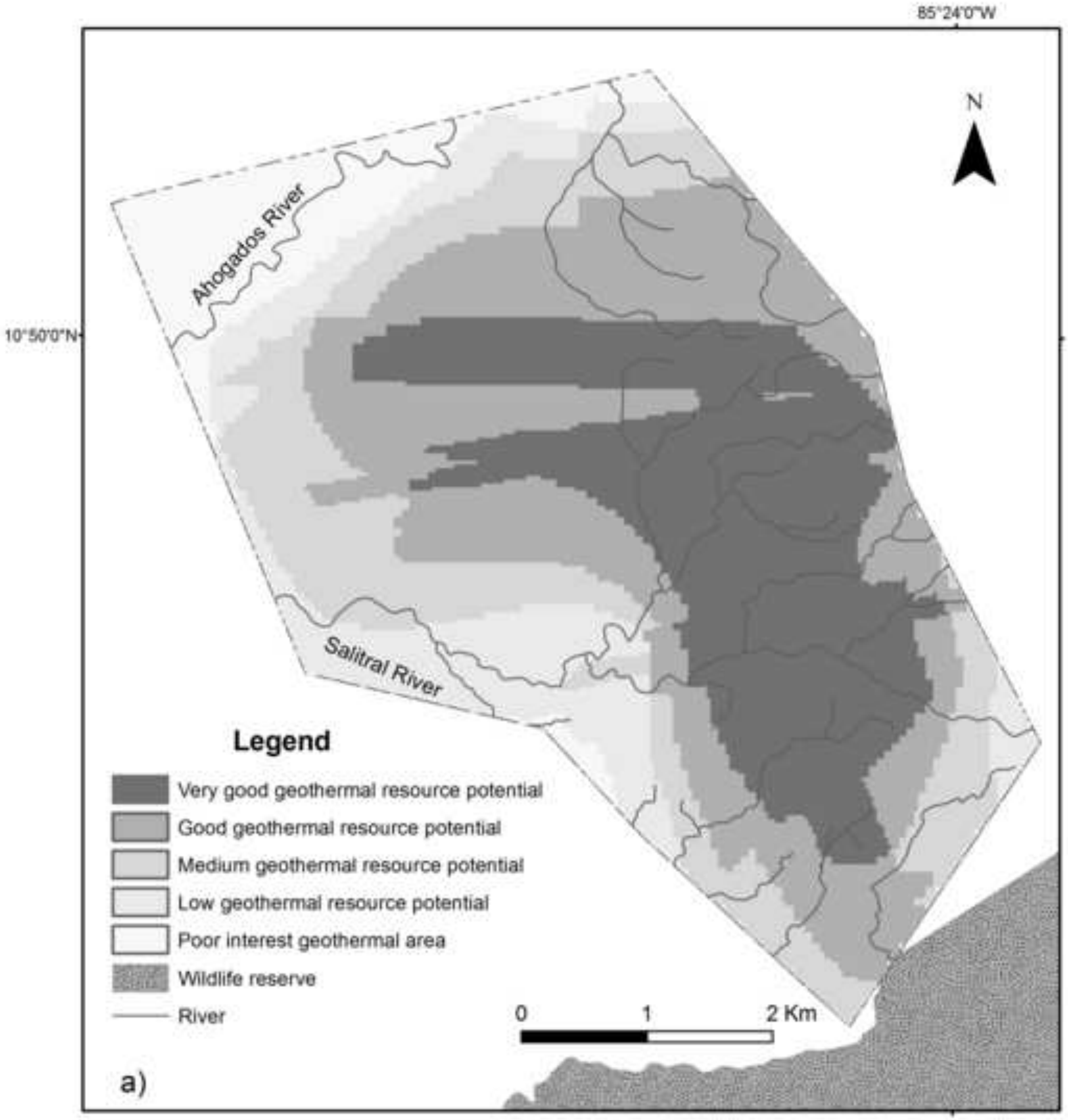

Figure 8b
Click here to download high resolution image

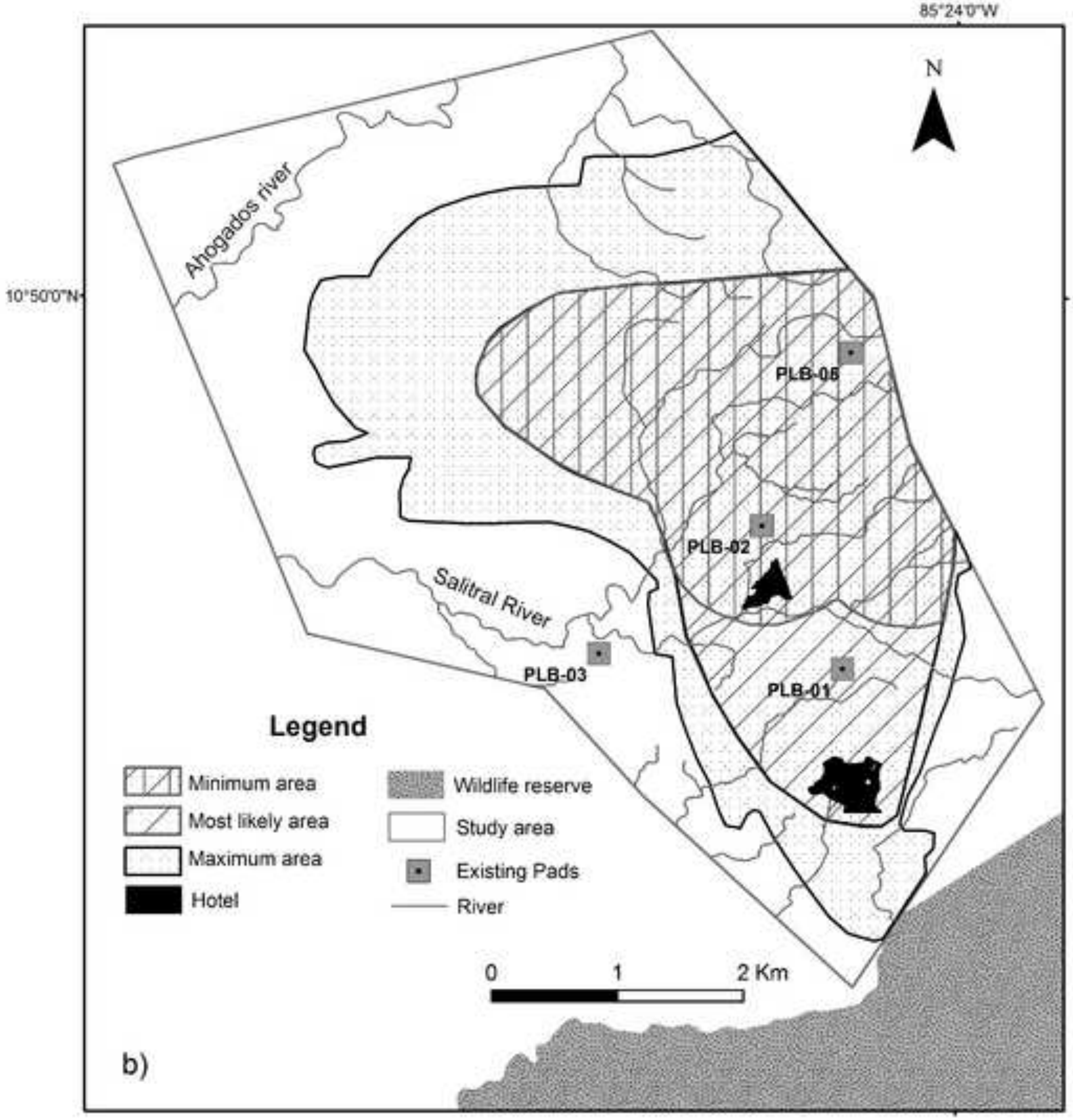

Figure 9

Click here to download high resolution image

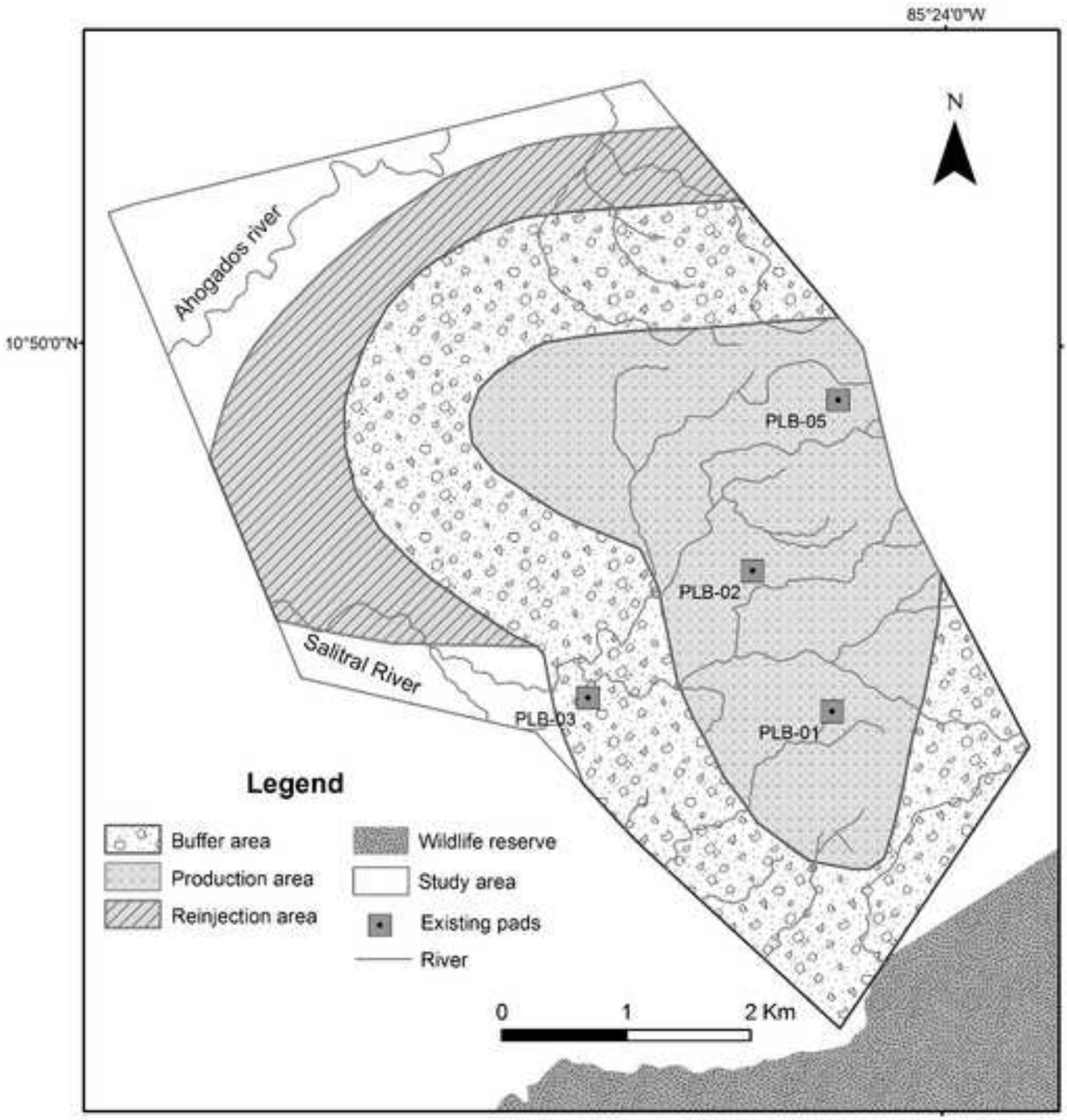

Figure 10

Click here to download high resolution image

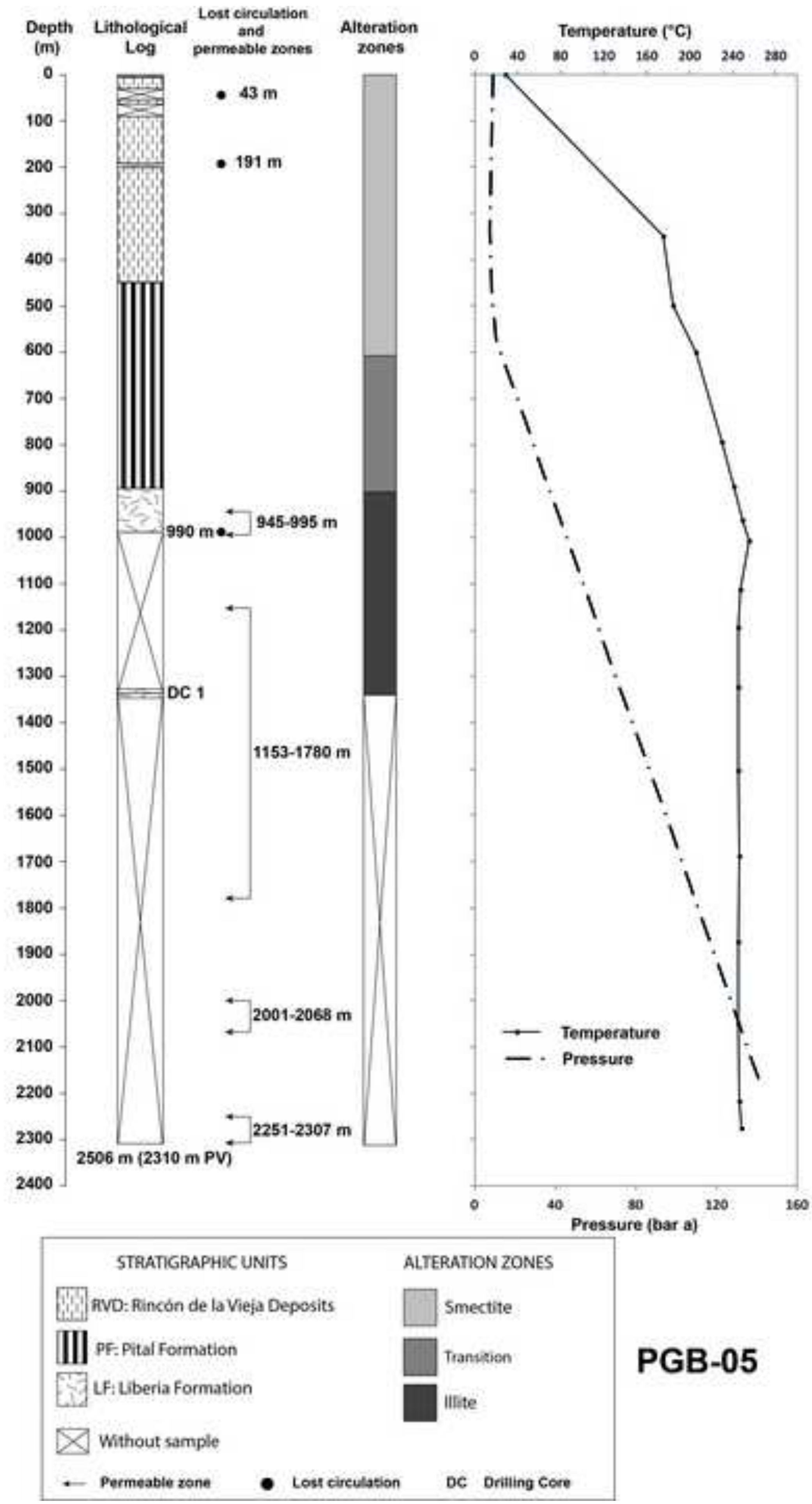

Figure 11
Click here to download high resolution image

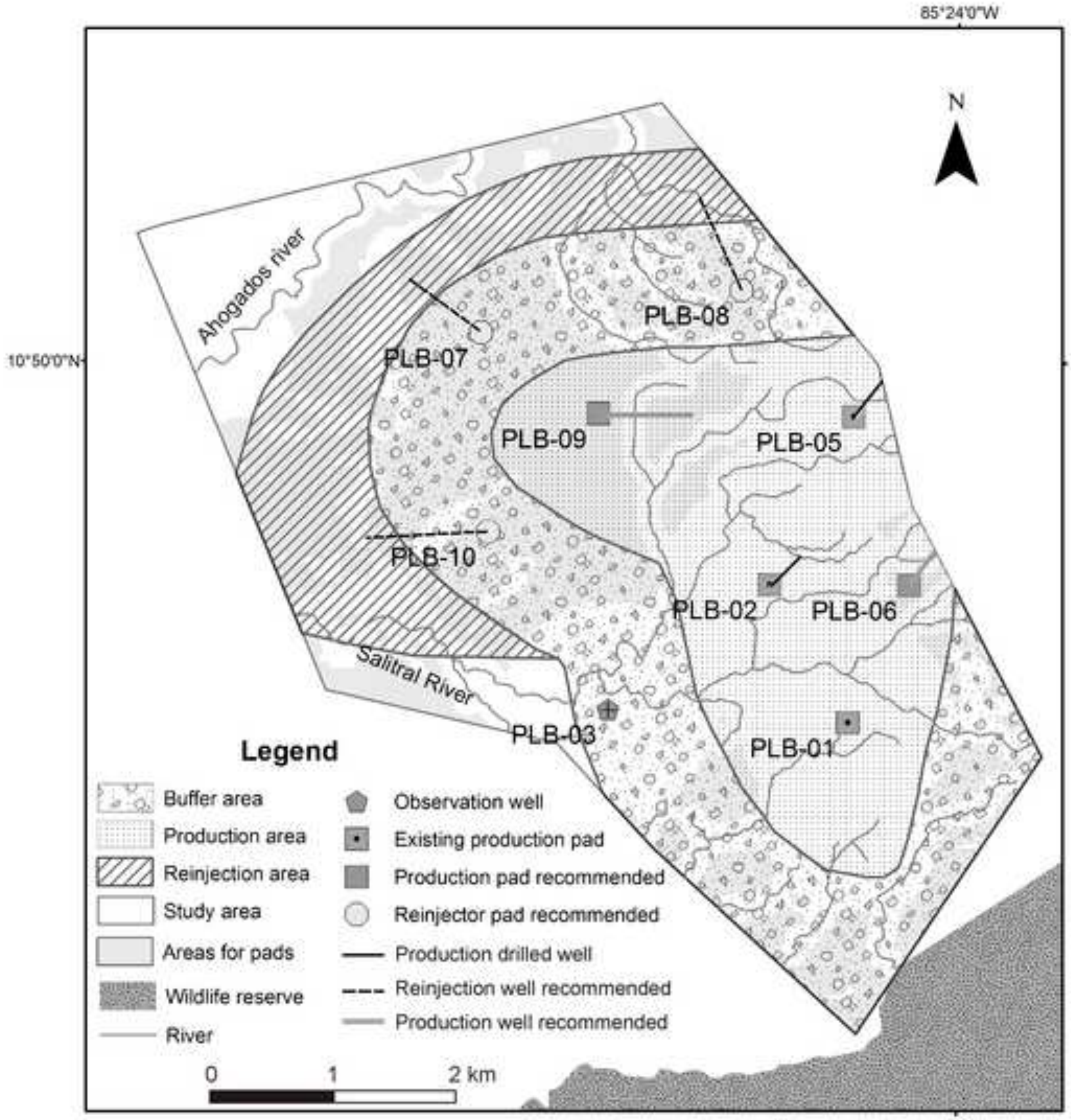

Table 1

Relation of the zones of alteration, resistivity, depth and temperature, for the hydrothermal system of the Borinquen geothermal zone

Hydrothermal alteration zones	Resistivity ohm	Depth m	Temperature ℃
Smectite	0-10	from 150 to 900	T ≤150
Transition	10 - 40	from >900 to 1100	150 < T < 220
Illite	≥ 40	>1100	T ≥ 220

Table 2

Value of suitability and weight assigned to the thematic layers of the selected geothermal resource zoning scenario.

Value	Suitability degree	Resistivity (Ωm)	Thermal gradient ºC/100 m	Tectonic structures distance m
1	Low			
2		10-30	1 – 10	
3			10 – 15	
4	Medio	30 - 40	15 – 20	>250
5				
6		40 - 50	20 – 25	75 - 250
7	Alto	50 - 60	25 -30	
8		60 - 75	30 -35	25 - 75
9		75 -105	35 – 55	0 - 25
Peso		0.35	0.55	0.1

Table 3

Values used in the calculation of the electric potential by the method of the USGS Heat in Place method and the Monte Carlo simulator

	Case 1 Minimum	Case 2 Most likely	Case 3 Maximum
Properties of rocks			
Density (g/cm3)	2.40	2.50	2.60
Heat capacity (J/g °C)	0.795	0.795	0.795
Porosity	0.05	0.05	0.1
Properties of fluid			
Density (g/cm3)	0.820	0.802	0.781
Heat capacity (J/g-°C)	4.186	4.186	4.186
Properties of reservoir			
Area (Km^2)	7.31	9.85	17.6
Thickness (m)	1000	1200	1500
Temperature (°C)	240	250	260
Other properties			
Reinjection temperature (°C)	165	165	165
Recovery Factor	0.10	0.15	0.20
Efficiency of conversion	0.45	0.45	0.45
Charge factor	0.90	0.90	0.90
Energy in the rock (kJ)	**9,93758E+14**	**1,897E+15**	**4,66563E+15**
Energy in the fluid (kJ)	**9,4094E+13**	**1,68648E+14**	**8,19932E+14**
Total energy	**1,08785E+15**	**2,06565E+15**	**5,48556E+15**
Plant life (years)	**30**	**30**	**30**
Maximum Plant Capacity (MWe)	**57**	**164**	**579**

Table 4

Thermohydraulic characteristics of Borinquen wells (estimation of vapor and liquid flow is calculated based on 6 absolute pressure rods).

Well	Depth (m)	Evaluation Date	Head Pressure Bar ab	Total flow (kg/s)	Enthalpy kj/kg	Vapor flow (kg/s)	Liquid flow (kg/s)	Production Index (kg* Bar /s)	Power vapor (MWe)
PGB 01	2594	10/02/14	9.44	43.0	1190	10.70	32.30		4.83
PGB 02	2107	11/11/15	10.34	114.0	1262	32.30	81.70	5.8	14.57
PGB 05	2310	11/01/15	10.14	57.0	1252	15.90	41.10	2.4	7.16
Total				214.0		58.90	155.10		26.56
Average				71.3	1245	19.63	51.70		8.85
Total without PGB1				171.0		48.2	122.80		21.73
Average without PGB1				85.5	1259	24.1	61.4		10.86